CELLULAR AND MOLECULAR MECHANISM OF ACTION OF THE AMYLOID-BETA OLIGOMER ABETA STAR 56

A DISSERTATION SUBMITTED TO THE FACULTY OF THE GRADUATE SCHOOL OF THE UNIVERSITY OF MINNESOTA BY

Fatou Amar

IN PARTIAL FULFILLMENT OF THE REQUIREMENTS FOR THE DEGREE OF DOCTOR OF PHILOSOPHY

ADVISOR: Sylvain E. Lesné, Ph.D.

January 2016

Acknowledgements

First and foremost, I want to thank my advisor Dr. Sylvain E. Lesné. It has been an honor to be his first Ph.D. student. He has taught me, both consciously and unconsciously, how good neuroscience research is done. I appreciate all his contributions of time, ideas, and funding to make my Ph.D. experience productive and stimulating. The joy and enthusiasm he has for his research was contagious and inspiring for me, even during tough times in the Ph.D. training. I am also thankful for the excellent example he has provided as a successful young scientist in neurodegenerative research.

I would also like to thank past and present members of the Lesné laboratory, who contributed immensely to my personal and professional development at the University of Minnesota, especially Mathew (Matt) A. Sherman who has been instrumental in completing my thesis project as he performed the purification of crucial biological materials for *in vitro* experiments. I am also very grateful for the opportunity to have worked with Megan S. Larson who generated some of the preliminary data for my thesis project.

I am thankful for our collaborators, notably Dr. Alain Buisson, Dr. Travis Rush and Dr. José Martínez Hernández who performed some of the calcium imaging and trained me on the technique to myself perform the rest of the calcium imaging. I am grateful for the valuable discussions and collaboration with the laboratory of Dr. Karen Ashe. A warm thank you to the collaborators who graciously provided reagents and valuable feedbacks. This includes Dr. Rakez Kayed, Gloria Lee, Peter Davis, Jurgen Gotz, Pritam Das and David Benett.

I appreciate the financial support that I have received throughout my graduate career from the NIH, the N. Bud Grossman Center for Memory Research and Care, and the Graduate Program in Neuroscience.

Finally, I would like to thank my family for all their love and encouragements. For my parents who raised me with love and supported me in all my pursuits. I am truly grateful for all their sacrifice. For my dear brother Babacar and my grandmother (Yaye) Nogaye. And lastly for my loving, supportive, encouraging, and patient husband Khadim whose faithful support during the final stages of this Ph.D. is so appreciated. Thank you.

Abstract

Alzheimer's disease (AD) is a progressive neurodegenerative disorder, with asymptomatic and symptomatic phases. Hallmark lesions of AD include extracellular deposits of fibrillar amyloid-β (A β) and intracellular Neurofibrillary tangle formations (NFTs). However, recent evidence seems to support soluble oligomeric forms of amyloid proteins as bioactive species in AD. Amyloid-β oligomers (Aβo), such as Aβ*56, Aβ dimers and trimers have been demonstrated to be synaptotoxic species in AD. In particular, one of these oligomers, Aβ*56, was found to cause cognitive decline in the AD mouse model Tg2576, despite the absence of plaques and neuronal loss. In addition, cross-sectional studies suggest its possible involvement in the asymptomatic or preclinical phase of AD. However, it is currently unclear how this specific oligomer (Aβ*56) influences cellular and molecular processes to lead to cognitive deficits. My thesis focused on how Aβ*56 is able to disrupt cognition at the cellular and molecular level. First, we demonstrate that Aβ*56 forms a complex with NMDA receptors (NMDARs) resulting in an aberrant increase in intracellular calcium driven by synaptic NMDARs and the specific activation of the Ca^{2+}/calmodulin dependent protein kinase CaMKIIα. Active CaMKIIα induces selective pathological changes in tau in vivo and in vitro, involving hyperphosphorylation and missorting. Importantly, other forms of endogenous Aβ oligomers do not appear to trigger these effects. Furthermore, other kinases such as GSK3, Cdk5 and fyn are not modulated by Aβ*56 in vitro. Interestingly, CaMKII phosphorylation is elevated in brain tissue of aged individuals, correlating with Aβ*56 abundance. These findings indicate that distinct Aβ oligomers activate specific

neuronal signaling pathways in a highly selective manner in vitro. By extrapolation, these observations may have important consequences relative to our understanding of the different stages of AD.

Table of content

List of figures

Abbreviations

α7-nACh: α7-nicotinic acetylcholine receptors

α-Syn: α-synuclein

Aβ: amyloid-β protein

AD: Alzheimer's disease

ADDLs: Amyloid Beta-Derived Diffusible Ligands

AMPA: α-amino-3-hydroxy-5-methyl-4-isoxazolepropionic acid receptors

APP: Amyloid precursor protein

CDK5: cyclin-dependent protein kinase-5

EphB2: Ephrin-type B2 receptor

Erk1/2: extracellular signal-regulated kinases 1 and 2

fAD: familial AD

GSK3: Glycogen synthase kinase-3

LBs: Lewy bodies

MARK: microtubule affinity-regulating kinases

MBD: microtubule-binding domains

NFTs: neurofibrillary tangles

NMDA: N-Methyl-D-Aspartate

O-GlcNAc: O-linked N-acetylglucosamine

PHF: paired helical filament

PKA: protein kinase A

PKB: protein kinase B

PKC: protein kinase C

PrP^C the cellular prion protein

PS1: presenilin-1 protein

PS2: presenilin-2 protein

PSEN1: presenilin-1 gene

PSEN2: presenilin-2 gene

RAGE: insulin receptors, the receptor for advanced glycation end-products

Chapter 1

Introduction

I. Introduction to Alzheimer's disease

Alzheimer's disease (AD) is the most common cause of dementia, which is often associated with multiple social and functional deficits such as memory impairment, communication and language deficits, inability to focus and pay attention, compromised reasoning and judgment, impaired visual perception, that are severe enough to hinder a person's daily living. AD makes up 60-80% of dementia cases according to the Alzheimer's Association (www.alz.org). In 2015, 5.3M Americans suffer from AD, the great majority of whom are 65 years or older. The annual incidence of AD increases steadily starting at age 65 and doubles after 85 years of age (Hebert et al., 1995). More than 90% of AD cases appear to be sporadic with no known genetic cause (Bekris et al., 2010). However, 1 to 6% showed AD-linked mutations that lead to the early-onset of clinical symptoms generally before the age of 60 (Bekris et al., 2010, Bateman et al., 2011). The number of people diagnosed with AD is projected to triple by 2050 reaching a resounding 16 million Americans, making it an urgent issue that needs immediate resolving.

Dr. Alois Alzheimer first described Alzheimer's disease in 1906 on a 56-year-old subject who presented with rapidly progressive dementia that failed to fall within the characteristics of 'senile dementia' because of its early onset, and disease severity

(Alzheimer, Förstl, & Levy, 1991). The German physician characterized the disease as 'pre-senile dementia' until it became clear that pre-senile and senile dementia share the same neuropathologies as demonstrated by Blessed, Tomlinson and Roth in 1968 (Burns, Tomlinson, & Mann, 1997). The term "Alzheimer's disease" was coined by his colleague Dr. Emil Kraepelin in 1910 and to later include both types of dementia (Katzman, 2008).

Following postmortem analysis, brains of patients showed a severe degeneration of neurons in the cerebral cortex with other pathologies. Abnormalities in the brain of an AD patient are first characterized by shrinkage of total brain volume with severe degradation of brain regions involved in learning and memory processes. Microscopic analysis showed formation of what Dr. Alzheimer referred to as extracellular Fischer's plaques and intracellular fibrillar structures (Alzheimer et al., 1991). These lesions were later referred to as amyloid plaques and neurofibrillary tangles (NFTs) respectively and are to date the two hallmarks of AD.

Amyloid plaques are mainly composed of a 39-43 amino acid protein amyloid-beta (Aβ) peptide, a product of the subsequent cleavage of the amyloid precursor protein (APP) by proteolytic enzymes initially termed secretases, β- and γ-secretases respectively (Eanes & Glenner, 1968; Glenner & Wong, 1984; "Kang et al., 1987; Simans et al., 1993). Following amyloidogenic APP processing, Aβ is released outside the cell as a soluble protein, however it can aggregate as diffused (non-congophilic) or dense core plaques. These amyloid plaques are found abundantly in different areas of the brain including the frontal, the parietal and temporal lobes.

Although the majority of AD cases are sporadic, mutation in the *APP*, presenilin-1 (*PSEN1*) and presenilin-2 (*PSEN2*) genes have been identified in early-onset AD. Certain of these genetic mutations cause dominantly inherent AD and increase production of the 42-amino acid form of Aβ (Aβ42). An increase in the ratio of Aβ42:Aβ40 appears to be more aggregation-prone and seems to promote more formation of neurotoxic assemblies (Chen & Glabe, 2006; Kuperstein et al., 2010; Mann et al., 1996). Aβ42 is of particular importance as it has been shown to be the more toxic species of Aβ (Zhang et al., 2002). These findings explains the coincidence of an increase in Aβ42 levels with the familial AD-linked *PSEN1* mutation carrier compared with cases of sporadic AD (Hellström-Lindahl et al., 2009).

Neurofibrilary tangles (NFTs), the other hallmark of AD, are mainly composed of the microtubule-associated protein tau (Avila et al, 2004; Binder, Guillozet-Bongaarts et al., 2005; Gamblin et al., 2000; Iqbal et al., 1998; King et al.,1999; Delacourte and Defossez, 1986). Tau can undergo hyperphosphorylation, truncation and conformational changes leading to the formation of intracellular fibrillar aggregates of the protein that make up the NFTs (Binder et al., 2005; Luna-Muñoz et al., 2005). Similar to the amyloid plaques, NFTs can be very abundant in the diseased brain and are found in brain areas that are important for learning and memory processes.

In addition to the changes in tau and Aβ, multiple other abnormal protein changes have been implicated in AD. For instance, intracellular inclusions mainly containing α-synuclein (α-Syn) known as Lewy bodies (LBs) and Lewy neurites (LNs) are found in

close to 60% of sporadic AD and familial AD cases (Baba et al., 1998; Hamilton, 2000; Lippa et al., 1998). Additionally subjects with the LB variant of AD generally display faster rate of cognitive decline than subjects with AD alone (Olichney et al., 1998). Interestingly the effects **α**-Syn appear to have in AD seems to be dependent on dysregulation of soluble levels of **α**-Syn and not fibrlar **α**-Syn (Larson et al., 2012; Lee et al., 2002; Scott et al., 2010).

Understanding the cellular and molecular mechanism of the disease will require understanding the part these proteins play and how they are related to one another.

II. The amyloid cascade hypothesis

The amyloid cascade hypothesis postulates that the amyloid-β protein (Aβ) is the causative initiator in AD pathology. According to Hardy and Heggins in their original report, Aβ depositions precede NFTs formation, cell degeneration, vascular damage and behavioral deficit which are proposed to be direct consequences of amyloid deposition (Hardy & Higgins, 1992). Two decades later, the majority of the data appears to still support the idea that Aβ is the primary initiator of AD pathogenesis. However, the concept that Aβ aggregation has a unique and critical role as the key initiator of AD pathology revealed many layers of complexity.

The strongest data supporting the role of Aβ as disease initiator comes from human genetics. Autosomal dominant familial AD (fAD) is caused by mutations in three genes, *APP*, *PSEN1* and *PSEN2*, which are all inherently involved in A β production. As previously noted, *APP* is the gene precursor for the amyloid-beta protein. *PSEN1* and

PSEN2 on the other hand are the genes encoding for the presenilin-1 (PS1) and pesenilin-2 (PS2) proteins. PS1 and PS2 are the catalytic subunits of the γ-secretase complex that cleaves APP to generate Aβ (Bettens et al., 2013). Therefore, many mutations to any of these two genes have the same consequence as the mutations on *APP* which is to typically increase Aβ production.

Familial AD-related mutations lead to accelerated accumulation of Aβ plaques and cause early-onset dementia (Bettens et al., 2013; Goate et al., 1991; Levy et al., 1990; Tomiyama et al., 2008; Tsubuki, Takaki, & Saido, 2003). Duplication of the *APP* gene located on chromosome 21 increases Aβ production and causes age-related cognitive impairment (Cabrejo et al., 2006; Rovelet-Lecrux et al., 2006; Sleegers et al., 2006), as patients with Down syndrome show increased levels of Aβ42 and develop dementia in their fifties. While the physiological roles of the PS are not clear (Borchelt et al., 1996; Thinakaran & Parent, 2004), their effects on APP metabolism are now well documented. The brains of individuals with *PSEN* mutations have particularly abundant deposits of Aβ42 (Cruts et al., 1996; Gómez-Isla et al., 1997; Lemere et al., 1996). Moreover, transgenic animals overexpressing mutant, but not wild type, *PSEN1* produce more Aβ42 (Borchelt et al., 1996; Scheuner et al., 1996) and cells transfected with mutant *PSEN* produce more Aβ42 (Borchelt et al., 1996).

Furthermore, several studies show that Aβ accumulations can cause toxicity in neurons leading to cognitive deficit in mouse models with *APP* or *PSEN* mutations. Loss of synaptic terminals and LTP deficits have been demonstrated in studies of transgenic mice overexpressing mutant *APP* (Chapman et al., 1999; Spires et al., 2005). Aβ peptides are

also capable of reducing metal ions leading to the production of hydrogen peroxide (H_2O_2). This in turn mediated an elevation of oxidative stress, one of the early pathological events of AD (Atwood et al., 2003; Behl, Davis, Lesley, & Schubert, 1994; Hensley et al., 1994; Huang et al., 1999).

The amyloid cascade hypothesis postulates that tau is an effector of A β toxicity (Götz et al., 2001; Lewis et al., 2001). In mice, A β seems to worsen tau pathology in animals expressing P301L mutation, a tau mutant that leads to NFTs formation. Reduction of endogenous tau protein levels in transgenic animals expressing APP with fAD mutations prevented A β -induced toxicity in those animals (Rapoport et al., 2002; Roberson et al., 2007). In vitro neurons expressing human tau showed an exacerbation of A β -induced toxicity. Further, deletion of endogenous tau in neurons damped A β -induced toxicity in those neurons (Lewis et al., 2001; Rapoport et al., 2002). As demonstrated by several studies, A β aggregation appear to be required for high levels of cortical tau pathology (Knopman et al., 2003; Price & Morris, 1999). Altogether, these observations support the concept that A β plaques have a unique and critical role as the initiating agent of AD pathology with downstream effects being tau pathologies, neuronal loss and cognitive dysfunction.

However, amyloid plaques correlate poorly with neuronal cell death and clinical symptoms both temporally and anatomically in sporadic AD (Gómez-Isla et al., 1997; Terry et al., 1991; Dickson et al., 1995; Giannakopoulos et al., 2003; Bennett et al., 2004). The brain regions that develop plaque depositions first and more severely do not coincide with regions where neuronal death is initiated and is more prominent.

For instance, cell loss begins in areas like the hippocampus and the entorhinal cortex, which have relatively low amounts of Aβ plaques compared to areas such as the frontal lobes (Braak & Braak, 1991; Serrano-pozo et al., 2011). It became evident that tau correlates more tightly with neuronal loss than Aβ plaques (Arriagada, Marzloff, & Hyman, 1992; Gómez-Isla et al., 1997; Serrano-pozo et al., 2011). Neuropathological studies have as well documented a level of Aβ plaques deposition in individuals with intact cognitive functions, though these individuals may be in a stage when clinical symptoms are yet to be manifested but disease processes like pathological Aβ changes has already started (Pike et al., 2007), a concept discussed later. Indeed, clinically cognitively normal subjects with amyloid plaque burden display subtle cognitive deficits with detailed neuropsychometric testing and accelerated hippocampal atrophy when compared with plaque-free controls (Chetelat et al., 2012; Donohue et al., 2014). In human AD tauopathy as measures by AT8, an antibody for paired helical filament (PHF) tau phosphorylated at S202, appeared to precede Aβ plaques deposition (Braak et al., 2011; Braak et al., 2013). In mice overexpressing APP with disease-linked mutations, cognitive deficit precedes frank Aβ plaques deposition (Hsia et al., 1999; Mucke et al., 2000), creating a discrepancy that lead some to challenge the amyloid hypothesis. However, these findings may also be supporting an altered amyloid hypothesis in which Aβ "aggregates" other than the plaques are mediators of impairment in AD. In deed, in the past 15 years there has been emerging evidence that soluble forms of Aβ may be the bioactive species in AD. Neuropathological studies have shown that fibrillar

amyloid plaques correlate poorly with cognitive function (Arriagada et al., 1992; Bennett et al., 2004; Giannakopoulos et al., 2003; Terry et al., 1991). Rather, soluble Aβ, not plaque levels, was found to correlate better with synaptic loss in transgenic APP mice and in brains of patients with AD (Lue et al., 1999; L Mucke et al., 2000). The role of soluble Aβ as in mediating synaptic dysfunction and cognitive impairment will be discussed further in the next section.

Challenge to the amyloid cascade hypothesis also includes the fact that transgenic animal models overexpressing APP developed Aβ pathology and cognitive dysfunction but do not recapitulate all the features of full-blown AD. Transgenic animal models of AD do not display tau NFTs and the majority of them lack overt neuronal loss at the degree found in AD ("Games et al., 1995; Masliah et al., 1996; Hsiao et al., 1996; Irizarry et al., 1997; Sturchler-Pierrat et al., 1997). A potential explanation for the lack of NFTs in Aβ AD mouse models, that would still support the amyloid cascade hypothesis, is that there may be species difference in the tau protein between humans and mice. There are six isoforms of adult human tau emanating from the alternative splicing of a single tau gene (Goedert et al. 1989a, 1989b; Kosik 1989). Each one of these isoforms either contain 3 (3R) or 4 (4R) domains with the inclusion or exclusion of a repeat region coded by exon 10 of the tau gene (Hutton et al. 1998; Spillantini et al. 1998; Poorkaj et al. 2001). On the other hand mouse tau isoforms only contain 4R as opposed to similar levels of 3R and 4R tau isoforms in human. Additionally, there are 14 amino acids difference in the N-terminus of the tau protein sequence between mouse anad human tau. All these differences may be the reason for the lack of NFTs in *APP* mouse models of AD. Indeed,

it has been documented that deletion of endogenous mouse tau in animals expressing wild-type human tau leads to the formation of NFTs in those animals (Andorfer et al., 2003). Additionally it was proposed that species difference in inflammatory responses (Schwab et al., 2004) or brain aging (Loerch et al., 2008) may be cause for the "shortcomings" of amyloid-β models of AD. Altogether, these studies rather support the idea that APP models may be representing an earlier stage of AD where Aβ pathology is accompanied with synaptic deficit and cognitive dysfunction without overt neuronal loss in the some of the amyloid models (Ashe & Zahs, 2010), although the loss of monoaminergic neurons has been reported in brains of APP/PS1 mouse model of AD but still no NFTs (Liu et al., 2008).

III. Amyloid beta oligomers

Sequential cleavage of the transmembrane glycoprotein APP by the otein glγ-secretase enzymes that generates Ae can lead to the formation of low-molecular weight (low-*n*) aggregates such as dimers and trimers to large aggregates such as proto-fibrils (Haass & Selkoe, 2007). The proto-fibrils are intermediate assemblies that lead to fibrillization, directing Aβ plaque deposition (Harper et al., 1997; Walsh et al., 1997). On the other hand, we have soluble aggregates of Aβ ranging from low-*n* oligomers (e.g.dimers and trimers) to mid-range-molecular weight oligomers (e.g. Aβ*56) to large aggregates, some of which do not seem to contribute to the formation of plaques (Larson & Lesné, 2012). These deposits are referred to as soluble amyloid-β oligomers (Aβo) with several of them identified and studied in animal models of AD (Cheng et al., 2007;

Gandy et al., 2010; Lesné et al., 2006; Reed et al., 2011; Shankar et al., 2008). A β oligomers have been described to promote neurotoxicity, synaptic and network dysfunction (Mucke & Selkoe, 2012; Palop et al., 2007; Palop, Chin, & Mucke, 2006; Shankar et al., 2008). Amyloid- β dimers, trimers and A β and, a 56 kDa A β oligomer, have been identified in brain lysates of patients with AD and from transgenic animal models of AD. Cognitive testing assayed these three oligomers to establish their effects on neuronal function and cognition (Cleary et al., 2005; Lesne et al., 2006; Shankar et al., 2008).

Sodium dodecyl sulfate (SDS)-stable A β oligomers with an apparent molecular weight of 8 and 12 kDa (putative dimers and trimers) were identified in both soluble and insoluble fractions of AD brain tissue (McLean et al., 1999). Several other studies later found an elevation of A β dimers in AD brains and in transgenic mouse models expressing AD linked mutations (Kawarabayashi et al., 2004; Shankar et al., 2008). A β dimers have deleterious effects on neuronal function and cognition. Healthy rodents injected with A β dimers showed impaired brain functions (Reed et al., 2011; Shankar et al., 2008). Dimers derived from human brain tissue or cell lines have been shown to induce synaptic loss, impair long-term potentiation and disrupt memory (Cleary et al., 2005; Klyubin et al., 2008; Shankar et al., 2007, 2008; Walsh et al., 2002). It was further demonstrated that blockade of LTP was induced by Low-n oligomers (including dimers) and not monomers or large aggregates (Walsh et al., 2005). Natural, cell-derived Aβ oligomers inhibited hippocampal LTP when small volumes were microinjected into

the lateral ventricle of the brains of wild-type rats (Walsh et al. 2002). In addition, dimers derived from human AD brains have been shown to induce tau phosphorylation and cytoskeletal abnormalities in cultured hippocampal neurons (Jin et al., 2011).

Amyloid-β trimers are the earliest endogenous oligomeric Aβ species produced and secreted by neurons (Lesne et al., 2013). Trimers are present in brain tissue of transgenic mouse models such as the Tg2576 mouse as early as embryonic day 14 and its expression persists throughout life (Lesné et al., 2006). Similarly, in human Aβ trimers brain levels were detectable as early as one year of age (Lesné et al., 2013). In addition to the fact that trimers are the most abundant species of Aβ produced and secreted by primary neurons *in vitro* (Larson et al., 2012; Lesné et al., 2006), the formation of trimers *in vivo* appears to be dependent on the levels of Aβ production (Ma et al., 2007). These findings seem to support the hypothesis that Aβ trimers may be the building blocks for non-fibrilar assemblies of Aβ. The deleterious effects of Aβ trimers appear to be a conflicting topic. Aβ trimers are found in the Tg2576 transgenic mouse model prior to cognitive decline and do not seem to cause deficit when injected into healthy rodents (Lesné et al., 2006; Reed et al., 2011). However, there is one study that claims disruption of synaptic plasticity on hippocampal slices caused by application of trimers (Townsend et al., 2006). In 2012 pathological tau changes was described in association with the application of Aβ trimers *in vitro* (Larson et al., 2012). Additionally, in a transgenic rat model of Alzheimer's disease Aβ trimers were found to be the only oligomeric Aβ species present at 3 months of age, when a cognitive deficit was detected (Leon et al., 2010).

Another soluble Aβ species called Aβ*56 was first identified in an APP mouse model of AD overexpressing human *APP* with the Swedish mutation, Tg2576 (Lesné et al., 2006). Aβ*56 is a putative dodecamer detected with SDS-PAGE western blotting at 56 kilodaltons (kDa) that impairs memory in the absence of Aβ plaque depositions and frank neuronal loss (Lesné et al., 2006). The oligomer was since identified in other mouse models of AD, notably J20, Arc48 and 3xTgAD with cognitive impairment (Cheng et al., 2007; Oddo et al., 2006). In the Tg2576 mouse model that overexpresses human APP with a familial AD-linked mutation, the onset of a subtle cognitive decline at 6 months of age coincides with the detection of Aβ*56 in forebrain tissues. Further, when the purified soluble Aβ assembly was acutely injected in young healthy rats, it induced a transient memory impairment as assessed by Morris Water Maze (MWM) and Alternating Lever Cyclic Ratio (ALCR) assay (Lesné et al., 2006; Reed et al., 2011).

In humans, these different amyloid-β oligomers appear to have different temporal patterns with distinct but overlapping levels in different clinical groups of AD. Aβ dimers, trimers and Aβ*56 are found in brains of cognitively intact individuals and increases with age (Lesné et al., 2013). However, Lesne et al (2013) showed that dimers are elevated in subjects with probable AD compared to cognitively intact subjects. Amyloid-β trimers on the other hand sharply increased in the mild cognitively impaired (MCI) individuals and drops in subjects with probable AD (Larson and Lesne 2012; Lesne et al., 2013). Finally, Aβ*56 was elevated in subject without cognitive

impairment and dropped in subjects with MCI or probable AD (Lesne et al., 2013). Interestingly, A β *56 appears to correlate more strongly with tau-Alz50, a pathological conformer of tau, and tau phosphorylated at S202 (CP13), a phosphorylation site found in the early stage of AD, than either dimers or trimers (Lesne et al., 2013). The same study also showed an inverse correlation with synaptic proteins such as debrin and fyn. All of these changes (increased pathological soluble tau or decreased synaptic proteins) lead to neuronal dysfunction and cognitive impairment. Therefore, a correlation with these two entities can possibly suggest that A β *56 may be underlying the subtle cognitive deficits observed in people at risk for AD (Amieva et al., 2008; Bateman et al., 2012; Jack et al., 2010; Sperling et al., 2011). Supporting that hypothesis is the fact that A β *56 started to increase in subjects in their 40s when also age-associated memory impairment such as subtle deficits in declarative memory is first noticeable (Youngjohn & Crook, 1993). Together, with the fact that age is the greatest single risk factor in AD, all these findings seem to suggest that A β *56 may be important in the preclinical asymptomatic phase of AD, as A β *56 appeared to participate in the amyloid cascade before the onset of clinical symptoms.

IV. Mediators of Amyloid- β toxicity

Two decades ago, several lines of evidence pointed to strong associations between the degrees of cognitive impairment and synaptic alteration in AD subjects (DeKosky & Scheff, 1990; Terry et al., 1991). Further, numerous other studies support the hypothesis that A β , particularly soluble A β oligomers, cause cognitive deficits in part by

interfering with synaptic functions (Walsh et al., 2002; Cissé et al., 2011; McLaurin et al., 2006; McLaurin et al. 2006; Cisse et al. 2011a; Roberson et al. 2011, Larson et al 2012). Synthetic Aβ oligomers and soluble Aβ oligomers isolated from cell culture media or brain of subject with AD caused acute synaptic deficits when added to hippocampal slices or slice cultures (Gong et al., 2003; Shankar et al., 2007, 2008). Aβ has been proposed to induce synaptic dysfunction by interacting functionally and/or structurally with receptors at the synaptic membrane. These proposed receptors include α7-nicotinic acetylcholine receptors (α7-nACh), N-methyl-D-aspartate (NMDA) and α-amino-3-hydroxy-5-methyl-4-isoxazolepropionic acid (AMPA) receptors, insulin receptors, the receptor for advanced glycation end-products (RAGE), the cellular prion protein (PrP^C), and the Ephrin-type B2 receptor (EphB2) (Cissé et al., 2011; Gimbel et al., 2010; Koffie et al., 2009; Lacor et al., 2004, 2007; M. Larson et al., 2012; Laurén et al., 2009; Simakova & Arispe, 2007; Yan et al., 1999).

A. RAGE in amyloid-β-induced toxicity

The first membrane receptor identified to possibly be interacting with Aβ oligomers is RAGE. RAGE is a 35 kDa transmembrane receptor of the immunoglobulin super family. The receptor was originally proposed to interact with Aβ (Yan et al., 1996) and regulate Aβ accumulation in the brain (Deane et al., 2003). Consistent with this finding, deletion of RAGE was reported to rescue Aβ-induced LTP inhibition (Origlia et al., 2008). In addition, in a transgenic animal model of AD harboring the Swedish and the Indiana mutation on *APP* (J20), overexpression of RAGE enhanced cognitive deficit typically associated with this model (Arancio et al., 2004). However, the concentration (10 μM)

used to initially demonstrate the interaction of RAGE with A β oligomers largely exceeded the physiological concentrations of A β peptides in human brain, interstitial fluid and cerebrospinal fluid proposed to be in the low nM range (Shankar et al., 2008; Dominic M Walsh et al., 2002). Accordingly, these supraphysiological conditions at which A β readily aggregates into fibrils raise the possibility of a non-specific interaction between A β and RAGE. Finally, gene ablation of RAGE in another transgenic mouse model did not rescue cognitive impairment (Vodopivec et al., 2009) making this topic somewhat controversial. To date, a direct interaction of RAGE with A β has not been shown. More evidence is therefore needed to support or refute the interaction of RAGE with A β oligomers.

B. The prion protein and EphB2 as mediators of amyloid- β-induced toxicity

Two other membrane receptors (PrP^C and EpB2 receptors) have been proposed to mediate the effects of A β have bed synaptic dysfunction. The prion protein hypothesis however, has been highly controversial (Barry et al., 2011; Calella et al., 2010; Freir et al., 2011; Kessels et al., 2010; Laurén et al., 2009). In the past few years, several studies have argued for A β ddependent toxicity to be mediated by PrP^c, the cellular prion protein (Barry et al., 2011; Gimbel et al., 2010; Laurén et al., 2009). PrP^c has been shown to act as a receptor for synthetic forms of A β oligomers leading to the inhibition of long-term potentiation (Laurén et al., 2009). This same study reported that deletion of the *PRNP* gene encoding for PrP^c lead to decreased binding of A β o to the surface of the cells. Supporting these findings, antibodies targeting the 94–104 domain of PrP^C blocked the

inhibition of LTP triggered by soluble extracts of AD brain (Barry et al., 2011; Freir et al., 2011). More recently, several independent studies have reported that soluble A β eported thPrP^{c} at neuronal dendritic spines where it forms a complex with and leads to activation of the Src kinase Fyn (Larson et al., 2012; Um et al., 2012, 2013). Further, PrP^{C}-interacting oligomers were tightly correlated with cognitive deficit in transgenic models of AD (Kostylev et al., 2015). By contrast, numerous other groups have failed to demonstrate that A β -induced LTP inhibition/cognitive impairment is dependent on PrP^{C} (Balducci et al., 2010; Calella et al., 2010; Kessels et al., 2010) leading to an intense debate in the field in relationship to the role of PrP^{C} in AD. This discrepancy can be partly explained by the fact that the Aβ used in these studies were highly heterogeneous and abundance was highly diverse (Calella et al., 2010; Kessels et al., 2010; Cissé et al., 2011b; Lesne 2013). For instance, in Kessels et al. it was unclear whether Aβ oligomers were present in carboxyl terminal domain of the amyloid precursor protein (APPct100)-expressing slices. In other studies the transgenic animals used might have been too young (Calella et al., 2010; Lesne 2013), to lead to the changes observed previously in Lauren et al 2009.

The Ephrin B2 (EphB2) has also been proposed as a receptor for endogenous Aβ oligomers (Cissé et al., 2011a). Aβ dimers and trimers seem to be in some sort of a complex with the EphB2 receptor as they co-immunoprecipitate with the receptor (Cisse et al. 2011a). Amyloid Beta-Derived Diffusible Ligands (ADDLs) application to mature hippocampal neurons lowered EphB2 expression by 60% (Lacor et al., 2007). In addition, EphB2 expression was found decreased in human AD hippocampal extracts (Simon et al.

2009). Further, binding of A β oligomers to some putative receptors, for example, EphB2, triggers proteosomal degradation of the receptor, as treatment of cells with the proteasome inhibitor lactacystin blocked Aβ-induced depletion of EphB2 (Cissé et al., 2011a).

C. Involvement of the NMDA and AMPA receptors in amyloid- β -induced toxicity

Glutamate is the principal excitatory neurotransmitter in the vertebrate nervous system (Meldrum, 2000). It acts postsynaptically on glutamate receptors classified into ionotropic (NMDA, AMPA and Kainate) and metabotropic (mGluRs) receptors depending on the mechanism by which their activation gives rise to a postsynaptic current (Palmada & Centelles, 1998). Ionotropic glutamate receptors are ligand-gated cation channels, that opens in response to glutamate binding. The NMDA receptor is particular in this category because in addition to glutamate, activation requires binding of one of the coagonists Glycine or D-serine mostly depending on the brain region (Johnson & Ascher, 1987; Matsui et al., 1995). Another distinct feature of the NMDA receptor is the voltage sensitive block by Mg^{2+} lifted by depolarization during activation (Mayer et al., 1984). The NMDAR is a heterodimer of glycine-binding GluN1, glutamate-binding GluN2 and glycine-binding GluN3 subunits, meaning that two copies each of the GluN1and GluN2 and/or GluN3 subunits are required (Benveniste & Mayer, 1991; Clements & Westbrook, 1991). Opening of the NMDAR allows Ca^{2+} ion through the ion channel initiating signal transduction cascades that in turn modulate synaptic strength (Bliss & Collingridge, 1993).

Two type of NMDAR pools have been described: synaptic and extrasynaptic

NMDAR types (Cottrell et al., 2000; Petralia et al., 2010). These two types of receptors are different in the pathways they activate and how they activate them (Hardingham & Bading, 2010). For instance, the synaptic NMDARs activation leads to activation of pro-survival signaling pathways such as activation of the extracellular signal-regulates kinases 1/2 (ERK1/2) and cAMP response element-binding protein (CREB), whereas activation of extrasynaptic NMDARs leads to inhibition of pro-survival agents or activation of pro-apoptotic signaling such as the Forkhead box protein O 1 (FOXO1) and the mitogene-activated protein kinases (p38) that lead to excititoxicity (Hardingham & Bading, 2010).

Glutamate receptors are good candidates for mediating Aβ-induced synaptic toxicity as oligomeric Aβs have been demonstrated to alter glutamatergic synaptic transmission thereby, causing synapse loss (Hsia et al., 1999; Mucke et al., 2000; Shankar et al., 2007; Walsh et al., 2002). NMDA and AMPA receptors, ionotropic glutamate receptors, play a pivotal role in long-term potentiation (LTP), a cellular process believed to underlie learning and memory. Induction of LTP promotes synaptic plasticity, however long-term depression (LTD) induction promotes synaptic loss (Kullmann and Lamsa 2007). A β oligomers have been suggested to indirectly block NMDA receptors partially by shifting NMDAR-dependent signaling cascades toward pathways involved in the induction of LTD and synaptic loss (Hsieh et al., 2006; Kim et al., 2001; Li et al., 2009; Shankar et al., 2007). This blockade of the NMDAR and induction of LTP may be due to desensitization (L. Liu et al., 2004) or internalization of the receptor at the synapse (Hsieh et al., 2006; Snyder et al., 2005), though the exact mechanisms explaining these changes are still unclear.

In addition to the synaptic NMDAR, A β -induced deleterious effect may be mediated by extrasynaptic NMDARs (S. Li et al., 2009; Shankar et al., 2007) with multiple potential down-stream effectors. A β o appear to block neuronal glutamate uptake at synapses, leading to a rise in glutamate levels in the synaptic cleft (Li et al., 2009), resulting in desensitization of the synaptic NMDARs. On the other hand, the increased glutamate levels can lead to spillover and activation of extra- or peri-synaptic NMDARs, which play a major role in LTD induction (L. Liu et al., 2004). Diverse lines of evidence suggest that extracellular oligomers can bind to pre- and postsynaptic elements on cultured neurons and in the AD cortex. Further, studies have shown A β co-localized with NMDARs at synapses (Dewachter et al., 2009; Lacor et al., 2007). Finally, memantine-HCl (Namenda®) an uncompetitive NMDA receptor antagonist has been demonstrated to improve measures of cognition, activities of daily living, global outcome, and behavior in patients of moderate to severe AD (Tariot et al., 2004). However, a directed interaction between the NMDARs and any of the A β oligomers is yet to be established.

V. Kinases, tau phosphorylation and Alzheimer's disease

Tau aggregates as paired helical filaments (PHFs) that constitute neurofibrillary tangles (NFTs) in AD and other tauopathies. Intracellular NFTs deposition is preceded by hyperphosphorylation and conformational changes of tau (Grundke-Iqbal et al., 1986; Iqbal et al., 1994). Tau protein is a microtubule-associated protein that is important for neuronal cytoskeleton stabilization (Harada et al., 1994; Chen et al., 1992; Hirokawa et al., 1988). The region responsible for tau binding to microtubules contains four repeat domains R1, R2, R3 and R4 also called microtubule-binding domains (MBD). Each

repeat domain contains a conserved consensus motif KXGS, which can be phosphorylated at serine, resulting in the destabilization of the neuronal cytoskeleton (Sengupta et al., 1998; Trinczek, 1995).

In addition to phosphorylation, tau can undergo multiple other post-translational modifications including ubiquitination, acetylation, methylation and O-linked **N**-acetylglucosamine (O-GlcNAc) (Arnold et al., 1996; Cohen et al., 2011; Cook et al., 2013; Cripps et al., 2006; Funk et al., 2014; Guo et al., 2014; Min et al., 2010; Morishima-Kawashima et al., 1993). Ubiquitination of tau has been identified in PHFs isolated from AD brains (Cripps et al., 2006; Morishima-Kawashima et al., 1993). Multiple studies have described methylation of tau at lysine and arginine residues (Funk et al., 2014; Guo et al., 2014). Acetylation has as well been described in AD (Cohen et al., 2011; Cook et al., 2013; Min et al., 2010). Recently a study published at nature neuroscience also describes acetylation, methylation and ubiquitination lysine residues in endogenous mouse tau (M. Morris et al., 2015). Yet tau phosphorylation is still the most widely studied post-translation modification of tau. Tau can be phosphorylated at numerous sites, 44 of which are found in AD, 28 of those are exclusively found in AD (Martin et al., 2013). Phosphorylation of tau at some of these sites has been demonstrated to induce tau conformational changes and to attenuate tau binding to microtubules (Gendron & Petrucelli, 2009).

Tau can be phosphorylated by multiple different kinases. Tau protein kinases belonging to the proline-directed protein kinases (PDPK), protein kinases non-PDPK and tyrosine protein kinases (TPK) are responsible for phosphorylation of tau. The most studied tau protein kinases linked to AD include but are not limited to Glycogen synthase kinase-3

(GSK3), cyclin-dependent protein kinase-5 (CDK5) and mitogen-activated protein kinases (MAPK), extracellular signal-regulated kinases 1 and 2 (Erk1/2), microtubule affinity-regulating kinases (MARK), protein kinase A (PKA), protein kinase B (PKB/Akt), protein kinase C (PKC), Fyn and Ca^{2+}/calmodulin dependent protein Kinase II (CaMKII) (Martin et al., 2013).

A. GSK3, tau phosphorylation

GSK3 has two main isoforms GSK3 α and GSK3 β. Phosphorylation at serine 21 (for GSK3 α isoform), at serine residues 9 and 389 (for GSK3 β isoform) inhibits GSK3 activity whereas phosphorylation at tyrosine 279 (for GSK3 α isoform) and at tyrosine 216 (for GSK3 β isoform) increases GSK3 activity (Bhat et al., 2000; Cole, Frame, & Cohen, 2004; Stambolic & Woodgett, 1994; Thornton et al., 2008; Wang et al., 1994). GSK3 can efficiently phosphorylate substrates following "priming" that is when substrates were previously phosphorylated at a site four amino acids upstream of the phosphorylation site targeted by GSK3 (Dajani et al., 2001), making tau a better substrate for GSK3. The structure of GSK3 is devoid of activation segment phosphorylation and is proposed to be using a mechanism of catalytic activation coupled to binding of phosphorylated substrates (Dajani et al., 2001). Twenty-nine of the 42 sites of tau phosphorylated by GSK3 are found in brains of AD patients (Hanger, Seereeram, & Noble, 2009; Sergeant et al., 2008) suggesting a link between AD and GSK3 induced tau hyperphosphorylation. These sites include phosphorylation at S396 and S404, that have been identified to be involved in the formation of PHF (Augustinack et al., 2002; Greenberg et al., 1992) and S202 and Thr205 (AT8). GSK3 β has been proposed to link A β to tau pathology. First, overexpression of GSK3 β in transgenic mice induces tau

hyperphosphorylation leading to neurodegeneration (Lucas et al., 2001). A β peptide increases GSK3 β activity, tau phosphorylation and apoptotic neuronal death *in vitro* (Yamaguchi et al., 1996; Zheng, Bastianetto, Mennicken, Ma, & Kar, 2002). It appears that GSK3-induced hippocampal degeneration and learning impairment are mediated by tau proteins, as knocking the *tau* gene in mice rescued GSK3-induced hippocampal degeneration and learning deficits (Gómez de Barreda et al., 2010). Moreover, GSK3 β phosphorylated at tyrosine 216 (active form) is elevated in the frontal cortex of AD brains (Leroy et al., 2007). Finally, in AD patients, GSK3 β co-localizes with NFTs (Pei et al., 1997; Yamaguchi et al., 1996).

B. CDK5, tau phosphorylation

Cdk5 is activated when co-activators p35/p39 or p25/p29 interact with the kinase. P35 can undergo proteolytic cleavage by the calcium-dependent calpains to generate p25 and p29. Binding of Cdk5 to p35/p39 is enough to activate Cdk5. However, the kinase is hyper-activated when Cdk5 binds to the more stable cleavage proteins p25/p29 (M. S. Lee et al., 2000; Martin et al., 2013; Patzke & Tsai, 2002). Cdk5 is exclusively activated in neurons due the distribution pattern of its activators p35 and p39 (Guidato et al., 1998; Miyajima et al., 1995) and is involved in the regulation of neuronal cytoskeleton dynamic (Hallows et al., 2003; Smith, 2003) , and synaptic functions (Samuels et al., 2007).

Cdk5 is able to phosphorylate tau at 11 sites, each of which is found in AD. Hyperactivation of Cdk5 in the presence of a mutant form of tau P301L has been demonstrated to induce tau hyperphosphorylation and NFTs formation (Cruz, Tseng,

Goldman, Shih, & Tsai, 2003; Noble et al., 2003). Additionally, long-term activation of Cdk5 in mice (during 27 weeks) results in the NFT formation in the cortex and hippocampus (Cruz et al., 2003). Consistent with these findings, p35 overexpression potentiates A β -induced apoptosis in neuronal cultures while Cdk5 inhibition reduces A β peptide-induced toxicity (Alvarez, Toro, Cáceres, & Maccioni, 1999; Chang et al., 2010; Lopes, Oliveira, & Agostinho, 2010). Moreover, in AD brains, the p25/p35 ratio and the level of the hyperactive complex CDK5/p25 are increased (Camins et al., 2006). Finally tau becomes a better substrate for GSK3 β after its phosphorylation by Cdk5, probably by activating tau priming for GSK3 tau phosphorylation (Sengupta et al., 1997).

C. CaMKII, tau phosphorylation

The calcium calmodulin dependent protein kinase II (CaMKII) is a Ca^{2+}-activated enzyme that is highly abundant in the brain, where it constitutes 1–2% of the total protein. Four genes (α, β, γ, and δ) encode the numerous different isoforms of CaMKII. α and β-subunits are the predominant isoforms in the brain. The enzyme may contain one or both subunits that form dodecameric holoenzymes. Each isoform of these subunits consists of a catalytic domain, an autoinhibitory domain, a variable segment and a self-association domain.

Entry of calcium into the cytosol leads to the coupling of Ca^{2+} with calmodulin (CaM). The Ca^{2+}/CaM complex binds to a region that overlaps with the pseudosubstrate region within the autoinhibitory domain, which normally inhibits the catalytic domain of enzyme. This process activates the subunit and exposes Thr286/287 site on the

autoinhibitory domain for the α and β-subunits respectively. Consequently, exposure of Thr286/287 triggers the phosphorylation of the site by a neighboring subunit (Rich & Schulman, 1998), that renders the holoenzyme autonomous and independent of calcium levels at that point (Lou, Lloyd, & Schulman, 1986; S. Miller, 1986; Saitoh & Schwartz, 1985; Yang & Schulman, 1999).

Following activation, CaMKII can phosphorylate several substrates one of which is the microtubule associated protein tau. CaMKII can phosphorylate tau at serines 131, 214, 262, 356, 416 and threonines 135, 212, though not the sole kinase for these sites, and 5 of these sites are found phosphorylated in AD brains (Litersky et al., 1996; Singh et al., 1996; Yamamoto et al., 2005; Yoshimura, 2003).

Several studies have shown that CaMKII is both necessary and sufficient to induce LTP. Numerous CaMKII inhibitors have been derived from the autoinhibitory domain of the holoenzyme to investigate a role of CaMKII in long-term potentiation (LTP) induction. CaMKII inhibitors such as KN62 and KN93, block the Ca^{2+}-dependent activity of the enzyme by interfering with calmodulin binding (Davies et al., 2000; Sumi et al., 1991; Terasawa et al., 1990), and prevent LTP induction (Otmakhov et al., 1997). However, KN92 and KN93 can also inhibit other members of the CaMK family including CaMKI and CaMKIV (Ichinose et al., 2011; Sato et al., 2006). In addition, these compounds act as open channel blocker of voltage-gated potassium channels, independently of CaMK inhibition, further complicating their experimental use. Therefore, genetic methods, in addition to the pharmacological paradigm, were employed to demonstrate that CaMKII is indeed involved in the induction of LTP. Partially knocking out α-CaMKII (45%) reduced the magnitude of LTP in these animals (Hinds et al., 1998; Silva et al., 1992;

Stevens et al., 1994). Moreover, a CaMKIIα mutation that replaced Thr286 by alanine more completely abolished LTP (Giese et al., 1998). Finally, postsynaptic application of CaMKII enhances the response to applied glutamate (Davies et al., 1989; Montgomery et al., 2001), a process known to be prompted by LTP. Further, synapses that are potentiated by CaMKII cannot undergo LTP and conversely, synapses that have undergone LTP are virtually insensitive to CaMKII (Lledo et al., 1995; Pettit et al., 1994). This involvement of CaMKII in LTP induction might explain how CaMKII-mediated tau phosphorylation can lead to synaptic dysfunction.

VI. Summary

Alzheimer's disease is a progressive neurodegenerative disorder that is characterized by severe neuronal loss in the brain, with shrinkage of the total volume of the brain, enlargement of ventricle and degeneration of important brain regions like the hippocampal formation. Microscopically, AD is characterized by two legions: extracellular amyloid plaques and intracellular NFTs. Amyloid plaques are mainly composed of the Aβ peptide that can form insoluble aggregates for plaque depositions or soluble aggregates that may not always participate to plaque formation. The soluble Aβ assemblies are also referred to as soluble Aβ oligomers (Aβo). Multiple mutations on the amyloid precursor protein gene (APP) or the presenilin 1 and 2 gene (PSEN1/2) have been demonstrated to cause the early onset familial form of AD. However, the vast majority of AD cases are sporadic (over 95%) meaning there is no known single cause for the disease. The amyloid cascade hypothesis postulates that Aβ is the initiator agent in AD and that other pathological changes such as neuronal cell death and cognitive

deficits are downstream consequences of A β accumulation. However, because amyloid plaques do not strongly correlate with symptoms and because cognitive impairment and synaptic dysfunction precede plaque deposition in transgenic animals with the familial AD mutations, the hypothesis has been altered to now advance soluble Aβ oligomers as bioactive species in AD (Lue et al., 1999; Mucke et al., 2000). Several studies have demonstrated the presence of A β o in AD and animal models of the disease. These different oligomers, mainly dimers, trimers and A β *56, have been demonstrated to have deleterious effects. They can cause neuronal dysfunction and cognitive deficits at what seems to be different stages of AD (Larson and lesne 2012; Lesne et al., 2013).

Multiple surface receptors at the membrane have been proposed to be mediating A β -induced toxicity. The suggested receptors for mediating A β actions include the receptor for advanced glycation end-products (RAGE), glutamate receptors (AMPA, NMDA), the cellular prion protein (PrP^c), Ephrin B2 receptor (EphB2).

Several Intracellular kinases are involved in the disease process. Kinases such as GSK3, Cdk5, Fyn and CaMKII are modulated in AD brains and have been demonstrated to phosphorylate tau. The amyloid cascade hypothesis partly postulates that tau is an effector of A β -induce toxicity. The above-cited kinases can phosphorylate tau at multiple different sites that are found in AD. Phosphorylation of tau by these different kinases can lead to the hyperphosphorylation, conformation changes of tau and subsequent neuronal dysfunction and cognitive impairment. Cumulatively, the evidence so far suggest a crucial role of multiple A β oligomers in disease progression and the involvement of multiple receptors and kinases that lead to the vast pathology of the

disease. However, which of these oligomers is associated with which signaling cascade change is still mostly unknown. This is to the exception of dimers that have been associated with PrP, fyn to tau.

Chapter 2

A β *56-induced selective alteration of neuronal signaling in a mouse model of alzheimer's disease (Tg2576)

I. Introduction

The classical view in Alzheimer's disease (AD) is that extracellular amyloid-β (Aβ) plaques induce a signaling cascade that leads to pathological changes in the microtubule-associated protein tau. These changes in tau will then result in the formation of neurofibrillary tangles (NFTs), causing neuronal dysfunction that leads to cell loss. Neuronal degeneration in turn leads to the symptoms observed in AD. However, according to our current understanding, AD may be initiated by soluble oligomeric forms of Aβ inducing pathological changes in tau (Jin et al., 2011; Larson & Lesné, 2012; Mairet-Coello et al., 2013; Roberson et al., 2007), which in turn leads to the dysfunction and degeneration of the neuronal elements underlying cognition, including neuronal cells and their synapses in the brain (Ittner & Götz, 2011). In the past decade, several groups have documented the effects of various putative endogenous soluble forms of Aβ oligomers (Aβo), most notably Aβ dimers, trimers and Aβ*56, on memory (Cleary et al., 2005; S. Lesné et al., 2006; Reed et al., 2011), or its presumed molecular substrate long-

term potentiation or LTP (Shankar et al., 2008; Townsend et al., 2006; Dominic M Walsh et al., 2002).

The Aβ assembly called Aβ*56 in reference to its apparent molecular weight was originally identified in brain tissue of young amnestic Tg2576 mice used as model of AD (S. Lesné et al., 2006). Similar observations (Cheng et al., 2007; Leinenga & Gotz, 2015; Meilandt et al., 2009; Oddo et al., 2006) from several independent groups validated the existence of this Aβ species in other cognitively impaired transgenic mouse models of AD overexpressing mutant forms of the human amyloid precursor protein APP. In addition, brain infusion of Aβ*56 purified from brain tissue caused transient memory deficits in young healthy rodents, demonstrating the memory impairing capability of this Aβo (S. Lesné et al., 2006). Recent studies further confirmed the presence of Aβ*56 in postmortem human brain tissue and cerebrospinal fluid (Lesné et al., 2013). In these cross-sectional studies, the brain abundance of this Aβo started to rise abnormally in the fifth decade of life preceding increases in Aβ dimers and trimers by two decades and coinciding with the age at which subtle cognitive deficits first appear (Salthouse, 2009). Importantly, this elevation in brain Aβ*56 levels was associated with aberrant changes in the tau protein typically seen in early stages of the symptomatic phase of AD (Lesné et al., 2013). Overall these findings indicate that the Aβ oligomer Aβ*56 might alter memory and neuronal function during the presymptomatic phase of AD. To further understand the role of Aβ*56 in AD, it becomes fundamental to identify the molecular mechanism by which Aβ*56 disrupts tau biology and neuronal physiology.

II. Results

*A. Interaction of A β *56 with the NMDA receptor in Tg2576 and human brain*

Oligomeric A β assemblies have been suggested to alter NMDAR-dependent synaptic plasticity experimentally as they can block hippocampal long-term potentiation (LTP) (Shankar et al., 2007; Townsend et al., 2006; Walsh et al., 2002). Various studies found that NMDA receptors activity can be modulated by the presence of A β (Chen et al., 2002; Um et al., 2012; Zhang et al., 2010). Since A β *56 can impair memory in absence of neuronal loss (Lesné et al., 2006; Reed et al., 2011) and since glutamate receptors are involved in the molecular mechanism underlying learning and memory, we hypothesized that the deleterious effect of A β *56 on cognition could be mediated by alteration of glutamate receptors, in particular the NMDAR.

*A.1 Age-dependent Co-immunoprecipitation of A β *56 with the NMDAR subunits in mouse and human*

We previously reported that Aβ*56 can be detected in Tg2576 (an animal model of AD overexpressing human APP with the Swedish mutation) brain lysates enriched in extracellular proteins starting at 6 months of age (Lesne et al., 2006). Alongside other APP derivatives, this oligomeric Aβ assembly can also be found in PSD (post-synaptic density)-containing lysates (MB fraction) (Larson et al., 2012a; Larson et al., 2012b) (**Fig. 1A**). The presence of Aβ*56 in the MB fraction puts it in a location for possible binding with a putative receptor through which the oligomer can transduce a deleterious

intracellular biological signal. Since Aβ*56 causes memory impairment, we sought to determine whether Aβ*56 could interact with glutamate receptors because of their importance in the molecular substrate of memory. We therefore performed co-immunoprecipitation experiments on membrane extracts using various antibodies against glutamate receptor subunits or other receptors previously described as interacting with synthetic Aβ oligomers: N-Methyl-D-Aspartate receptor (NMDAR) subunits GluN1, GluN2A, GluN2B, α-amino-3-hydroxy-5-methyl-4-isoxazolepropionic acid receptor (AMPAR) subunits GluA1, GluA2, the α7-acetylcholine receptor subunit (α7), the metabotropic glutamate receptor mGluR5 and the receptor tyrosine kinase Ephrin B2 (**Fig. 1B**). The relative amount of Aβ*56 detected varied across immunoprecipitations with different GluN antibodies and reflected their abundance in the forebrain. In addition, no other Aβ species were detected with 6E10 or 4G8 antibodies (data not shown). It is worth noting that, under our experimental conditions, antibodies targeting other receptors did not capture any soluble Aβ species. Using either membrane-associated (MB) or extracellular-enriched (EC) protein fractions known to contain Aβ*56, we confirmed that Aβ*56 co-immunoprecipitated with GluN1 in the MB extracts of 13-month-old Tg2576 mice but not in the extracellular-enriched (EC) protein fractions which do not contain the NMDAR subunit GluN1 (**Fig. 1C**). Consistently, reverse co-immunoprecipitations with either 6E10 or 4G8 (**Fig. 1D**) also showed a co-capture of Aβ*56 with the NMDAR subunit. Similar findings were observed using the A11 antibody raised against non-fibrillar amyloid oligomers (**Fig. 1E**), confirming the oligomeric nature of the Aβ assembly pulled down by GluN1. In addition, the relative abundance of putative Aβ*56:GluN1 complexes increased with aging when comparing transgenic mice at 2, 9

and 24 months of age (**Fig. 1F**). Similar to mouse brain tissue, we found apparent Aβ*56:GluN1 complexes in human brain tissues (**Fig. 2**) from old human subjects (80-90 years of age, n = 6**, Table 1**) without cognitive impairment, while none were detected in brains of young individuals (10-20 years of age, n = 6). Altogether these biochemical experiments suggested the existence of an Aβ*56:NMDAR complex.

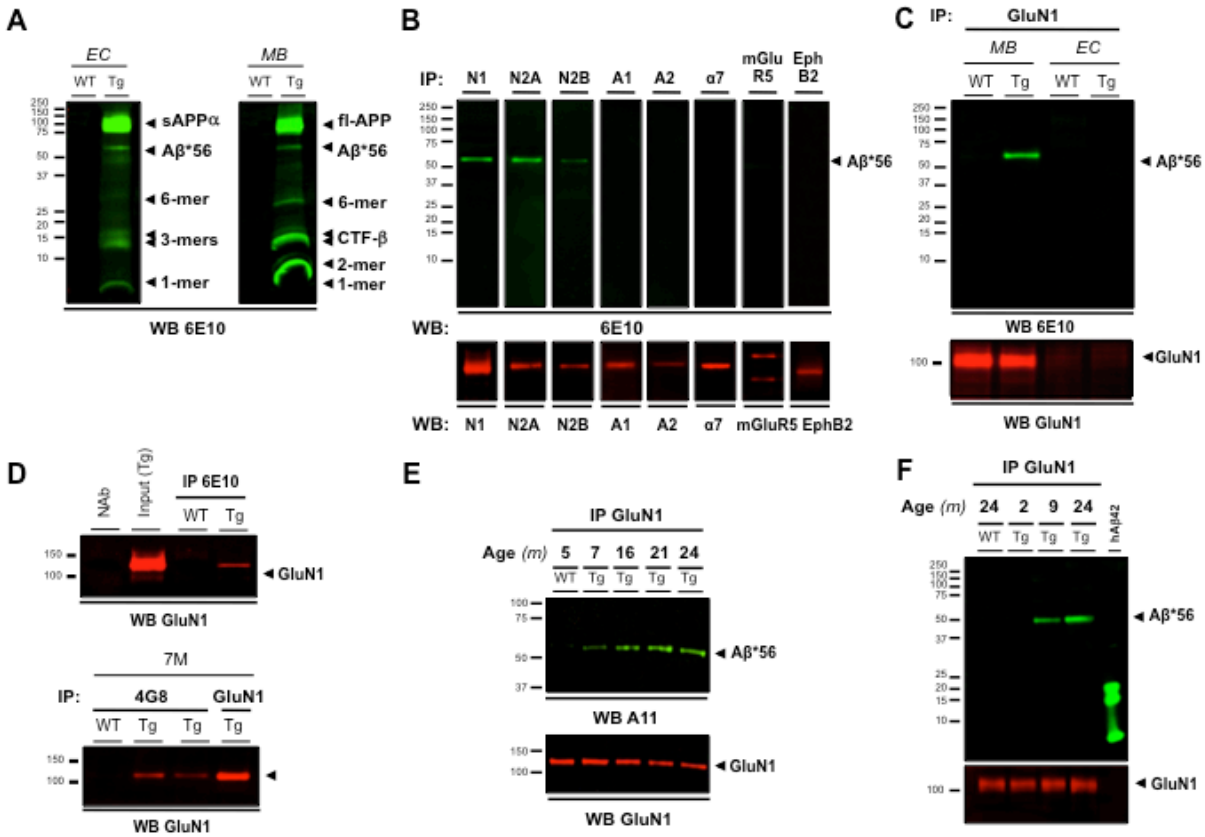

Figure 1. Co-immunoprecipitation of Aβ*56 with the NMDA receptor subunit GluN1 in Tg2576 brain tissue. (**A**) Representative western blot profile of APP and Aβ molecules in Tg2576 mice (Tg) and wild-type (WT) littermates at 13 months of age using 6E10. EC: soluble extracellular-enriched fraction, MB: membrane-associated protein fraction (*n* = 6 animals/genotype). (**B**) Selective co-immunoprecipitation of Aβ*56 with NMDAR subunits GluN1, GluN2A, GluN2B but not AMPA receptor subunits (GluA1, GluA2), α7-nicotinic acetylcholine receptor subunit (α7), the metabotropic glutamate receptor mGluR5 and Ephrin B2 using membrane extracts of Tg2576 mice. Aβ was detected with 6E10 (*n* = 6 animals/genotype/condition). (**C**) Representative 6E10 western blot following immunoprecipitation with GluN1 antibodies from either MB or EC protein extracts from 15-month-old Tg2576 mice (Tg) and wild-type (WT) littermates. EC: soluble extracellular-enriched fraction, MB: membrane-associated protein fraction (*n* = 4

animals/genotype). (**D**) Reverse co-immunoprecipitation of Aβ*56:NMDAR complexes using 6E10 (*B*) or 4G8 (*C*) antibodies as capture antibodies with MB lysates from 7-month-old WT and Tg2576 mice. NAb, no antibody condition (*n* = 3-5 animals/genotype/condition). (**E**) A11 detection of GluN1 pull-downs confirmed the selective age-dependent interaction between the Aβ oligomer Aβ*56 and GluN1 in Tg2576 mice at ages when Aβ*56 is present in brain tissue (*n* = 5 animals/age/genotype). (**F**) Immunoprecipitation of Aβ*56/GluN1 complexes in Tg2576 mice at the indicated ages using 6E10 as detection antibody (*n* = 6 animals/age). Non-denatured synthetic human $A\beta_{1-42}$ (5 ng) was used as internal standard.

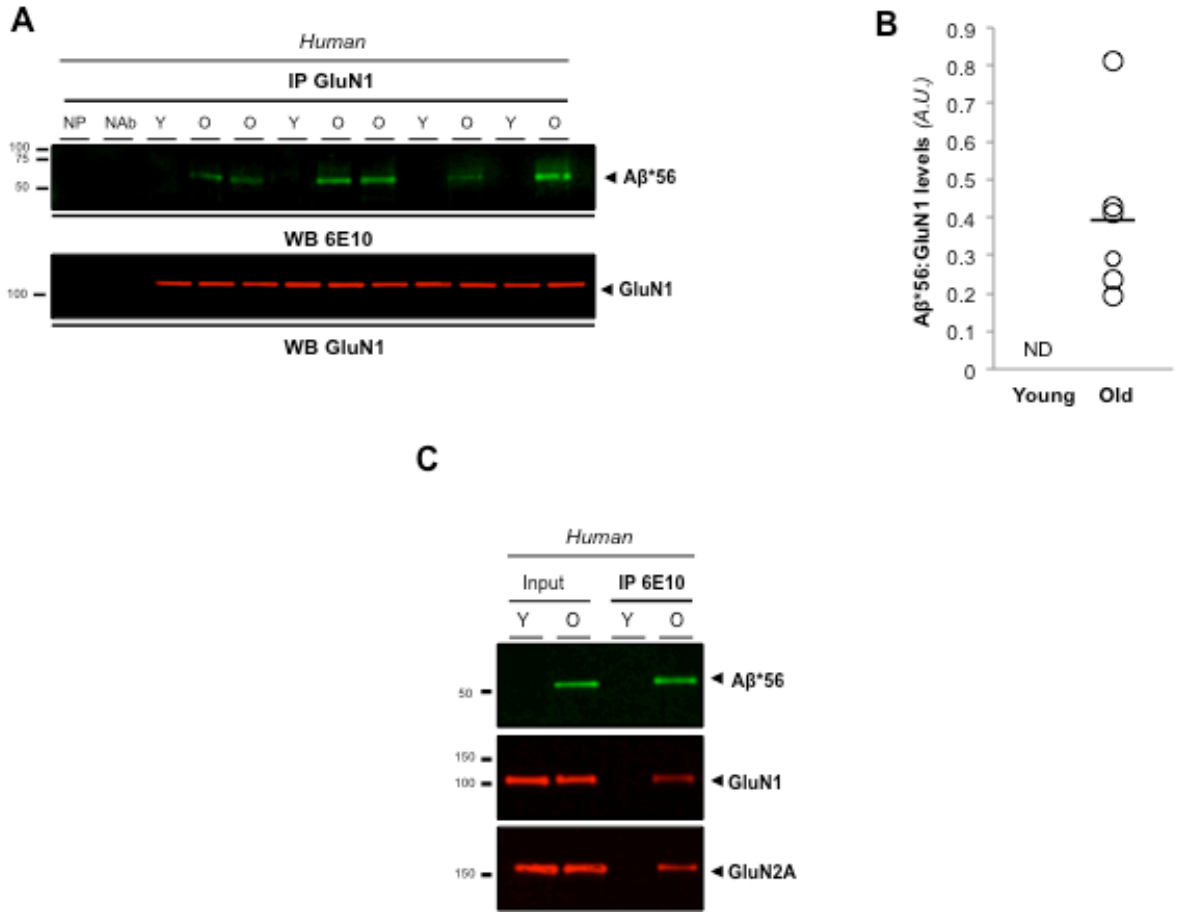

Figure 2. Co-immunoprecipitation of Aβ*56 with the NMDA receptor subunit GluN1 in human brain tissue. (**A**) Aβ*56 immunoprecipitated with GluN1 in brain tissue of aged human subjects with no cognitive impairment (O) but not in brain tissue of younger individuals (Y). 6E10 was used to detect Aβ (*n* = 6/group/experiment). NP: no protein condition; NAb: no antibody condition. (**B**) Aβ*56:GluN1 ratios from the experiment shown in (*a*). Each point corresponds to the mean value measured for three independent experiments and the bold horizontal line indicates the group average. (**C**) Reverse co-immunoprecipitations of Aβ*56:GluN complexes immunoprecipitated with 6E10 and revealed with GluN1 and GluN2A in brain tissue of aged human subject with no cognitive impairment (O) but not in brain tissue of younger individuals (Y). (*n* = 6/group/experiment).

Table 1. Characteristics of the human specimens used.

Group	**Young** (n = 6)	**Old** (n = 6)
Age of death *(years)*, Mean ± SD	16.40 ± 2.41	83.96 ± 2.88
Last MMSE Score, Mean ± SD	N.A.	28.17 ± 1.73
Amyloid Burden *(% of area)*, Mean ± SD	N.A.	1.49 ± 0.94
Tangle density *(#/mm^2)*, Mean ± SD	N.A.	0.63 ± 1.03
NIA-Reagan score, Count (Score)	N.A.	3 (2), 3 (3)
Braak score, Count (Score)	N.A.	3 (I), 1 (II), 2 (III)

Abbreviations: MMSE, mini-mental status examination; N.A., Not available.

*A.2 Interactions of Aβ*56 with the NMDAR in vitro*

Though the results so far seem to suggest complexing of Aβ*56 with the NMDAR subunits, it is unknown whether there is a direct interaction between the two. To demonstrate that Aβ*56 can directly interact with NMDAR subunits, we applied Aβ*56 purified from aged APP transgenic mouse brains onto HEK293T cells transfected with GluN1 and/or GluN2B. Vehicle and monomeric Aβ were used as negative controls. Preparations of isolated Aβ species including monomers and Aβ*56 derived from transgenic animals were obtained using a modified protocol previously described for purifying Aβ oligomers endogenous to human brain tissue (Larson et al., 2012a) (**Fig. 3**). Purified Aβ*56 was applied to cells for 60 minutes as previously reported (Larson et al., 2012a). Aβ*56 co-localized with GluN-transfected HEK293T cells treated with the Aβ assembly (**Fig. 4A**). Consistently, application of decreasing concentration of Aβ*56 to

the GluN-transfected HEK293T cells resulted in a concentration dependent decrease of Aβ*56 co-localized with GluNs (**Fig. 4B**). At 0.025 pM, co-localization between Aβ*56 and GluN was no longer detectable. To assess which subunit might be responsible for the interaction, cells were then transfected with discrete GluN subunits. Following the application of Aβ, Aβ*56 readily co-localized with GluN1 but not with GluN2B indicating that Aβ*56 may be binding to the NMDAR through a direct interaction with GluN1 (**Fig. 4A**). These findings support the interaction of Aβ*56 with the NMDAR subunit GluN1.

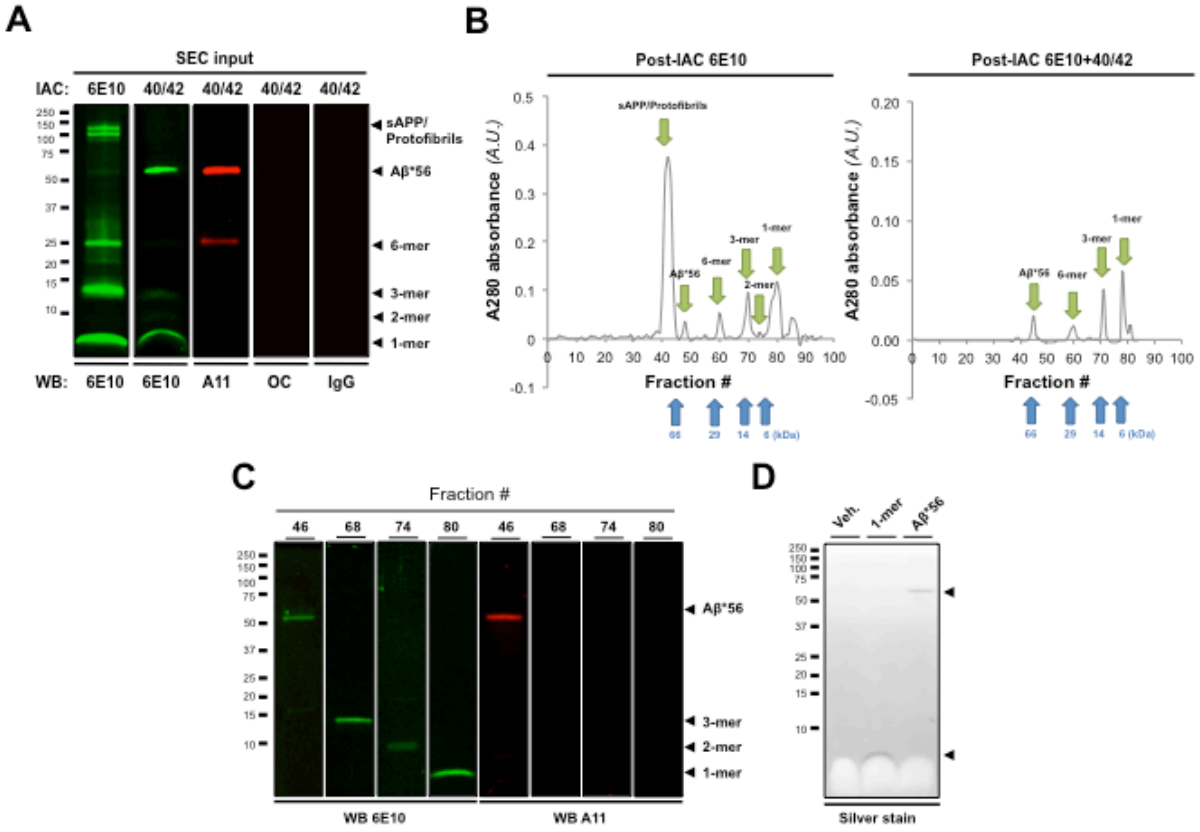

Figure 3. Biochemical characterization of soluble Aβ species present in APP transgenic brain tissues. Immuno-affinity capture (IAC) of soluble Aβ species was either performed using crosslinked 6E10 or with a 1:1 mixture of 40- and 42-end specific Aβ antibodies (labeled 40/42). (**A**) Representative western blotting profiles of soluble APP/Aβ oligomers affinity-purified from 15-18 month-old Tg2576 with 6E10 antibodies and of captured Aβ species following a sequential round of IAC with our 40/42 column

using 6E10, A11 (targeting non-fibrillar amyloid oligomers) or OC (targeting fibrillar amyloid oligomers) (right panels) illustrate the various input material used for segregation by size-exclusion chromatography. Detection with anti-IgG-IR680 was used as negative control. (**B**) Typical size-exclusion chromatograms observed using a Tricorn Superdex™ 75 column following IAC-6E10 or IAC-40/42. Several peaks (green arrows) corresponding to the APP/A β species seen by western blot are clearly observed with elutions at predicted molecular weights (blue arrows correspond to 4 out of 6 molecular weight standards used). (**C**) Representative western blot images of the respective SEC fractions isolated in (*B*) using 6E10 (in green, left panels) or A11 (in red, right panels). (**D**) Silver staining confirmed the apparent purity of the isolated species. Examples for SEC fractions containing A β monomers and A β *56 are shown.

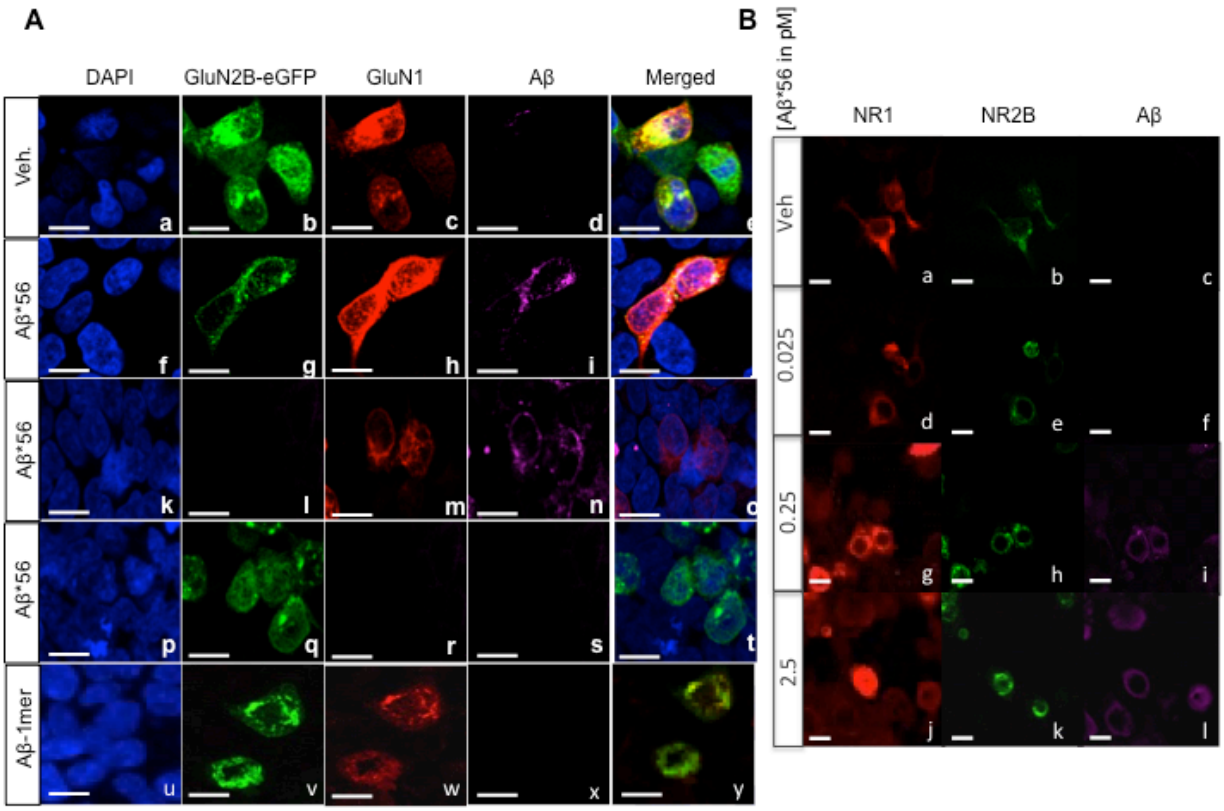

Figure 4. Colocalization of Aβ*56 with the NMDAR subunit GluN1 in HEK293 cells. (**A**) Representative confocal images of Aβ*56 binding to HEK293 cells transfected with NMDAR subunits GluN1 or GluN2B-eGFP. After 1 hour of 2.5uM Aβ*56, Aβ or Veh treatment, cells were immunostained for GluN1 (red channel, [c, h, m, r, w]), Aβ (magenta, [d, i, n, s, x]) and nuclei were stained with DAPI (blue channel, [a, f, k, p, u]). (**B**) Representative confocal images of A β *56 binding to HEK293 cells transfected with NMDAR subunits GluN1 or GluN2B-eGFP. After 1 hour of 2.5, 0.25, 0.025uM A β *56, or Veh treatment. (Scale bars = 15 μ m; n = 6 dishes/group).

B. ***Increased Activation of CaMKII by Aβ*56***

NMDAR-mediated neuronal responses depend on the subcellular localization of the receptors at the plasma membrane, *i.e.* synaptic or extrasynaptic, and involve known distinct, opposing or overlapping signaling pathways (Hardingham & Bading, 2010). Briefly, the activation of extracellular signal-regulated kinases (ERKs), cyclic AMP-response element binding protein (CREB) and Ca^{2+}/calmodulin dependent kinases (CaMK) have been traditionally linked to mediating the effect of synaptic NMDA receptors. By contrast, the activation of the p38 kinase, Forkhead box protein O (FOXO) and the inhibition of ERK and CREB are believed to be the downstream effectors of extrasynaptic NMDAR (Hardingham & Bading, 2010). We therefore assessed key components of these major common pathways in Tg2576 mice at an age when Aβ*56 is present (7 months) or absent (4 months). There was no change of phosphorylation in the cell survival-promoting kinases ERKs and CREB at S133 or in the cell death-inducing kinase p38 at T180/Y182 (**Fig. 5**). Since the gene expression activity of the FOXO member FOXO-1 relies upon nuclear translocation, we examined its relative abundance in extracts enriched in intracellular proteins (IC) and in extracts containing nuclear proteins (MB) (Larson et al., 2012b; Lesne et al., 2006). Similar to other intracellular messengers, we did not observe any overt changes in the biochemical segregation of FOXO-1 across ages and genotypes (**Fig.6**).

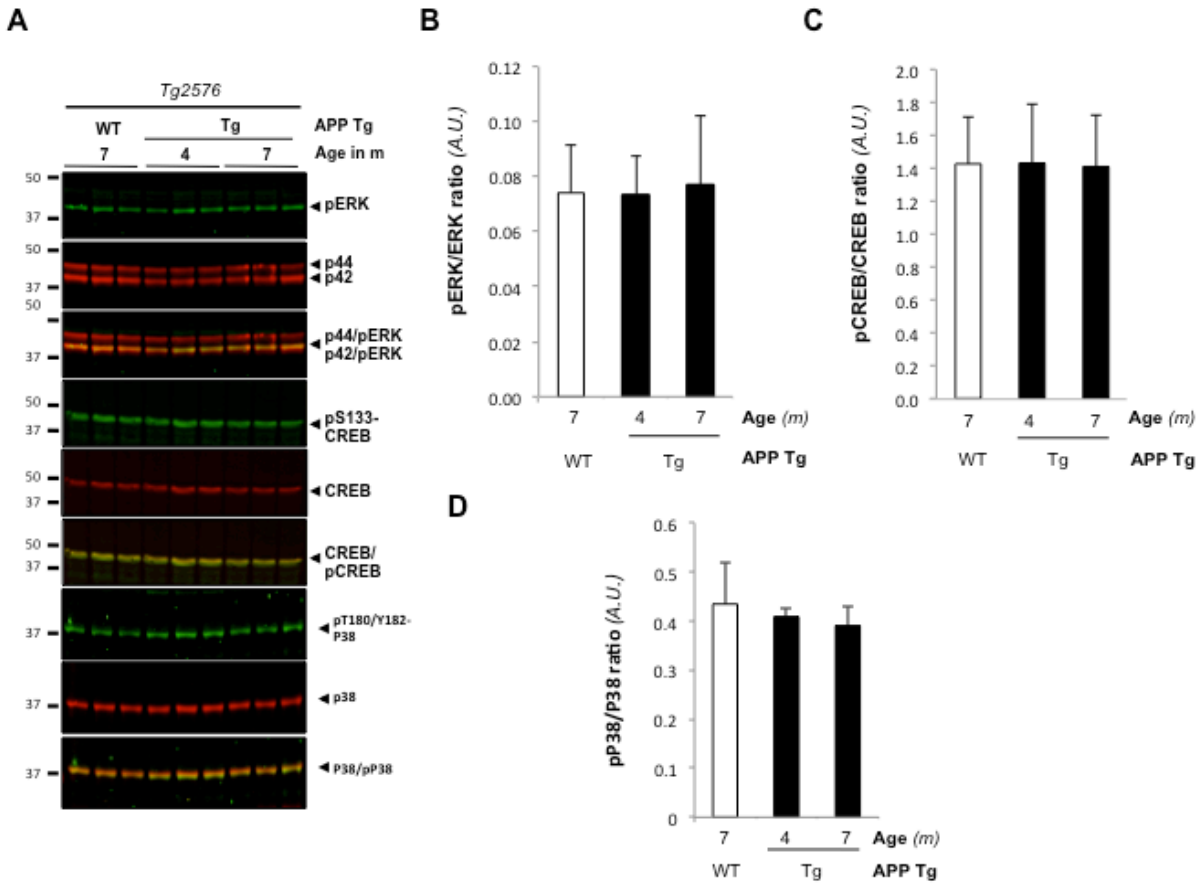

Figure 5. The major pathways regulated by extrasynaptic NMDA receptors are not altered in 7-month-old Tg2576 mice. (**A**) Representative western blot analysis of signaling pathways traditionally activated by NMDAR in brain tissues of wild-type and Tg2576 mice. Phosphoproteins were detected in the 800nm channel (green) while total protein levels were measured in the 680nm channel (red). Unless indicated otherwise, IC protein extracts were used. (**B-D**) Quantification of the respective phospho/total protein ratios for ERK *(b)*, CREB *(c)* and p38 *(d)* in the various age groups studied. No statistical differences were observed in the aforementioned proteins between groups. (Histograms represent the mean ± standard deviation; two-way ANOVA [$F_{(7,28)} = 38.7825$, $P = 0.0001$] followed by Student *t* test with Bonferroni correction, $^{\star}P < 0.05$, $n = 5$/group).

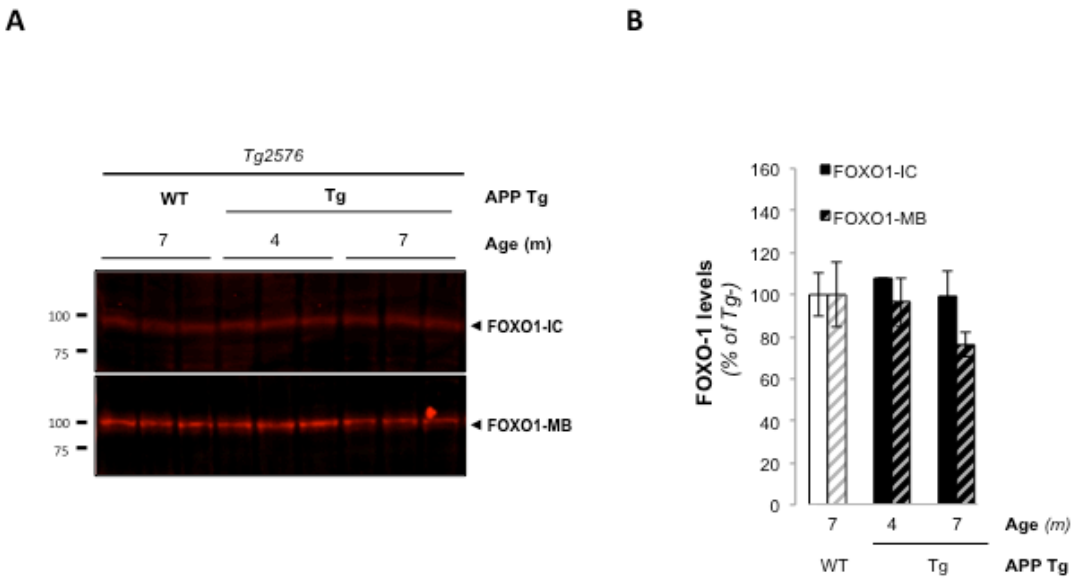

Figure 6. FOXO-1 levels are not altered in 7-month-old Tg2576 mice. (**A**) The relative abundance of FOXO-1 protein in intracellular (IC) and membrane-associated (MB) pools was used to assess putative translocation of the transcription factor in the forebrain of mice studied. The MB fraction contains nuclear proteins as opposed to extracellular and intracellular-enriched extracts (Larson *et al.*, 2012). (**B**) No statistical differences were observed in IC and MB levels of FOXO-1 between groups. (Histograms represent the mean ± standard deviation; two-way ANOVA [$F_{(7,28)}$ = 38.7825, P = 0.0001] followed by Student t test with Bonferroni correction, $^{\star}P < 0.05$, n = 5/group).

When the ionotropic glutamate receptor (GluN or NMDAR) is activated, the receptor becomes permeable to cations, notably calcium ions (Ca^{2+}) that rush across the membrane into the cytoplasm of the cell, leading to a significant influx of extracellular Ca^{2+}. Increased intracellular calcium then binds to calmodulin to activate CaMKII (Hardingham & Bading, 2010). Considering that the CaMKII isoform has previously been linked to neuronal toxicity in neurodegenerative disorders other than AD (Coultrap et al., 2011; Picconi et al., 2004) and the lack of observed changes in CREB phosphorylation mediated by CaMKIV in 7-month-old Tg2576 mice, we assessed CaMKII activity by measuring its phosphorylation state at T286 (**Fig. 7**). Phosphorylation at T286 increased by ~2.5-fold in 7-month-old Tg2576 mice compared

to younger 4-month-old Tg2576 littermates or age-matched wild-type (WT) and Tg5469 animals (**Fig. 7A,B**) overexpressing human wild-type APP at a level similar to that of mutant APP in Tg2576 mice (Ma et al., 2007). This apparent elevation in pT286-CaMKIIα (thereafter denoted as pCaMKII) in Tg2576 mice was transient and declined to 26% and 32% in 12- and 16-month-old mice, respectively, compared to control levels. Importantly, Aβ*56 levels correlated with pCaMKII in 6 to 9-month-old transgenic animals, with no changes observed for total CaMKII levels ($R^2 = 0.4777$, $P = 0.0128$, $n = 12$; **Fig. 8**). Supporting our biochemical findings, pCaMKII immunoreactivity was markedly enhanced in the synaptic fields of Tg2576 CA1 pyramidal neurons at 7 months of age (**Fig. 7C**). Moreover, the observed cellular distribution of pCaMKII was consistent with the preferential translocation of CaMKII to the synapse once phosphorylated (Merrill et al., 2005). Based on this observation, we biochemically assessed whether pCaMKII was accumulating in PSD (post-synaptic density)-containing lysates (MB fraction) of Tg2576 mice over time. We found that active CaMKII accumulated in an age-dependent manner in this fraction (**Fig. 7D,E**), further validating imaging analyses. Overall, these results indicate a supraphysiological activation of CaMKII at synapses associated with the onset of Aβ*56 detection in Tg2576 mice.

To directly demonstrate that Aβ*56 caused a selective exacerbation of CaMKII activity, we applied endogenous soluble Aβ oligomers purified from APP transgenic mouse brains at pathophysiologically relevant concentrations (pM to nM range) onto primary cultured cortical neurons. Preparations of apparent Aβ monomers, dimers, trimers and Aβ*56 derived from transgenic animals were obtained using a protocol previously described for purifying Aβ oligomers endogenous to human brain tissue

(Larson et al., 2012a) (**Fig. 3**). Due to the low abundance of Aβ*56 in brain tissue and recovery yields following our two-step purification method, Aβ*56 was applied to cells in a dose-dependent manner ranging from 1 to 25 pM. By contrast, low-molecular weight soluble Aβ species were applied at concentrations (1-5 nM) previously found to be biologically active in our *in vitro* system (Larson et al., 2012a). To attempt inducing a sustained effect on CaMKII that might recapitulate the exposure of neurons to Aβ*56 *in vivo*, primary cortical neurons were exposed to each purified Aβ molecule for 60 min as previously described (Larson et al., 2012a) (**Fig. 7F** and **Fig. 3**). While baseline levels of pCaMKII were readily detected in vehicle-treated neurons, application of increasing concentrations of Aβ*56 induced a dose-dependent potentiation of CaMKII phosphorylation, which plateaued at an average of 2.89-fold starting at 5 pM (**Fig. 7F, G**). Time course experiments using 2.5 pM Aβ*56 applications indicated that CaMKII activity peaked after 1 hour of treatment and declined to baseline within 8 hours (**Fig. 7H, I**). Consistent with the elevation in CaMKII phosphorylation, confocal immunofluorescence analyses revealed a translocation of pCaMKII to postsynaptic densities in neurons treated with 2.5 pM Aβ*56 for 60 minutes (**Fig. 9)**. Z-stack reconstruction analyses confirmed a 2.53-fold elevation of pCaMKII colocalization with PSD-95 in neurons exposed to Aβ*56 (**Fig. 7K, L**). Furthermore, neuronal cell death as determined by lactate dehydrogenase assay indicated that the concentrations of Aβ*56 used were not cytotoxic under our experimental settings (**Fig. 10A**). Different from Aβ*56, applications of Aβ monomers, dimers or trimers at 1 nM onto cortical neurons did not alter CaMKII phosphorylation compared to vehicle-exposed cells (**Fig. 10B, C**). Finally, *in vitro* application of Aβ*56 did not trigger the activation of ERK, CREB or p38

kinases (**Fig. 11**), similar to what was observed in 7-month-old Tg2576 animals. These findings indicate that CaMKIIα becomes hyperactive in the presence of Aβ*56.

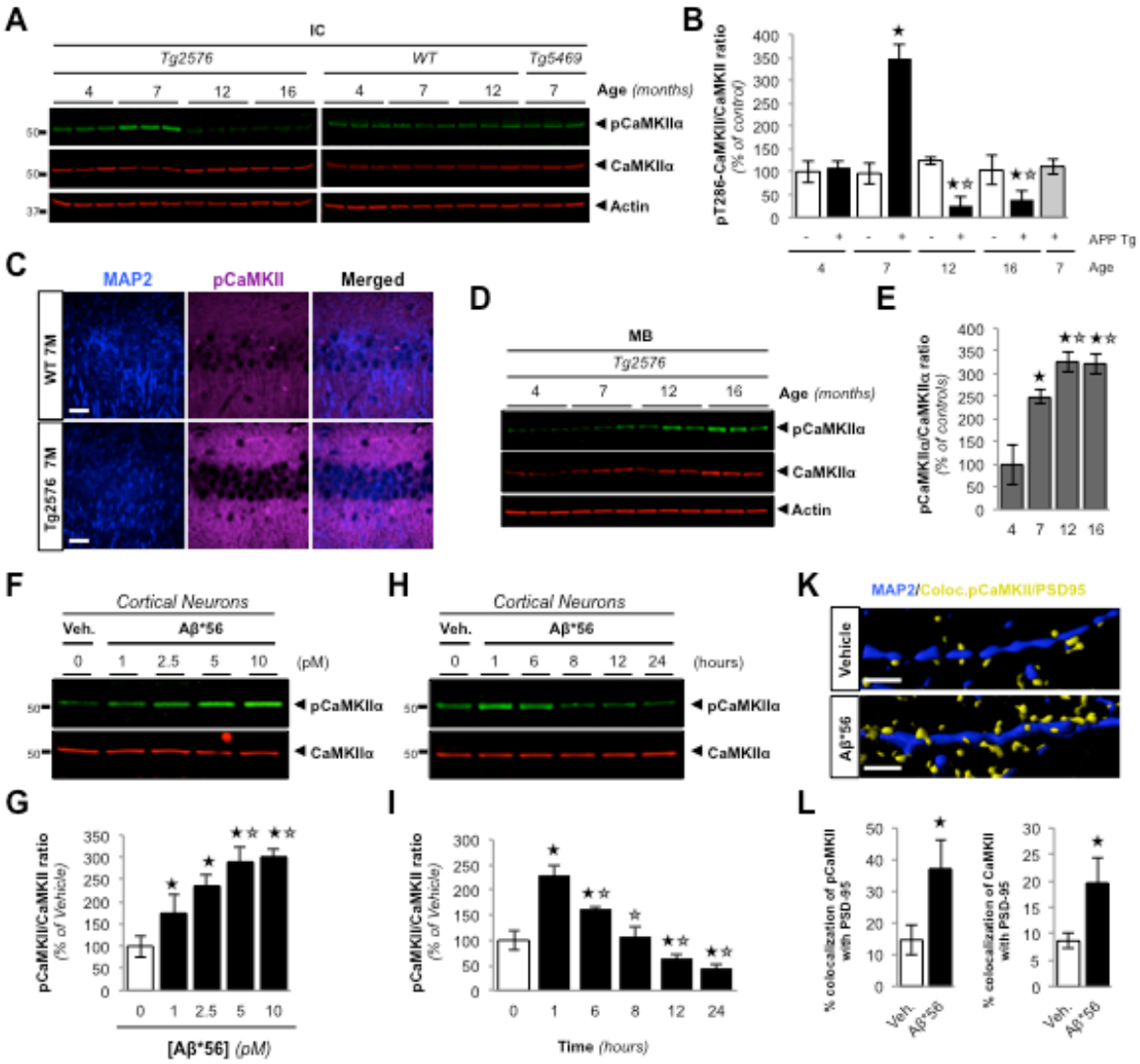

Figure 7. CaMKII is abnormally phosphorylated at T286 in brain tissue of 7-month-old Tg2576 mice and in cortical neurons treated with Aβ*56. (**A**) Representative western blotting images for pT286-CaMKIIα and CaMKIIα in intracellular protein extracts of 4-, 7-, 12- and 17-month-old Tg2576 as well as in age-matched wild-type and Tg5469 mice, which overexpress the wild-type human form of APP_{695} at a similar level than the APP^{Swe} transgene in Tg2576 mice. (**B**) Quantification of the phosphorylated/total CaMKII ratio revealed a ~3.5-fold increase in T286 phosphorylation at 7 months of age compared to younger Tg2576 animals. Of note, the activation of CaMKII was reduced in Tg2576 mice older than 12 months of age. White bars, wild-type mice; Black bars, Tg2576 mice; Grey bars, Tg5469 mice. (Histograms represent the mean ± standard deviation; two-way ANOVA [$F_{(7,28)} = 38.7825$, $P < 0.0001$] followed by Student *t* test

with Bonferroni correction, ★$P < 0.05$ *vs.* 4-month-old WT mice, ☆$P < 0.05$ *vs.* 4-month-old Tg2576 mice, n = 6-9/age/genotype). The ANOVA revealed a significant effect of the transgene ($F = 8.4721$, $P = 0.0305$), of age ($F = 44.793$, $P < 0.0001$) and transgene*age interaction ($F = 52.3397$, $P < 0.0001$). (**C**) Confocal imaging analysis of pT286-CaMKIIα expression and cellular localization in CA1 pyramidal neurons of 7-month-old WT and Tg2576 mice. Dendrites labeled with the microtubule-associated protein 2 (MAP2) are shown in blue and pT286-CaMKIIα (pCaMKII) is shown in magenta. Please note the apparent increase in pCaMKII immunoreactivity along the dendritic projections but not in the soma of pyramidal cells. Scale bar = 20 μm. (**D**) Representative western blotting images for pT286-CaMKIIα and CaMKIIα in membrane-associated protein extracts of 4-, 7-, 12- and 17-month-old Tg2576 mice. (**E**) Quantification of the phosphorylated/total CaMKII ratio revealed an age-dependent increase in T286 phosphorylation starting at 7 months of age compared to younger Tg2576 animals. (Histograms represent the mean ± standard deviation; one-way ANOVA [$F_{(3,24)} = 30.4023$, $P < 0.0001$] followed by Student t test with Bonferroni correction, ★$P < 0.05$ *vs.* 4-month-old WT mice, ☆$P < 0.05$ *vs.* 7-month-old Tg2576 mice, n = 6/age). (**F**) Western blot images for pT286-CaMKIIα and total CaMKIIα in DIV12-14 primary mouse cortical neurons treated with vehicle or increasing concentrations of brain-derived Aβ*56 for 60 minutes. (**G**) Densitometry analyses revealed a dose-dependent elevation of the pT286-CaMKII/total CaMKII ratio in neurons exposed to Aβ*56. (Histograms represent the mean ± standard deviation; ANOVA [$F_{(4,30)} = 14.6822$, $P < 0.0001$] followed by Student t test with Bonferroni correction, ★$P < 0.05$ *vs.* vehicle, ☆$P < 0.05$ *vs.* 1 pM condition, n = 6-8/group). (**H**) Western blot images for pT286-CaMKIIα and total CaMKIIα in DIV12-14 primary mouse cortical neurons treated with 2.5 pM of brain-derived Aβ*56 for 1, 6, 8, 12 or 24 hours. (**I**) Densitometry analyses revealed a transient elevation of the pT286-CaMKII/total CaMKII ratio in neurons exposed to 2.5 pM Aβ*56 that lasted up to 8 hours. (Histograms represent the mean ± standard deviation; ANOVA [$F_{(4,34)} = 17.4461$, $P < 0.0001$] followed by Student t test with Bonferroni correction, ★$P < 0.05$ *vs.* vehicle, ☆$P < 0.05$ *vs.* 1 hour condition, n = 6/group). (**K**) Representative images of dendrites illustrating the cellular distribution of the pCaMKII/PSD-95 colocalization channel with respect to MAP2 in neurons treated with vehicle or 2.5 pM Aβ*56 for 60 minutes. MAP2, pCaMKII and PSD-95 were, respectively, visualized with AlexaFluor405, AlexaFluor488 and AlexaFluor647 conjugated secondary antibodies and colocalization analyses between pCaMKII and PSD-95 were performed using the Imaris7.x colocalization tool (Bitpane Scientific Software). Upon creating a colocalization channel (shown in yellow), Z-stacks of images were transformed for volume rendering and voxel count analysis. Scale bar = 3 μm. (**L**) Quantification of the voxels occupied by the colocalization channel between pCaMKIIα/PSD-95 or total CaMKII/PSD-95 revealed a marked accumulation of pCaMKII and CaMKII at postsynaptic sites under Aβ*56 exposure. (Histograms represent the mean ± standard deviation; Student t test, $F_{(1,14)} = 37.339$, ★$P < 0.05$ *vs.* Vehicle, n = 8 ROIs/group).

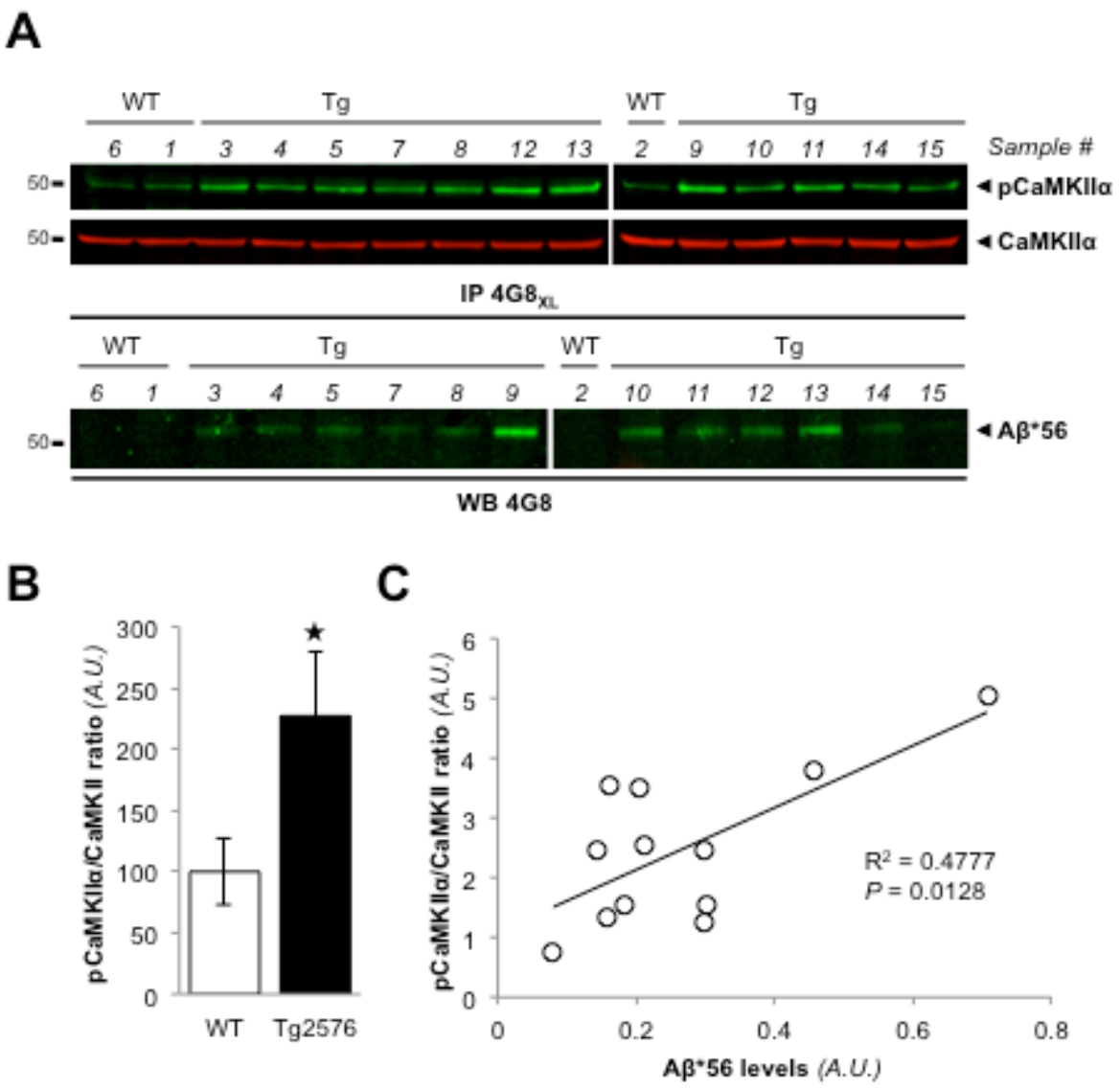

Figure 8. Relationship between CaMKIIα activity and Aβ*56 expression in young Tg2576 mice. (**A**) Representative western blot analyses of pT286-CaMKIIα (green), total CaMKII (red) in brain tissues of WT and Tg2576 mice at 6 to 9 months of age. Aβ*56 was detected with 4G8 following immunoprecipitation with crosslinked 4G8 ($4G8_{XL}$) using 200 µg of MB extracts. (**B**) Quantification of the averaged CaMKII activity in WT and Tg2576 animals as assessed by analyzing the pCaMKII/CaMKII ratio. (Histograms represent the mean ± standard deviation; $F_{(1, 13)} = 4.7843$, Student *t* test, $^{\star}P < 0.05$ *vs.* WT mice, $n_{WT} = 3$ and $n_{Tg2576} = 12$). (**C**) Regression analysis between the pCaMKII/CaMKII ratio and A β *56 levels in all transgenic animals studied ($P = 0.0128$, $n = 12$).

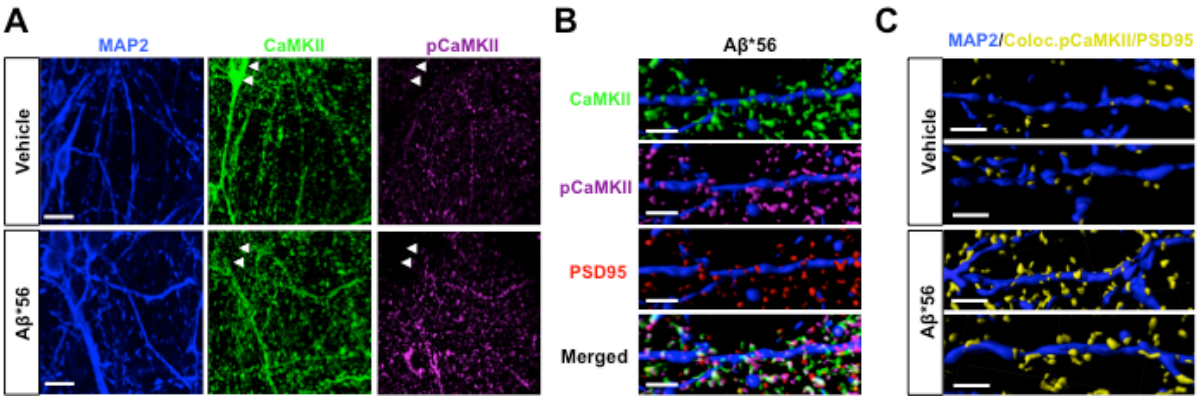

Figure 9. Aβ*56-induced translocation of pCaMKIIa to postsynaptic sites in primary cortical neurons. (**A**) Representative immunofluorescence images of MAP2 (blue), CaMKII (green) and pT286-CaMKII (magenta) in primary cortical neurons treated with vehicle or 2.5 pM Aβ*56 for 60 minutes. Arrowheads indicate the cell bodies of neurons. Please note the marked reduction in CaMKII labeling in the cell bodies of Aβ*56-treated neurons compared to vehicle-treated cells. Scale bar = 20 µm. (**B**) Software-generated three dimension rendering of MAP-2 (blue), CaMKII (green), pCaMKII (magenta), PSD-65 (red) immunoreactivities in Aβ*56-treated neurons. The merged image is presented below. Scale bar = 3 µm. (**C**) Using two fluorescence pairs (pCaMKII/PSD95 and CaMKII/PSD-95), the corresponding colocalization channels were created for comparison and clarity purposes between treatment conditions (Vehicle *vs.* 2.5pM Aβ*56). Examples of the cellular distribution of the pCaMKII/PSD-95 colocalization channel (shown in yellow) on two dendrites are presented. Scale bar = 3 µm.

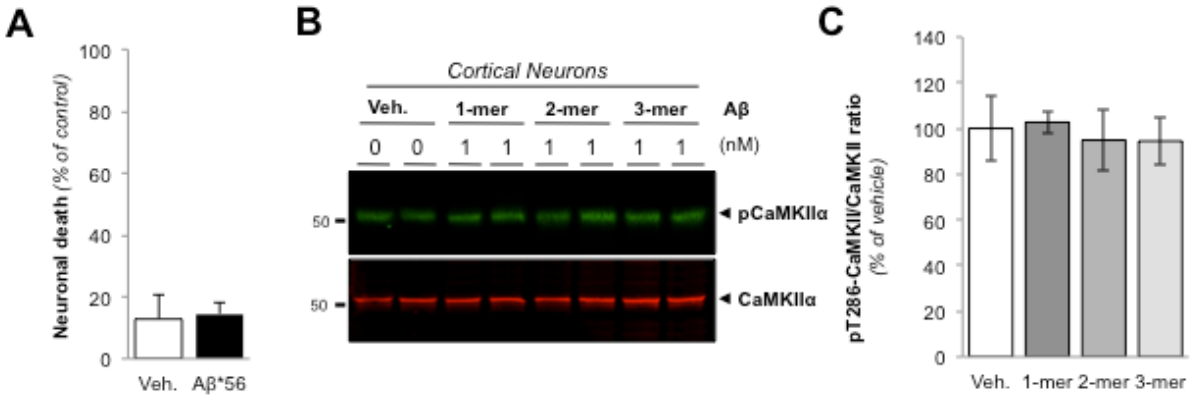

Figure 10. CaMKII activation is not induced by low-*n* Aβ oligomers purified from APP transgenic mice. (**A**) Neuronal death of primary cortical neurons exposed to 2.5pM Aβ*56 or Vehicle for 60 minutes as determined by LDH assay. Full kill condition (100% cell death) consisted in applying 0.1% Triton X-100 onto cells in order to disrupt the neuronal plasma membrane. (Histograms represent the mean ± standard deviation; one-way ANOVA [$F_{(2,21)} = 529.3333$, $P < 0.0001$] followed by Student *t* test with Bonferroni correction, $^{\star}P < 0.05$ *vs.* Vehicle, n = 9-12/condition). (**B**) Western blot analysis of

pCaMKII α and total CaMKII α in primary cortical neurons exposed to discrete 1 nM A β oligomers. Duplicate wells are displayed. (**C**) Quantification of the respective pCaMKII α/CaMKII α ratio revealed no statistically significant changes across groups under our experimental conditions. (Histograms represent the mean ± standard deviation; ANOVA followed by Student *t* test with Bonferroni correction, $^{\bigstar}P < 0.05$ *vs.* 4-month-old Tg2576 mice, $^{\star}P < 0.05$ *vs.* 7-month-old Tg2576 mice, n = 4-6/group).

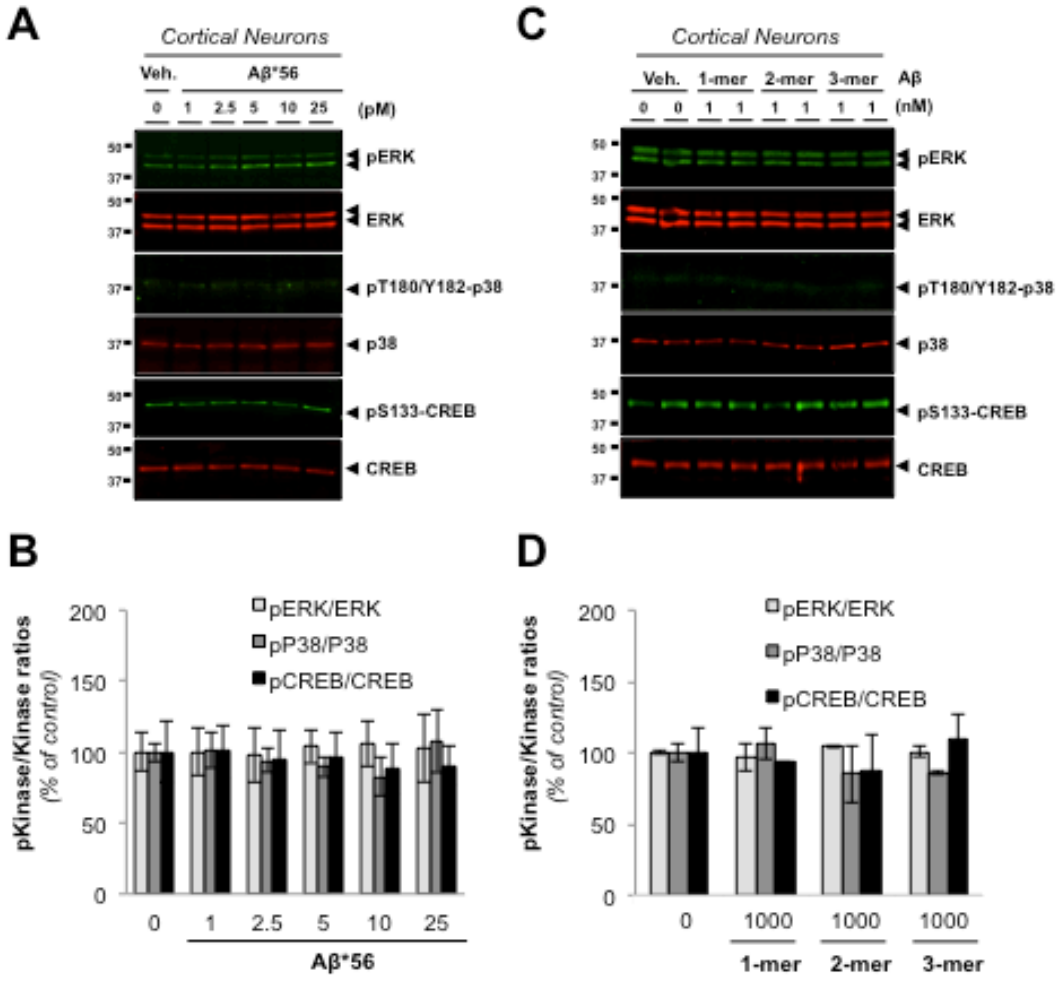

Figure 11. The major pathways regulated by extrasynaptic NMDA receptors are not altered by endogenous Aβ oligomers in mouse cortical primary neurons following a 60-minute exposure. (**A**) Representative western blot analysis of signaling pathways traditionally activated by NMDAR in primary cortical neurons treated with either vehicle or various concentrations of Aβ*56. Phosphoproteins were detected in the 800nm channel (green) while total protein levels were measured in the 680nm channel (red). (**B**) Quantification of the respective phospho/total protein ratios for ERK, P38 and CREB revealed no overt changes under our conditions. (Histograms represent the mean ± standard deviation; one-way ANOVA [$F_{(4,21)} = 0.0833$, $P = 0.8974$, $F_{(4,21)} = 0.4967$, $P = 0.7390$ and $F_{(4,21)} = 0.3286$, $P = 0.8526$ respectively] followed by Student *t* test with Bonferroni correction, n = 5-6/group). (**C**) Western blot analysis of ERK, P38 and CREB

in primary cortical neurons exposed to either vehicle or low molecular weight Aβ molecules (1 nM) for 60 minutes. (**D**) Quantification of the respective phospho/total protein ratios for ERK, P38 and CREB revealed no statistically significant changes under our settings. (Histograms represent the mean ± standard deviation; one-way ANOVA [$F_{(3,16)} = 0.6586$, $P = 0.5894$, $F_{(3,16)} = 1.8590$, $P = 0.3772$ and $F_{(3,16)} = 0.6222$, $P = 0.6370$ respectively] followed by Student *t* test with Bonferroni correction, n = 5/group).

*C. Aβ*56-Induced Enhanced Synaptic NMDAR-Dependent Calcium Influx*

For its initial activation, CaMKII depends on intracellular Ca^{2+} changes (Coultrap & Bayer, 2012). Taking into consideration the apparent binding of Aβ*56 to the NMDAR subunits, the activation of an intracellular signaling pathway traditionally associated with synaptic NMDAR stimulation and the lack of activation of cellular messengers modulated by extrasynaptic NMDARs (Hardingham & Bading, 2010), we sought to examine the effect of Aβ*56 on synaptic NMDAR-dependent calcium influx. Calcium transients were visualized in mouse cortical neurons transfected with GCaMP6f, a genetically engineered calcium indicator, and bicuculin/4-aminopyridine (Bic4AP, a GABA receptor antagonist and potassium channel blocker, respectively) was applied onto cells for 15 seconds to stimulate the NMDAR, since this paradigm was previously characterized to selectively activate synaptic NMDARs in primary cultured neurons (Hardingham & Bading, 2002; Léveillé et al., 2008). In the absence of Aβ*56, the Bic4AP pulse induced a lasting elevation of eGFP fluorescence (**Fig. 12A, B**). In the presence of 2.5 pM Aβ*56 (a 30-minute pretreatment followed by a 5 minute recording period), application of Bic4AP resulted in an enhanced and sustained influx of calcium mediated by synaptic NMDARs (**Fig. 12A,B**). Upon calculating the peak amplitude and the global magnitude of the recorded responses (**Fig. 12C, D**), Aβ*56 potentiated

synaptic NMDAR-induced Ca^{2+} influx by ~4.5-fold compared to cells exposed only to vehicle (a respective 4.99 ± 0.16- and 3.94 ± 0.16-fold increase compared to control cells).

To demonstrate that NMDAR-mediated Ca^{2+} currents are specifically enhanced in the presence of Aβ*56, we exposed the cells to a series of sequential bath stimulations with Bic4AP preceding or following a 15-min exposure to 2.5 pM Aβ*56; then we subjected the cells to Bic4AP/MK801 stimulations to block opened synaptic NMDARs. Finally, the same cells were exposed to another Bic4AP bath stimulation to ensure that synaptic NMDAR were indeed blocked (**Fig. 12E**). Adding the NMDAR-antagonist MK801 led to an 82% reduction in NMDAR-mediated Ca^{2+} influx in cells exposed to Aβ*56 (**Fig. 12E, F**). The lack of potentiated Ca^{2+} influx triggered by the subsequent Bic4AP stimulation indicated that extrasynaptic NMDARs were not involved in the potentiation induced by Aβ*56 (**Fig. 12E, F**). Together, these findings were consistent with the selective activation of CaMKII by synaptic NMDARs.

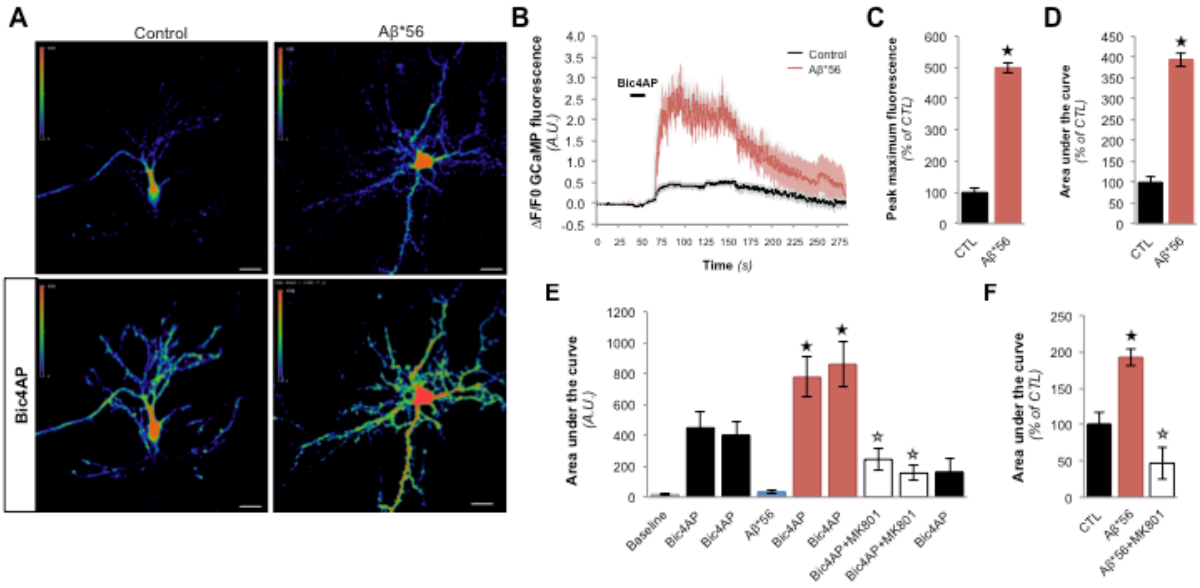

Figure 12. Aβ*56 enhances synaptic NMDAR-dependent calcium transients in primary cultured neurons. (**A**) Representative confocal images for GCaMP6f-transfected neurons in presence or absence of Aβ*56 at rest or following stimulation of synaptic NMDARs with Bic4AP (see methods). Scale bars = 20 µm. (**B**) Fluorescence responses of GCaMP-transfected neurons following synaptic NMDAR activation in the presence (red) or absence (black) of Aβ*56. Bold solid lines correspond to the average response while the flanking upper and lower grey-shaded areas indicate the standard deviation. The black bar indicates the exposure of Bic4AP. (**C**) Quantification of the maximum GCaMP fluorescence ratio revealed an ~5-fold increase in neurons exposed to Aβ*56 following simulation of synaptic NMDARs ($F_{(1,13)}$ = 21.122, Student *t* test, $^{\bigstar}P <$ 0.05, n = 6-9 cells per group). (**D**) Quantification of the area under the curve for the traces recorded indicated an ~4-fold potentiation of Ca^{2+} influx following synaptic NMDAR stimulation in presence of Aβ*56. ($F_{(1,13)}$ = 22.306, Student *t* test, $^{\bigstar}P < 0.05$, n = 6-9 cells per group). (**E**) Neuronal Ca^{2+} responses induced following sequential bath stimulations consisting of two 15-second Bic4AP exposures, a 15-minute Aβ*56 exposure (2.5 pM), two 15-second Bic4AP exposures, two 45-second Bic4AP+10µM MK801 exposures. Blockade of synaptic NMDAR was verified by applying a final Bic4AP application. (Histograms represent the mean ± standard deviation; one-way ANOVA [$F_{(8,51)}$ = 9.4731, $P < 0.0001$] followed by Student *t* test with Bonferroni correction, $^{\bigstar}P < 0.05$ *vs.* Bic4AP (stimulation #2), $^{\star}P < 0.05$ *vs.* Bic4AP post-Aβ*56 (stimulation #5), n = 8 cells/treatment). (**F**) Averaged Ca^{2+} responses in cortical neurons consecutively exposed to Bic4AP, Bic4AP post-Aβ*56 application and Bic4AP+MK801. (Histograms represent the mean ± standard deviation; one-way ANOVA [$F_{(2,40)}$ = 14.7673, $P < 0.0001$] followed by Student *t* test with Bonferroni correction, $^{\bigstar}P < 0.05$ *vs.* Bic4AP, $^{\star}P < 0.05$ *vs.* Bic4AP post-Aβ*56, n = 16 responses/treatment).

III. Discussion

The soluble Aβ oligomer, Aβ*56 is found in the MB fraction and appears to co-immunoprecipitate with the NMDAR subunits but not with the subunits of other glutamate receptors, nicotinic acetylcholine receptors or EphB2 receptors in mouse and in human brain tissue. Further Aβ*56 co-localizes with the NMDAR subunit GluN1 and not GluN2B in HEK293T cells. This complexing of Aβ*56 to the NMDAR seems to induce an enhanced influx of Ca^{2+} through the synaptic NMDAR receptor type *in vitro*. Moreover, CaMKII the main mediator of the synaptic NMDAR activation is hyper-activated and translocates to the PSD in the presence of Aβ*56 both *in vitro* and *in vivo.* Altogether these findings seem to suggest that Aβ*56, an oligomer shown to have deleterious effects on cognition in a transgenic animal model of Alzheimer's disease, can bind to the ionotropic glutamate receptor, synaptic NMDAR and enhanced activation of the receptor, leading to the increase activation of the downstream kinase CaMKII and localization of the activated kinase to the post synaptic density. It is worth noting that when examining the intracellular-enriched (IC) fraction the increased activation of CaMKII appeared to be transient both in the mouse model and in primary cortical neurons treated with Aβ*56. However, when the membrane-bound fractions are analyzed, the increase in CaMKII phosphorylation persisted and even increased further in the forebrains of older animals. Following activation, CaMKII translocated to the PSD where it is known to interact with anchored receptors. This data suggested a persistent Aβ*56-dependent increased activation of CaMKII. This is in agreement with fact that Aβ*56 levels remain elevated in the brain of Tg2576 mice starting at 6 months and even increase slightly further at later ages. Considering that the NMDA receptor is very

important for the cellular and molecular process underlying learning and memory and the involvement of abnormally activated CaMKII in multiple neurological disorders (Weeber et al. 2003; Picconi et al 2004; Yabuki et al. 2014) it is reasonable to believe that Aβ*56 is mediating its toxic effect via the NMDAR/CaMKII axis.

Chapter 3

A β *56-induced pathological tau changes in brains of Tg2576 mice

I. Introduction

Tau pathology in AD is thought to act as a downstream effector of A β in the disease process. The amyloid hypothesis suggests that disease-relevant tau pathological changes result from the accumulation of A β (Hardy & Higgins, 1992) . We proposed to determine whether the conformation and phosphorylation of tau molecules was altered in the presence of Aβ*56 *in vivo* and *in vitro*. As mentioned in the Introduction section, several kinases can phosphorylate tau at multiple sites thereby contributing to pathology in AD (Martin et al., 2013). In animal models, phosphorylation of tau at certain sites have been linked to specific neuronal dysfunction. For instance, tau phosphorylation at Y18, S409 and S416 are linked to cell cycle re-entry or CCR (Seward et al., 2013), which is a characteristic of cortical neuron in the AD brain. Neurons in most regions of the normal adult human brain do not divide (Altman & Das, 1965; Kuhn et al., 1996). However, in the AD brain (Arendt et al., 2010) and numerous mouse models of the disease (Li et al., 2011), neurons re-enter cell cycle but fail to divide. Instead, this ectopic CCR is proposed to account for a significant amount of neuronal loss in the AD brain (Arendt et al., 2010).

Phosphorylation of tau at S202 has also been proposed to be one of the earliest pathogenic tau changes that take place in the AD brain. CaMKII is one of the kinases that can phosphorylate tau at sites that are found in AD and during aging (Martin et al., 2013; Steiner et al., 1990). In addition to its hyperphosphorylation, the translocation of tau from the axon to dendritic spines constitute another pathological characteristic of tau, which has recently been proposed to contribute to synaptic dysfunction (Frandemiche et al., 2014; Hoover et al., 2010; Ittner et al., 2010).

Here we examined the effects Aβ*56 on tau phosphorylation and on its cellular distribution following Aβ*56-induced CaMKII hyper-activation.

II. Results

*A. Aβ*56-Induced hyperphosphorylation and misslocalization of tau*

One substrate of CaMKII is the tau protein at various serine residues including S262, S409 and S416, which are hyperphosphorylated in the AD brain (Martin et al., 2013; Steiner et al., 1990). Of particular interest, phosphorylation at S416 leads to a conformational change in the tau protein associated with the biochemical profile of AD (Steiner et al., 1990). We therefore examined the phosphorylation and conformation status of tau for changes commonly associated with AD (**Fig. 13A**). Across transgene and age groups, no obvious phosphorylation increases were detected at Y18, S262, S396/S404 and S409 (**Fig. 13A, B**). However we detected a 2.73 ± 0.22- and a 2.68 ± 0.34-fold increase in phosphorylation at S202 and S416, respectively, in 7 month-old Tg2576 forebrains compared to non-transgenic littermates (**Fig. 13A, B**). In addition, we

observed a delayed electrophoretic migration of pS416-tau molecules resulting in the detection of two additional bands of ~55 and 60 kDa as previously documented (Steiner et al., 1990) (**Fig. 13A**), which tau epitope and dephosphorylation assays confirmed as hyperphosphorylated 0N4R tau conformers (C. Liu & Götz, 2013) (**Fig. 14**). Both pS202- and pS416-tau protein levels present in IC extracts declined at 12 and 16 months of age compared to those detected in 7-month-old Tg2576 mice (**Fig. 15**) paralleling the transient elevation of pCaMKII observed (**Fig. 7**).

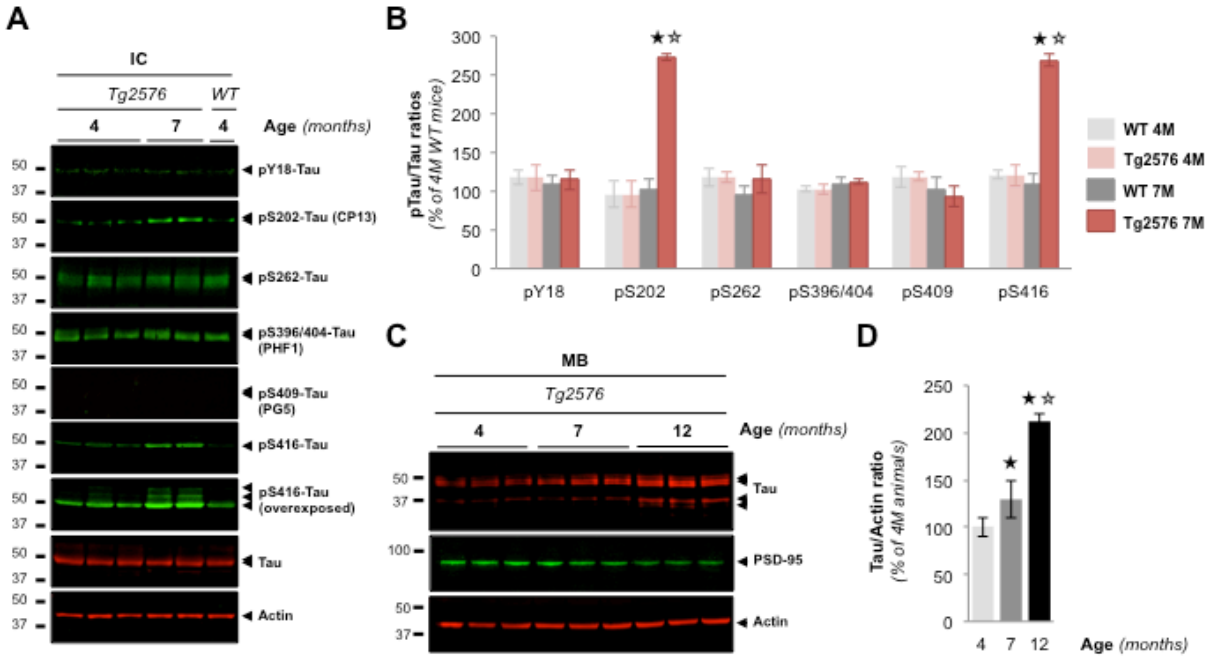

Figure 13. Hyperphosphorylation and missorting profile of soluble tau species in young Tg2576 mice. (**A**) Representative quantitative western blotting images for soluble tau species detected in intracellular-enriched fractions (IC) in 4-, 7-month-old Tg2576 as well as 4-month-old WT mice. (**B**) Quantification of the modified/total Tau ratio revealed a ~2.7- and 2.6-fold increase in pS202-Tau (CP13) and pS416-tau respectively at 7 months of age compared to younger Tg2576 animals. Light colors correspond to 4-month-old animals while darker colors represent data obtained in 7-month-old mice. (Histograms represent the mean ± standard deviation; two-way ANOVA [$F_{(2,21)}$ = 67.6019, $P < 0.0001$] followed by Student *t* test with Bonferroni correction, ★$P < 0.05$ *vs.* age-matched WT mice, ☆$P < 0.05$ *vs.* 4-month-old Tg2576 mice, n = 6-9/age/genotype). (**C**) Western blotting images for total soluble tau, PSD-95 and actin in membrane extracts (MB) of Tg2576 mice preceding (4 months) or concurrent with Aβ*56 detection (7 and 12 months). (**D**) Densitometry analysis indicated an abnormal accumulation of tau in

PSD-containing lysates of 7-month-old Tg2576 mice or older. (Histograms represent the mean ± standard deviation; one-way ANOVA [$F_{(2,18)} = 19.7636$, $P < 0.0001$] followed by Student *t* test with Bonferroni correction, $^{\bigstar}P < 0.05$ *vs.* 4-month-old Tg2576 mice, $^{\star}P < 0.05$ *vs.* 7-month-old Tg2576 mice, $n = 6$-9/age/genotype).

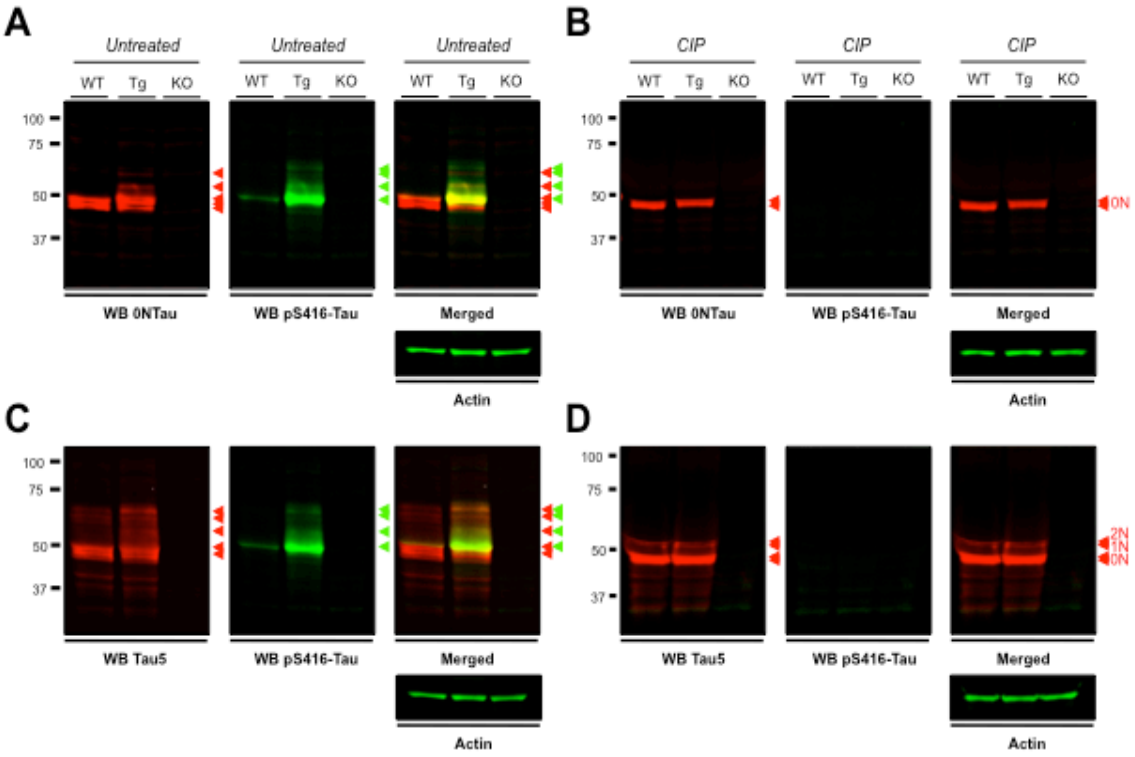

Figure 14. Epitope and dephosphorylation tau assays confirm the presence of hyperphosphorylated tau conformers detected by pS416-Tau antibodies. (**A,B**) Representative western blot analyses of 0N4R-Tau (0NTau) and pS416-Tau in untreated (*A*) or CIP-treated (*B*) IC fractions of 6-month-old WT, Tg2576 and *MAPT*-null mice. Actin was used as internal control (lower right inserts). (**C,D**) Representative western blot analyses of total Tau (Tau5) and pS416-Tau in untreated (*C*) or CIP-treated (*D*) IC fractions of 6-month-old WT, Tg2576 and *MAPT*-null mice. Actin was used as internal control (lower right inserts). ($n = 3$/genotype).

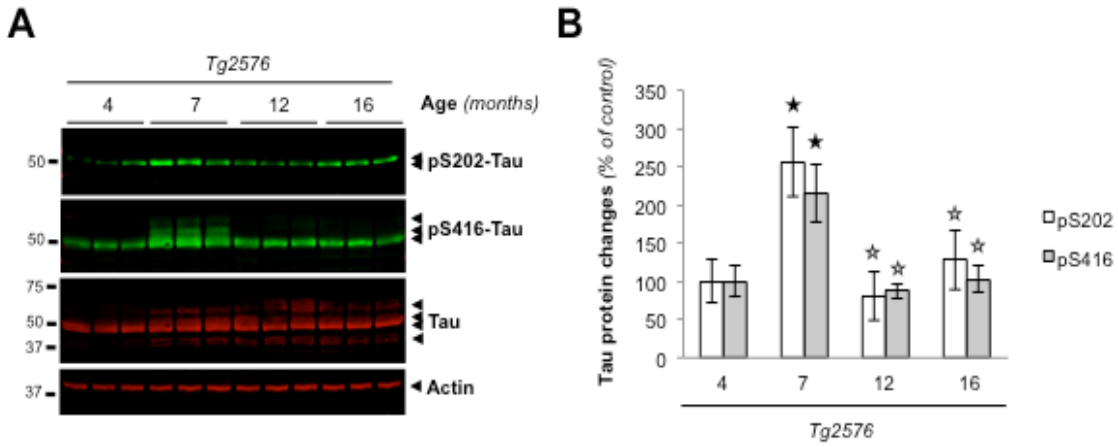

Figure 15. Temporal expression profile of pS202-Tau and pS416-Tau in Tg2576 mice. (**A**) Representative western blot analysis of pS202-Tau (CP13), pS416-Tau and total tau (Tau5) in IC fractions of Tg2576 mice at 4, 7, 12 and 16 months of age. Actin was used as internal control (red). (**B**) Quantification of the respective protein ratios (phosphorylated/total) for pS202- and pS416-Tau species in the various age groups studied. (Histograms represent the mean ± standard deviation; one-way ANOVA [$F_{(3,23)}$ = 23.4704, $P < 0.0001$ for pS202-Tau and $F_{(3,23)}$ = 25.6013, $P < 0.0001$ for pS416-Tau] followed by Student *t* test with Bonferroni correction, $^{\star}P < 0.05$, n = 6-9/group).

Consistent with this apparent specificity in the observed pattern of tau hyperphosphorylation, we observed that neither Cdk5 nor GSK3β, two of the major tau kinases, were abnormally activated in 7-month-old Tg2576 mice and in primary cortical neurons exposed to Aβ*56 (**Fig. 16**). At later ages, however, these kinases, which have been widely implicated in the downstream effects of Aβo became abnormal at 12 and 16 months of age (**Fig. 16**). Upon assessing the relative abundance of the two distinct classes of oAβ species, non-fibrillar ($A11^{+}$) and pre-fibrillar (OC^{+}), respectively, in the forebrain of Tg2576 mice, regression analyses indicated that OC-immunoreactive Aβ species (which Aβ*56 is not (M. E. Larson & Lesné, 2012; S. E. Lesné et al., 2013; S. Lesné et al., 2006)) were remarkably correlated to Cdk5 activation at 12 and 16 months of age (R^2= 0.7544, P = 0.0248 and R^2=0.8854, P = 0.0051 respectively; **Fig. 17**). Interestingly, none of the Aβ species measured using the 6E10, 4G8, 82E1, A11 or OC antibodies appeared to

be related to the changes we had observed in GSK3β activity between different age groups (**data not shown**). Accordingly, none of the additional tau sites linked to the aforementioned kinases were hyperphosphorylated (S396, S409 and S404, respectively; **Fig. 13A,B**) in 7-month-old Tg2576 mice further arguing against their potential involvement in mediating the initial signaling response induced by Aβ*56.

Since tau missorting to the PSD alters synaptic function (Frandemiche et al., 2014; Hoover et al., 2010; Zempel et al., 2010), we measured total tau levels in membrane extracts from forebrains of Tg2576 mice at 4, 7, and 12-months of age containing PSD-95 as described elsewhere (Larson et al., 2012a). Tau abnormally co-segregated with PSD-95 at 7 months of age, and further accumulated in 12-month-old Tg2576 animals (**Fig. 13C,D**). To support these biochemical changes, we performed immunofluorescent labeling followed by confocal imaging analyses (**Fig. 18**). In CA1 pyramidal neurons of 7-month-old Tg2576 mice, there was a striking increase of pS202-Tau in the soma and dendrites of the stratum radiatum (**Fig. 18,** *panel F*). By contrast, pS416-Tau was nearly exclusively detected in dendrites (**Fig. 18,** *panel G*), matching the distribution of pCaMKII (**Fig. 7C**). Importantly, pS202-Tau and pS416-tau colocalized at dendritic spines in transgenic mice (**Fig. 18** *panels I-L*). These results indicate that the ~2-fold elevation in CaMKII activity observed in Tg2576 at ages when Aβ*56 starts forming is associated with a ~2.5-fold increase in tau hyperphosphorylation at S202/S416 and missorting of this tau species into spines.

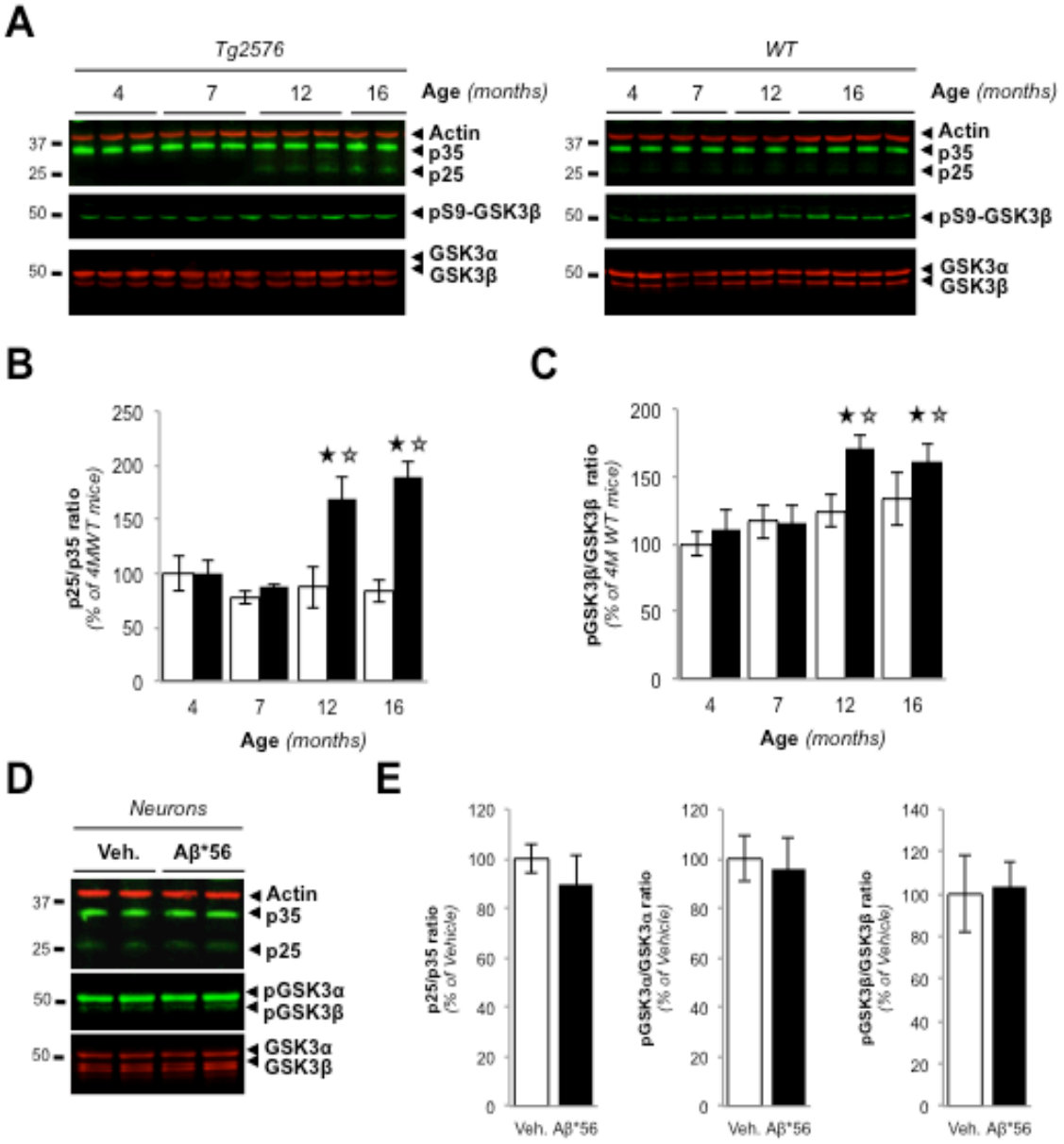

Figure 16. Temporal expression profiles of Cdk5 adaptor proteins and GSK3 in WT and Tg2576 mice. (**A**) Representative western blot analysis of Cdk5 adaptors (p35 and p25) and GSK3α/β in brain tissues of wild-type and Tg2576 mice at 4, 7, 12 and 16 months of age. Actin was used as internal control. (**B, C**) Quantification of the respective protein ratios for P25 *(B)* and GSK3 β *(C)* in the various age groups studied. The ANOVA analysis for the p25/p35 ratio revealed significant effects of the transgene (F = 8.8771, P = 0.0056), of age (F = 12.7530, $P < 0.0001$) and transgene*age interaction (F = 8.5758, P = 0.0003). The ANOVA for pGSK3 β /GSK3 β revealed significant effects of the transgene (F = 53.0123, $P < 0.0001$), of age (F = 26.5855, $P < 0.0001$) and transgene*age interaction (F = 12.1330, $P < 0.0001$). (Histograms represent the mean ± standard deviation; two-way ANOVA [$F_{(7,31)}$ = 10.4771, $P < 0.0001$ and $F_{(7,32)}$ = 23.3261,

$P < 0.0001$ respectively] followed by Student *t* test with Bonferroni correction, $^{\bigstar}P < 0.05$ vs. 4-month-old mice, $^{\star}P < 0.05$ vs. age-matched mice, *n* = 4-6/group). (**D**) Representative western blot analysis of Cdk5 adaptors (p35 and p25) and GSK3α/β in DIV14 mouse primary cortical neurons in absence or presence of 2.5pM Aβ *56 for 60 minutes. Actin was used as internal control. (**E**) Quantification of the respective protein ratios for P25 *(left panel),* GSK3 α (*middle panel*) and GSK3 β (*right panel*) in the tested conditions. (Histograms represent the mean ± standard deviation; [$F_{(1,8)} = 0.8911$, $P = 0.3728$, $F_{(1,8)} = 0.6679$, $P = 0.4374$ and $F_{(1,8)} = 0.0425$, $P = 0.8419$ for the p25/p35, pGSK3 α /GSK3 α and pGSK3 β /GSK3 β ratio respectively], Student *t* test, *n* = 5/group).

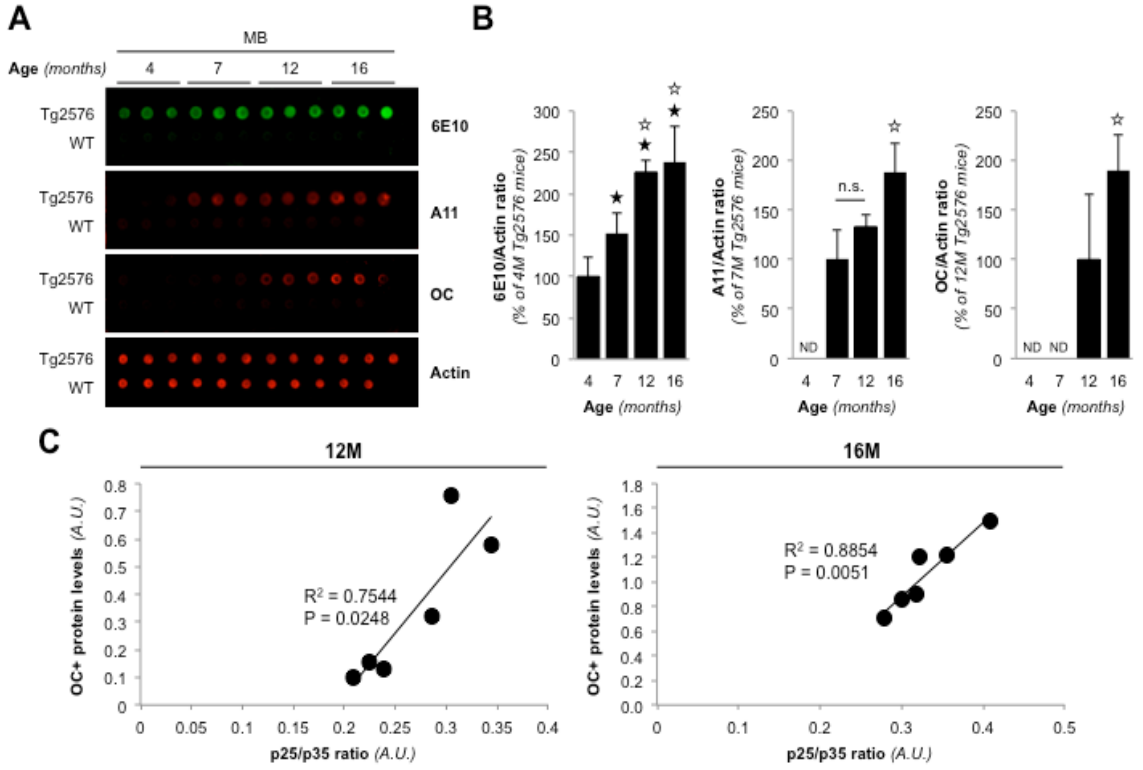

Figure 17. OC-positive Aβ oligomers are associated with Cdk5 activation in middle-aged Tg2576 mice. (**A**) Age-dependent accumulation of oligomeric Aβ conformers in MB lysates of Tg2576 mice by dot blotting analysis using A11 and OC antibodies. 6E10 was also used to measure APP/Aβ levels and actin was used as internal control. (*n* = 6 animals/age). (**B**) Normalized levels of Aβ species indicated an age-dependent accumulation of A11 and OC conformers in MB extracts of Tg2576 animals. (Histograms represent the mean ± standard deviation; one-way ANOVA [$F_{(3,20)} = 14.9375$, $P < 0.0001$, $F_{(2,15)} = 13.8173$, $P = 0.0004$, $F_{(1,10)} = 19.8003$, $P = 0.0012$ and respectively] followed by Student *t* test with Bonferroni correction; $^{\bigstar}P < 0.05$ *vs.* 4-month-old Tg2576 mice, $^{\star}P < 0.05$ vs. 7-month-old Tg2565 mice, n = 6/age). (**C**) Regression analyses between OC-immunoreactive Aβ species and Cdk5 activation assessed by the p25/p35 ratio at 12 and 16 months of age revealed positive correlations ($R^2 = 0.7544$, $F = 12.2901$ and $R^2 = 0.8854$, $F = 30.9039$, $n = 6$/age).

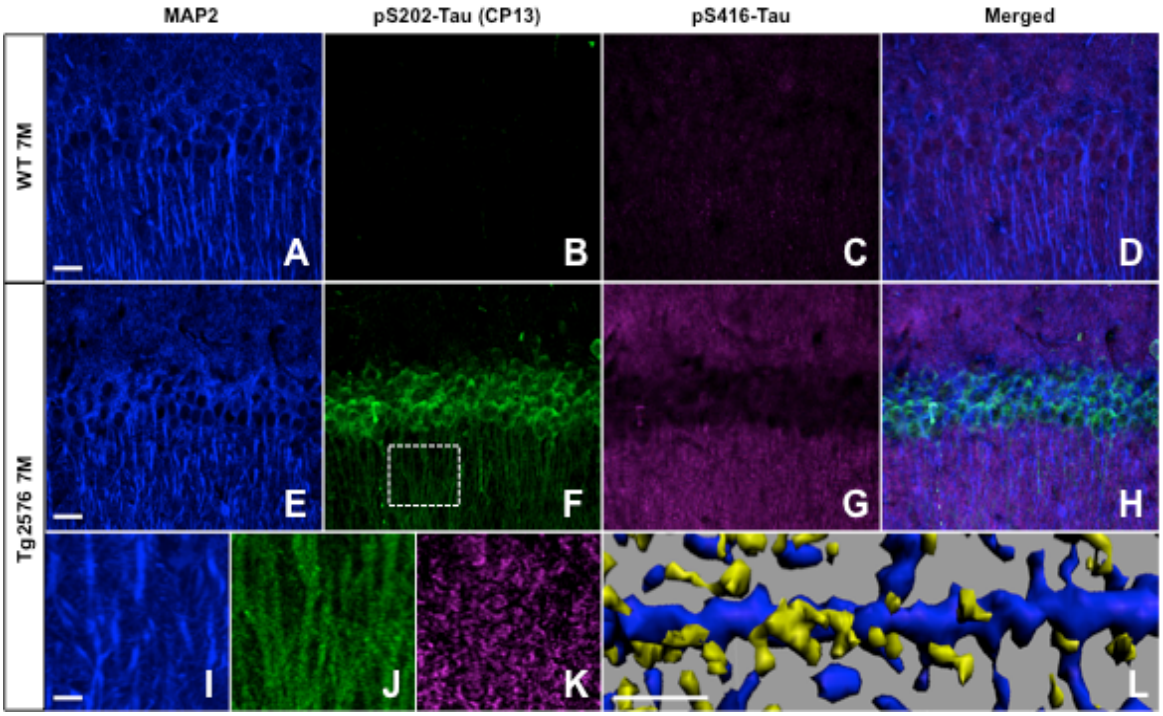

Figure 18. Abnormal phosphorylation and missorting of tau in the CA1 pyramidal neurons of 7-month-old Tg2576 mice . (**A-K**) Representative confocal images of CA1 hippocampal neurons immunostained for the microtubule-associated protein 2 (MAP2; blue channel, [A, E, I]), pS202-Tau (CP13; green, [B, F, J]) and pS416-Tau (magenta, [C, G, K]) revealed an aberrant accumulation and differential missorting of soluble tau species in 7-month-old Tg2576 mice. The bottom row images (I-K) illustrate the synaptic localization of pS416-tau in transgenic hippocampal cells. (**L**) Using Bitplane's Imaris 7.x suite, volume renderings of the MAP2, pS202-Tau and pS416-tau channels were created and a colocalization channel for the soluble tau species was generated (displayed in yellow). The resulting channel is shown with the 3D rendering of MAP2 to illustrate the colocalization of abnormal tau species at dendritic spines. (Scale bars = 20 μ m [A-H], 10 μ m [I-K],3 μ m [L],; n = 6 sections/animals; N = 3-6 animals /age/genotype).

To demonstrate that Aβ*56 is triggering these pathological changes in tau, we exposed primary cortical neurons to increasing concentrations of Aβ*56 previously shown to activate CaMKII, and examined the phosphorylation/missorting status of tau (**Fig. 19**). Mirroring the data observed in 7-month-old Tg2576 mice, tau phosphorylation was

unaltered at Y18, S262, S396/S404 and S409 in the presence of Aβ*56 (**Fig. 19A, B**). In contrast, neuronal levels of soluble pS202-Tau and pS416-Tau rose sharply in a dose-dependent manner in presence of increasing amounts of Aβ*56 (**Fig. 19A, B**). It is worth noting that although purified Aβ dimers and trimers can trigger a Fyn-mediated phosphorylation of tau at Y18 (Larson et al., 2012a), neither species induced the hyperphosphorylation of tau at S202 and S416 (**Fig. 20**). In parallel, an Aβ*56-mediated ~2 to 2.5-fold accumulation of tau was observed in membrane-enriched lysates containing PSD-95 (**Fig. 19C, D**). These *in vitro* findings demonstrate that Aβ*56 causes highly selective pathological changes in the tau protein.

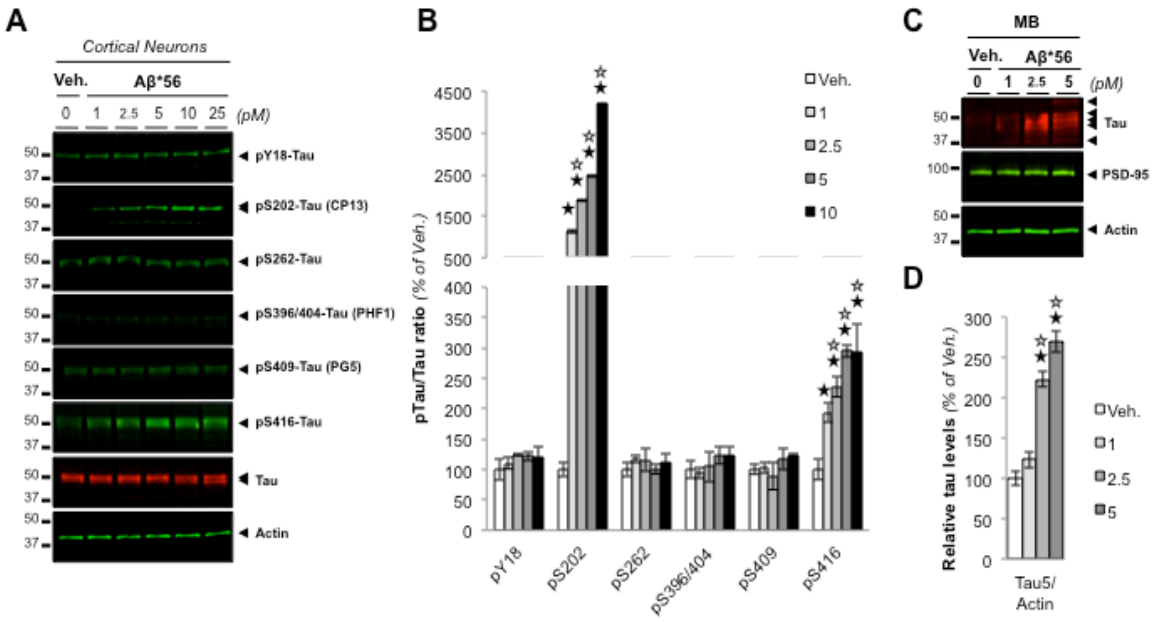

Figure 19. Selective tau hyperphosphorylation in primary neurons exposed to Aβ*56. (**A**) Western blot analysis of soluble tau species detected in mouse cortical neurons exposed to increasing concentrations of Aβ*56 for 60 minutes. (**B**) Quantification of the modified/total Tau ratio revealed a dose-dependent increase in both pS202-Tau and pS416-Tau compared to controls. Due to the large magnitude of the effects of Aβ*56 on pS202-Tau, the y-axis was broken. (Histograms represent the mean ± standard deviation; one-way ANOVA [$F_{(2,21)}$ = 67.6019, P < 0.0001] followed by Student t test with Bonferroni correction, ★P < 0.05 *vs.* vehicle-treated neurons, ☆P < 0.05 *vs.* 1 pM Aβ*56 condition, n = 6-8/treatment). (**C**) Western blotting images for total soluble tau detected with the antibody tau5, PSD-95 and actin in MB extracts of vehicle or Aβ*56 treated

neurons. (**D**) Densitometry analysis indicated an abnormal accumulation of tau in MB lysates in cells that received ≥ 2.5 pM Aβ*56. (Histograms represent the mean ± standard deviation; one-way ANOVA [$F_{(2,21)}$ = 67.6019, $P < 0.0001$] followed by Student *t* test with Bonferroni correction, ★$P < 0.05$ *vs.* vehicle-treated neurons, ☆$P < 0.05$ *vs.* 1 pM Aβ*56 condition, n = 6-8/treatment).

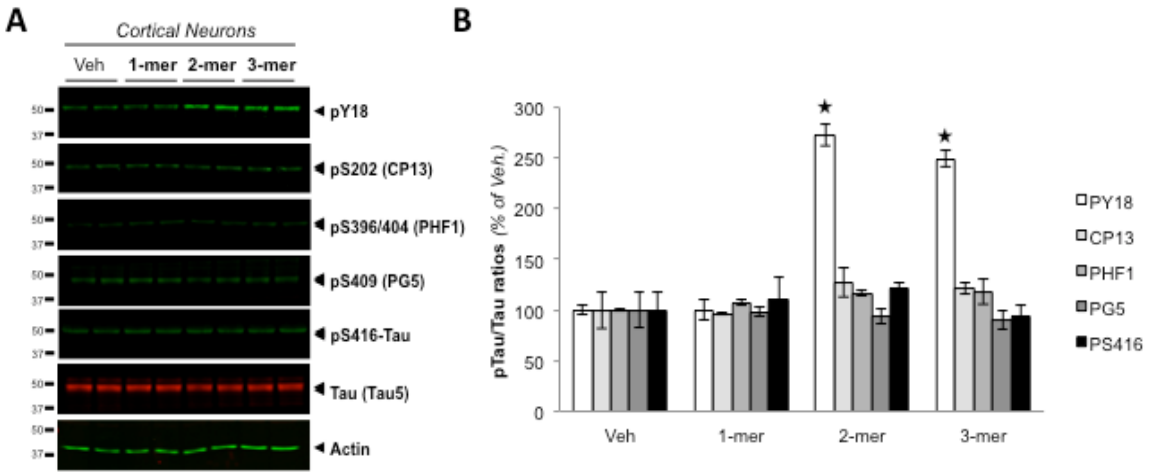

Figure 20. Brain-derived Aβ dimers and trimers do not induce tau hyperphosphorylation at Serine 202. (**A**) Western blot analysis of tau phosphorylation at Y18, S202, S396/404, S409 and S416 in primary mouse cortical neurons. Oligomeric Aβ were applied at 1nM (Aβ monomer equivalent) for 60 minutes. Tau5 was used to measure total tau levels and actin was used as internal control. (**B**) Densitometry analysis of tau protein changes relative to total tau levels detected with Tau5 confirmed that low-*n* Aβ oligomers trigger a Fyn-dependent phosphorylation of tau at Y18 as previously reported (Larson *et al.*, 2012). No changes were observed for the other phosphoepitopes tested. (Histograms represent the mean ± standard deviation; one-way ANOVA [$F_{(3,12)}$ = 177.8357, $P < 0.0001$; $F_{(3,12)}$ = 0.1351, P = 0.9372; $F_{(3,12)}$ = 0.3881, P = 0.7637; $F_{(3,12)}$ = 0.0393, P = 0.9891 and $F_{(3,15)}$ = 0.4221, P = 0.7399 for pY18-, pS202-, pS396/404-, pS409- and pS416-Tau respectively] followed by Student *t* test with Bonferroni correction; ★$P < 0.05$ *vs.* vehicle, n = 4-5/group).

*B. Aβ*56-Induced hyperphosphorylation and misslocalization of tau is dependent on CaMKII activity.*

To further demonstrate that the downstream signaling cascade induced by Aβ*56 is dependent on CaMKII, we applied Aβ*56 at a final concentration of 2.5 pM to primary cultured neurons pretreated with tatCN21, a selective inhibitor of CaMKII (Vest et al., 2007) for 15 min (**Fig. 21**). As previously described (**Fig. 7**), a 60 min exposure to 2.5pM

Aβ*56 triggered a 2.28-fold increase in CaMKII phosphorylation at T286 compared to vehicle-treated cells (**Fig. 21A, B**). Pretreatment with 1 μM tatCN21 prevented the elevation in pT286-CaMKII induced by Aβ*56 (118 ± 11.85 vs. 228.18 ± 10.95, $P < 0.05$) and, importantly, maintained CaMKII activity levels at baseline. As predicted, tatCN21 lowered the baseline levels of active CaMKII in the primary neurons.

Once the efficacy and the extent of the inhibition of CaMKII was established in the presence of Aβ*56, we evaluated a potential rescue of the tau phenotype (**Fig. 21C-E**). In the presence of 2.5 pM Aβ*56 alone, pS416-tau levels increased by ~2-fold (2.03 ± 9.79) compared to the vehicle control as shown in Fig. 19. In addition, a putative misfolded tau conformer was readily observed (**Fig. 21C**). Inhibiting CaMKII with tatCN21 blocked the aberrant hyperphosphorylation of tau at S416 and prevented the observed shift in the folding of tau proteins (**Fig. 21C, D**). Similar observations were made for tau phosphorylation at S202 (**Fig. 21E**).

Moreover, we addressed whether inhibiting CaMKII could block the apparent missorting of tau triggered by Aβ*56. Pretreating cortical neurons with tatCN21 completely abolished the translocation of tau to dendrites and into dendritic spines induced by Aβ*56 exposure (**Fig. 22A-C**). Furthermore, the biochemical segregation of tau into membrane-enriched compartments further supported these findings (**Fig. 22D,E**), indicating that tau hyperphosphorylation at S416 might be necessary to redistribute tau.

Finally, to demonstrate that NMDAR activity is required to mediate the effects of Aβ*56, primary neurons were first pretreated with the NMDAR-PSD uncoupling peptide tatNR2B9c (Aarts et al., 2002) in the presence or absence of Aβ*56. We found that disrupting the interaction between NMDAR and PSD-95 inhibited the hyperphosphorylation of tau at S202 and S416 induced by Aβ*56 (**Figure 23**), reminiscent of the protection conferred by the peptide from Aβ-induced toxicity (Ittner et al., 2010).

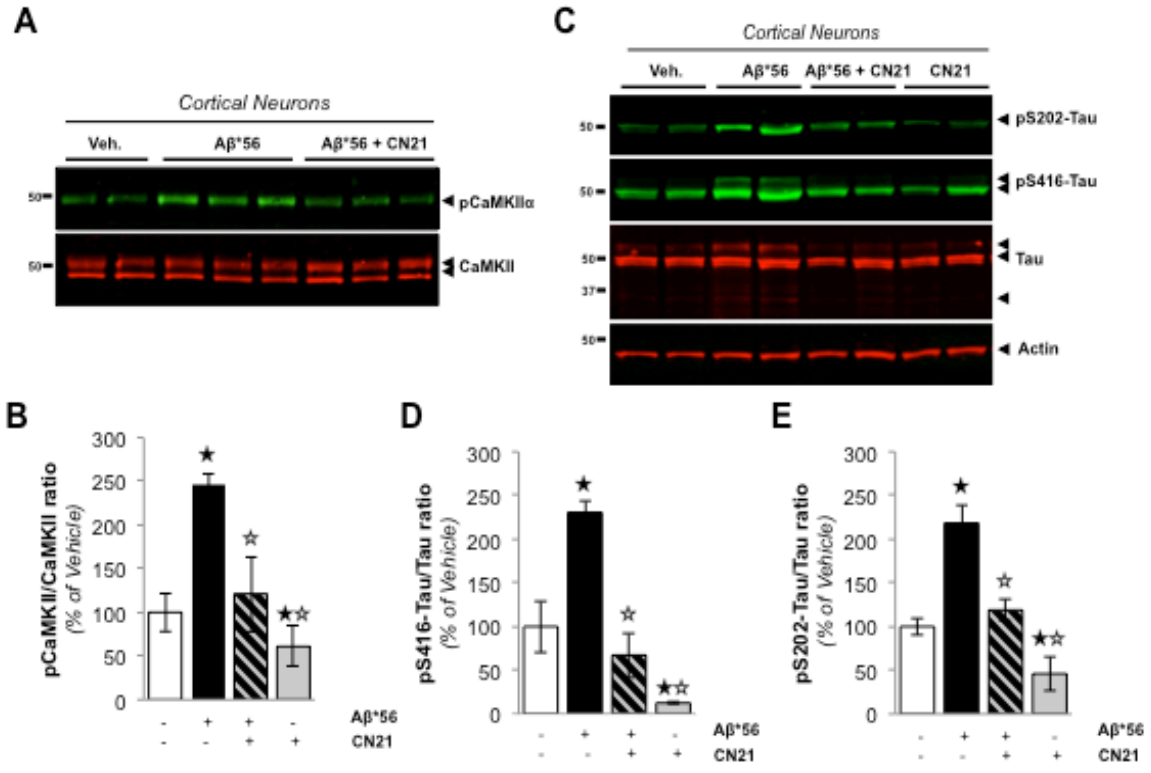

Figure 21. Inhibiting CaMKII prevents Aβ*56-induced tau hyperphosphorylation at S416. (**A**) Representative quantitative western blotting images for pT286-CaMKIIα and total CaMKII in primary cortical neurons pretreated with the CaMKII inhibitor tat-CN21 in presence or absence of 2.5 pM Aβ*56. (**B**) Quantification of the phosphorylated/total CaMKII ratio confirmed that the pretreatment with tat-CN21 prevented the over-activation of CaMKIIα triggered by Aβ*56 in primary neurons. (Histograms represent the mean ± standard deviation; two-way ANOVA [$F_{(3,35)} = 25.0063$, $P < 0.0001$] followed by Student t test with Bonferroni correction, $^{\bigstar}P < 0.05$ *vs.* vehicle-treated neurons, $^{\bigstar}P <$

0.05 *vs.* Aβ*56-treated neurons, n = 6-9/group). The ANOVA revealed a significant effects of Aβ*56 ($F = 26.7966$, $P < 0.0001$), of tat-CN21 ($F = 16.2025$, $P = 0.0003$) and Aβ*56xtat-CN21 interaction ($F = 27.4058$, $P < 0.0001$). (**C**) Western blot analysis for soluble pS416-Tau and total tau (as measured with the tau5 antibody) in mouse primary neurons pretreated with the CaMKII inhibitor tat-CN21 in presence or absence of 2.5 pM Aβ*56. (**D, E**) Quantification of the phosphorylated/total tau ratio confirmed that the pretreatment with tat-CN21 prevented the hyperphosphorylation of tau at S416 (*D*) and S202 (*E*) triggered by Aβ*56. (Histograms represent the mean ± standard deviation; two-way ANOVA [$F_{(3,35)} = 28.4569$, $P < 0.0001$ and $F_{(3,35)} = 24.8972$, $P < 0.0001$ respectively] followed by Student t test with Bonferroni correction, $^{\bigstar}P < 0.05$ *vs.* vehicle-treated neurons, $^{\bigstar}P < 0.05$ *vs.* Aβ*56-treated neurons, n = 6-9/group).

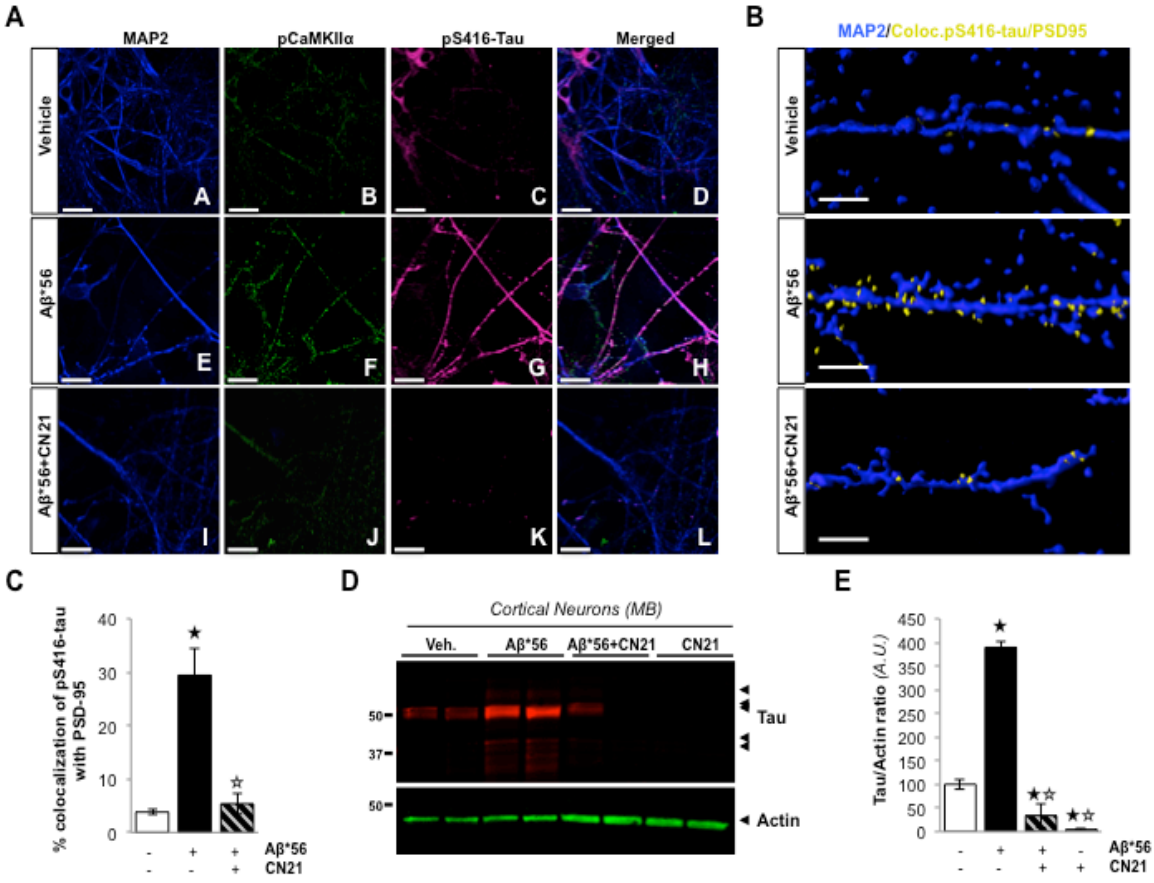

Figure 22. CN21 pretreatment prevents the missorting of tau in cortical primary neurons exposed to Aβ*56. (**A**) Representative confocal images of primary mouse cortical neurons immunostained for the microtubule-associated protein 2 (MAP2; blue channel, [A, E, I]), pT286-CaMKIIα (green, [B, F, J]) and pS416-Tau (magenta, [C, G, K]) revealed an abnormal cellular localization of soluble tau species in neurons treated with 2.5 pM Aβ*56 for 60 minutes. Please note the somatic distribution of pS416-tau in *C* while it is preferentially detected in dendrites in *G*. (Scale bar = 30 µm; n = 6 dishes/group). (**B**) Surface of dendrites labeled with MAP2, pS416-tau and PSD-95 illustrating the cellular distribution of the pS416-tau/PSD-95 colocalization channel (shown in yellow) with respect to MAP2 (in blue) in neurons treated with vehicle, 2.5 pM

Aβ*56 or tatCN21 pretreatment (15 minutes) followed by 2.5 pM Aβ*56 for 60 minutes. Scale bar = 3 μm. (**C**) Quantification of the colocalization of pS416-tau with PSD-95 in mouse primary neurons exposed to vehicle, 2.5 pM Aβ*56 or tatCN21 pretreatment (15 minutes) followed by 2.5 pM Aβ*56. (Histograms represent the mean ± standard deviation; one-way ANOVA [$F_{(2,20)} = 67.7832$, $P < 0.0001$] followed by Student *t* test with Bonferroni correction; $^{\bigstar}P < 0.05$ *vs.* vehicle, $^{\star}P < 0.05$ *vs.* Aβ*56-treated neurons, $n = 8$ ROIs/group). (**D**) Representative western blot images for soluble tau in MB extracts of neurons exposed to vehicle, Aβ*56, Aβ*56+CN21 and CN21 using tau5. Actin was used as internal standard. (**E**) Densitometric analyses revealed an abnormal ~4-fold accumulation of tau species in membrane-enriched lysates of neurons treated with Aβ*56, which was blocked by pretreating cells with tatCN21 for 15 minutes. (Histograms represent the mean ± standard deviation; one-way ANOVA [$F_{(3,12)} = 197.3191$, $P < 0.0001$] followed by Student *t* test with Bonferroni correction; $^{\bigstar}P < 0.05$ *vs.* vehicle, $^{\star}P < 0.05$ *vs.* Aβ*56-treated neurons, $n = 4$/group).

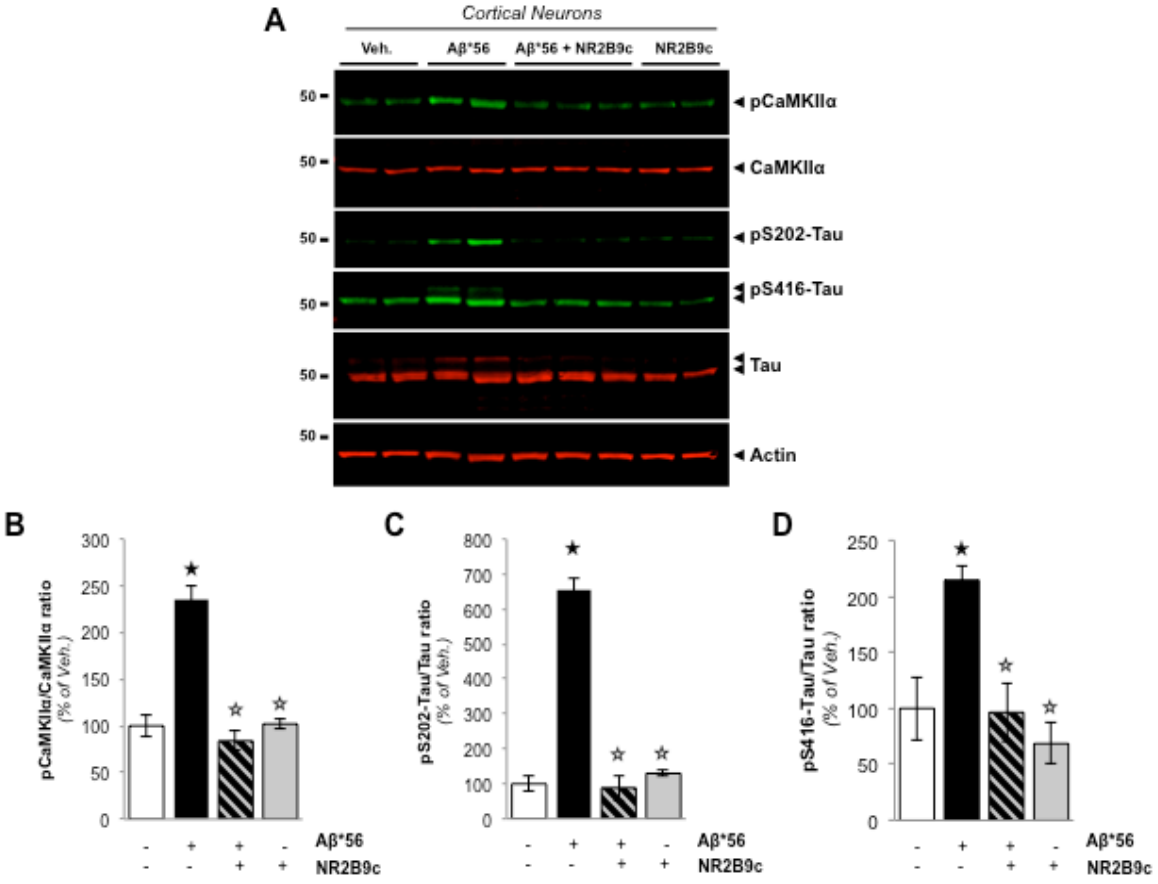

Figure 23. Uncoupling NMDAR from the PSD prevents Aβ*56-induced tau hyperphosphorylation at S416. (**A**) Representative quantitative western blotting images for pCaMKIIα, CaMKIIα, pS202-Tau, pS416-Tau, total Tau and actin in primary cortical neurons pretreated with the NMDAR uncoupling peptide tat-NR2B9c for 15 minutes in presence or absence of 2.5 pM Aβ*56. (**B, C, D**) Quantification of the pCaMKII/CaMKII (*b*) and phosphorylated/total tau ratios (*c, d*) confirmed that the pretreatment with tat-NR2B9c prevented the CaMKII overactivation and the hyperphosphorylation of tau

triggered by Aβ*56 in primary neurons. (Histograms represent the mean ± standard deviation; one-way ANOVA [$F_{(3,14)}$ = 252.0481, P < 0.0001, $F_{(3,14)}$ = 22.6029, P < 0.0001 and $F_{(3,12)}$ = 16.1364, P = 0.0009 respectively] followed by Student t test with Bonferroni correction; ★P < 0.05 *vs.* vehicle, ☆P < 0.05 *vs.* A β *56-treated neurons, n = 4-6/group).

III. Discussion

Here we demonstrated a hyperphosphorylation of tau at S416 and S202, two sites that are hyperphosphorylated in early stages of AD, in the presence of A β *56 both *in vivo* and *in vitro* via a CaMKII activity dependent pathway. CaMKII has multiple substrates one of which is tau. Since S416-tau is a substrate of CaMKII this could be the mechanism by which A β *56 induced hyperphosphorylation of tau at that. However, A β *56 also increases phosphorylation of tau at S202 which is not a direct target of CaMKII as it does not correspond to the consensus sequence of the kinase. Yet, inhibition of CaMKII activity leads to the return to basal levels of tau phosphorylation at S202. These findings lead us to think that the phosphorylation at S202 may follow a hierarchical phosphorylation process of tau as is observed in the case of GSK3 anad PKA (Hanger et al., 2009; T. Li & Paudel, 2006; Woods et al., 2001). We speculate that "substrate priming" at S416 may be responsible for the subsequent S202 phosphorylation.

Interestingly, the phosphorylation of tau by A β *56 at these two sites seems to be selective and specifically dependent on CaMKII activity. Other phosphorylations sites, such as Y18, S262, S409 and S396/S404, evaluated are unchanged in the presence of A β *56. Further, other well studied kinases in AD (e.g. Cdk5 and GSK3) are not modulated by A β *56 in vitro and in the 7 month old Tg2576 mice. It is worth noting that other A β species (monomer, dimer, trimers, protofibrils) studied did not affect tau

phosphorylation at S416 even though some of them have been shown to induce tau phosphophorylation at other sites such as Y18 (Larson et al., 2012). Further, this hyperphosphorylaton of tau in the presence of A β *56 is accompanied by a translocation of the protein into the PSD where it is not normally found, at least not at the resting state of the neuron. This A β *56-induced missorting of tau is dependent on pCaMKII as inhibition of the kinase directly or via internalization of the NMDAR leads to an abolition of the abnormal cellular distribution of tau. In conclusion, our findings suggest that A β *56 is mediating its deleterious effects by promoting an abnormal activation of CaMKII that leads to the specific and selective hyperphosphorylation of tau and consequently miss-localization of the tau into the dendritic spines.

Chapter 4
A β *56-induced pathological changes in neuronal signaling and tau state in another mouse model of Alzheimer's disease, J20

I. Introduction

Multiple mouse models have been generated to recapitulate the major neuropathological hallmarks of the disease, notably amyloid- β plaques and neurofibrillary tangles. The generation of these models is based on the genetics of AD or expression of human tau. A transgenic model of AD often contains human *APP* (hAPP) and/or *PSEN1/2* with the genetic mutations described in AD or contains the tau manipulations that lead to the formation of neurofibrillary tangles. Expression of mutant *APP* (hAPP) and/or *PSEN1/2* increase formation of the A β peptide and accumulation of the protein in plaques, soluble assemblies and several other APP fragments that can be biologically active. The Tg2576 mouse above used is one of these mouse models that

recapitulate certain aspects of AD, amyloidosis, tau hyperphosphorylation, cellular deficits and cognitive dysfunction. This line expressed human APP with the Swedish mutation (Hsiao et al., 1996). It is clear that A β *56 is found in this mouse model and leads to the previously described changes potentially mediating its deleterious effects. However, the soluble assembly A β *56 is also found in other mouse models such as the J20 (Cheng et al., 2007). J20 overexpresses hAPP with the Swedish and Indiana mutation (Mucke et al., 2000). Several A β species are detectable in the brain of this mouse with several other APP fragments. A β *56 is detectable at 3-4 months of age when spatial cognitive deficits are first detected (Cheng et al., 2007). We ask whether the presence of A β *56 in this mouse model leads to the changes we described in the Tg2576 mouse.

II. Results

As mentioned above A β *56 is expressed in the J20 at an earlier age than in the Tg2576. We analyzed the CaMKII/tau axis in these mice at 3 and 6 months of age as A β *56 has been shown to be expressed at 3 month of age. Similar to Tg2576 mice phosphorylation of CaMKIIα is significantly increased in the J20 at 3 and 6m month of age when compared to the age matched wild-type (WT) mice (**Figure 24A, B**). This increase in CaMKII though to a lesser extent follows the same profile, as when the IC fraction is examined the abnormal activation of CaMKII appears to be transient. The increase in CaMKII phosphorylation at 6 months is significantly lower than compared to 3 months J20 (**Figure 24A, B**). We found that CaMKII activity at 9 month in the intracellular

fraction of the J20 (IC brain lysates) is not significantly different from WT (**Figure 24C, D**).

Considering that CaMKII can phosphorylate tau and the increase in tau phosphorylation at S416 and S202 previously observed in the Tg2576 mice when Aβ*56 was present, we examined tau phosphorylation in the J20 mice when Aβ*56 is present. Similar to the Tg2576 mice pS202-tau and pS416-tau was selectively increased at 3 months and declined (by how many folds) at 6 months of age in the J20 brain lysates (**Figure 25**). The other tau phosphorylation site examined S262 was not significantly altered when comparing the 3 and 6 month J20 compared to the WT (**Figure 25**). These findings therefore demonstrate that the specific alteration of the CaMKII/tau axis by Aβ*56 is not specific to one mouse model but may be a general feature of AD mouse models.

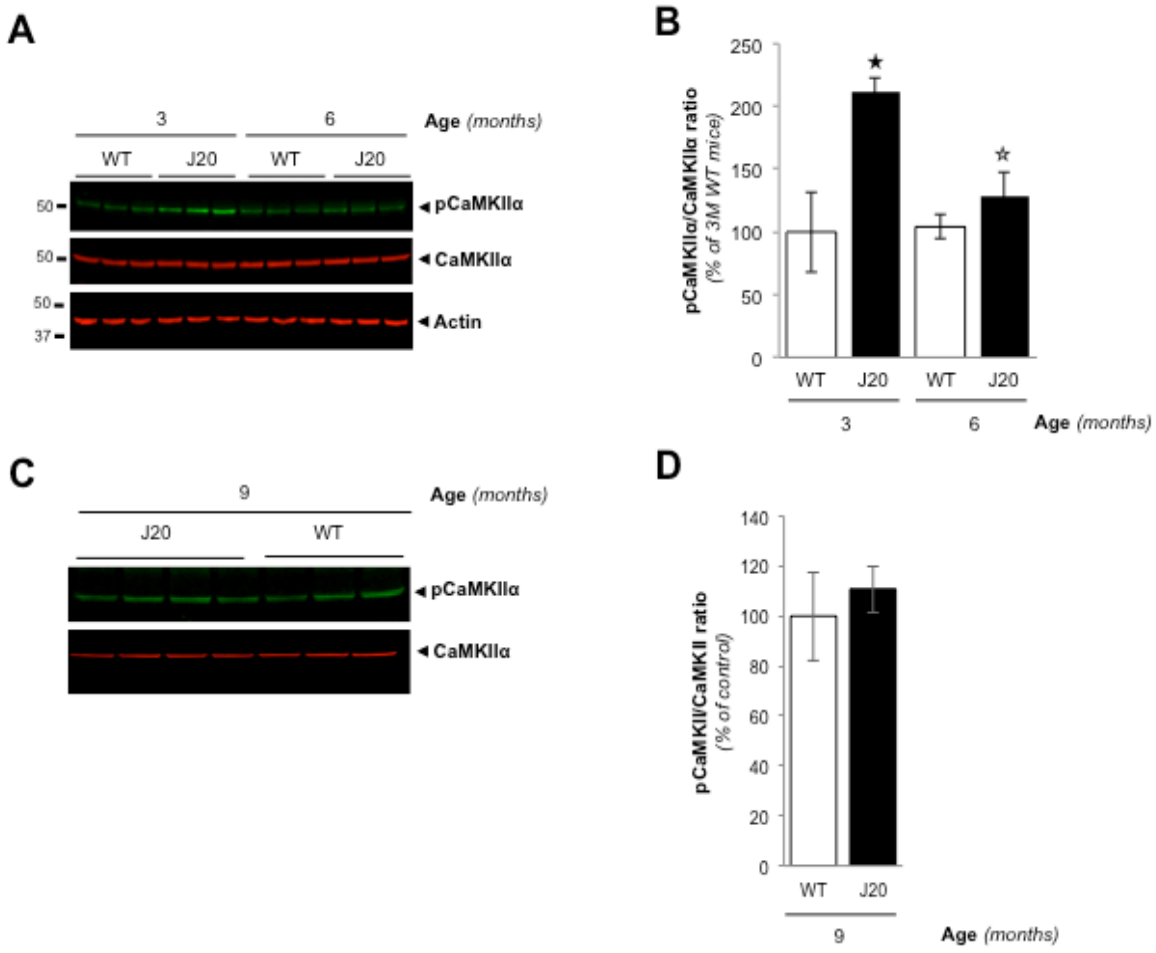

Figure 24. Aberrant phosphorylation of CaMKII in young J20 mice expressing Aβ*56. (**A, C**) Representative quantitative western blotting images for pCaMKIIα and total CaMKII in WT and J20 mice at 3, 6 and 9 months of age. (**B, D**) Quantification of the phosphorylated/total CaMKIIα ratio indicated that CaMKII is overactivated at ages in J20 when Aβ*56 is first detected (Cheng *et al.*, 2007). n = 5/group).

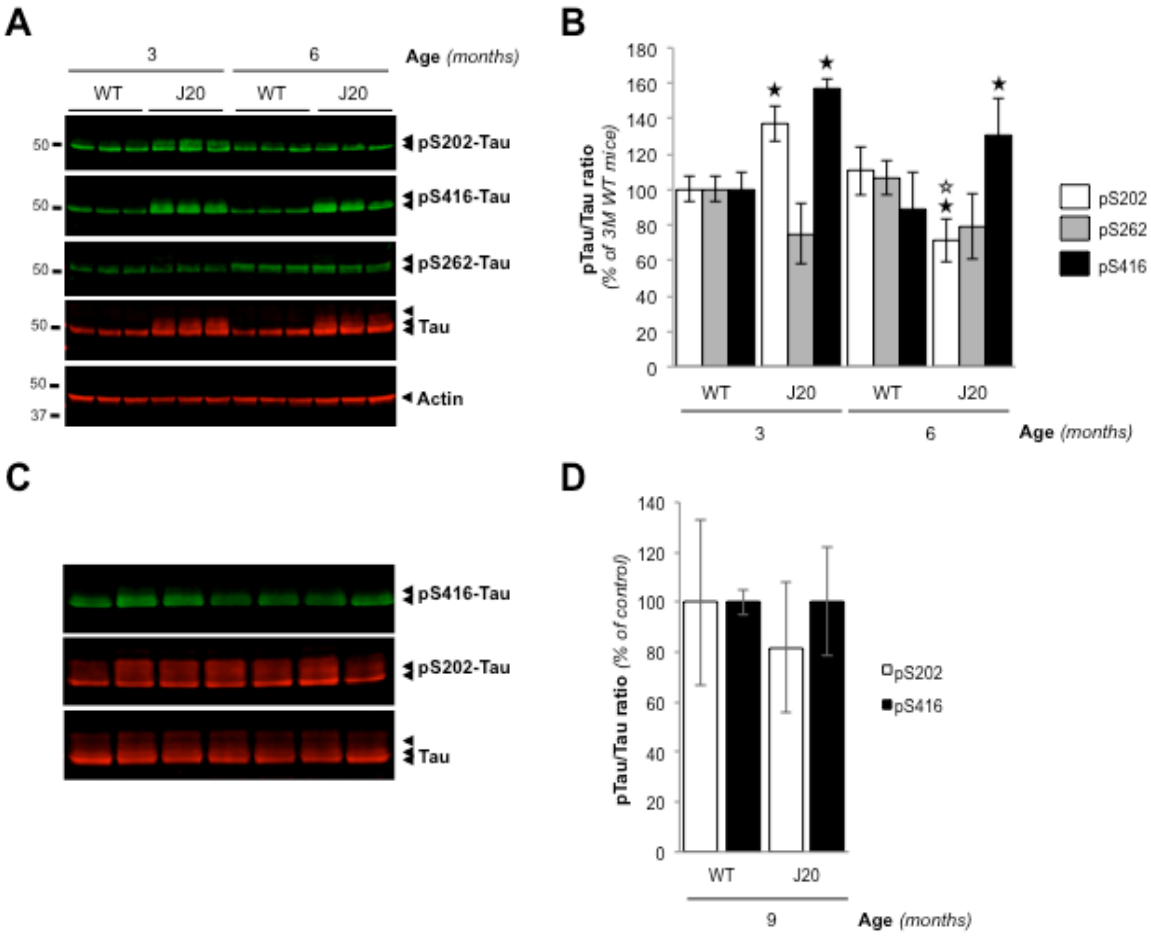

Figure 25. Aberrant phosphorylation of tau in young J20 mice expressing Aβ*56. (**A, C**) Representative quantitative western blotting images for pS202-Tau, pS416-Tau, pS262-Tau and total Tau our J20 cohort. (**B, D**) Quantification of the phosphorylated/total tau ratios confirmed that a selective hyperphosphorylation of Tau associated with Aβ*56 in J20 mouse brains similar to those observed in Tg2576 animals. The analysis for pS202-Tau revealed no significant effects of transgene ($F = 0.0053$, $P = 0.9426$) due to opposite variations with aging, but significant effects of age ($F = 15.4113$, $P = 0.0012$) and transgene*age interaction ($F = 21.9372$, $P = 0.0002$). The analysis for pS262-Tau revealed a significant effect of transgene ($F = 19.5346$, $P = 0.0004$), but no effects of age ($F = 0.9088$, $P = 0.3546$) or transgene*age interaction ($F = 0362$, $P = 0.8515$). Finally, the analysis for pS416-Tau revealed significant effects of transgene ($F = 45.4571$, $P < 0.0001$), of age ($F = 4.6441$, $P = 0.0367$) but no transgene*age interaction ($F = 0.3975$, P = 0.5373). (Histograms represent the mean ± standard deviation; two-way ANOVA [$F_{(3,16)} = 12.4513$, $P < 0.0001$, $F_{(3,16)} = 6.8265$, $P = 0.0036$ and $F_{(3,16)} = 16.8329$, $P < 0.0001$ for S202, S262 and S416 respectively] followed by Student t test with Bonferroni correction, ★$P < 0.05$ vs. 3-month-old WT mice, ☆$P < 0.05$ vs. 3-month-old J20 mice, n = 5/group).

III. Discussion

Examination of the J20 mouse indicated an abnormal increase in phosphorylation of CaMKII in this line at ages when A β *56 was detected. In the IC fraction the abnormal elevation of pCaMKII levels appeared to be transient as the levels decreased overtime even though the levels of A β *56 persist, just as has been observed in Tg2576 mice. The levels of CaMKII activity in the PSD containing fraction was not evaluated in this paradigm but it would not be unreasonable to predict a persistent increase in pCaMKII levels mirroring the levels of A β *56, similar to our observations in Tg2576 mice. Further, the Phosphorylation of tau at S202 and S416 showed an increase in the J20 at 3 months and declined toward normal levels at 6 and 9 month of age. This hyperphosphorylation of tau in the presence of A β *56 seems specific as other phosphorylation sites of tau examined were unchanged.

All these findings appear to support an important role of the CaMKII/tau axis in modulating the deleterious effects of A β *56 in mouse models of Alzheimer's disease. The prove of this concepts in these two mouse models with not only different AD associated mutation but also different backgrounds provides a general pathway A β *56 could be causing cognitive deficit in mice in general and possibly in human.

Chapter 5
Association of A β *56 with abnormal molecular changes in cognitively intact human subjects

I. Introduction

Alzheimer's disease is a progressive neurodegenerative disorder that initially presents

with difficulties in episodic memory and acquisition of new memories. Clinical diagnosis of probable Alzheimer's disease dementia is made when these impairments progress to include remote memory and executive functions severe enough to interfere with the patient's daily living. The stage preceding the diagnosis of probable AD is referred to as the mild cognitive impairment (MCI) phase during which cognitive deficit is apparent but not severe enough to meet the criteria for AD clinical diagnosis. Recent biomarker studies have demonstrated that the neuropathology of AD may begin years prior to the onset of clinical symptoms (Bateman et al., 2012; Moonis et al., 2005; J. C. Morris et al., 2009; Skoog et al., 2003; Storandt, Mintun, Head, & Morris, 2009). This stage is typically referred to as the asymptomatic or preclinical phase of AD.

The notion of a preclinical phase of AD was initiated when it became clear that amyloid plaques correlated poorly with cognitive function (Bennett et al., 2004; Giannakopoulos et al., 2003; Terry et al., 1991) and after neuroimaging studies have demonstrated that large proportion of non-demented older adults have significant amyloid deposition in the brain (Aizenstein et al., 2008; Mintun et al., 2006; Morris et al., 2014; Rowe et al., 2010). These findings have driven the hypothesis of the existence of a preclinical phase of AD with pathology accompanied by abnormalities in brain without apparent neurodegeneration (Price & Morris, 1999). In deed amyloid imaging studies have demonstrated an elevated amyloid deposition in the brains of presymptomatic carriers of autosomal dominant mutations linked to familial AD several years before expected age of onset (Klunk et al., 2007; Knight et al., 2011; Villemagne et al., 2009). Furthermore, amyloid positivity in cognitively normal subjects is associated with regional brain

atrophy (Chetelat et al., 2012; Dickerson et al., 2009; Mormino et al., 2009). Cerebrospinal fluid (CSF) studies also support the existence of an asymptomatic phase of AD. Amyloid plaque deposition in the brain is believed to echo a decrease in CSF Aβ1-42 levels in AD subjects compared to controls (Fagan et al., 2007; Sunderland et al., 2003). Low CSF Aβ1-42 has been associated with whole-brain atrophy (Fagan et al., 2009). In subjects with AD-linked mutation decreased CSF Aβ1-42 has been described several years before estimated age of onset (Moonis et al., 2005).

All these findings support the hypothesis of an asymptomatic phase of AD during which there is pathological processes occurring that precede cognitive dysfunction. This divides Alzheimer's disease in three stages two symptomatic stages that end in full blown AD preceded by a MCI stage and an asymptomatic phase usually referred to as preclinical AD.

II. Results

As previously mentioned Aβ*56 appears to play a role in the asymptomatic phase of AD. First of all Aβ*56 has been shown to increase in brains of cognitively intact older adults starting in the fifth decade of life with the levels of soluble tau increasing in parallel (Lesné et al., 2013). Further, in that study Aβ*56 strongly correlated with two pathological forms of soluble tau (tau-Alz50 and pS202-tau). CP13 (pS202-tau) is one of the earliest pathological tau changes (Andorfer et al., 2003). Supporting the involvement of Aβ*56 in the preclinical stage of AD is a negative correlations between Aβ*56 and

two postsynaptic proteins (Lesné et al., 2013).

Since Aβ*56 has been found to be elevated in cognitively unimpaired subject starting in their 40s and keep increasing over time but drops in MCI and AD brains we wondered whether pCaMKII which seems to be mediating the effects of Aβ*56 in mouse brain and *in vitro*, is modulated in the human brain when Aβ*56 is elevated. Using a subset of subjects from the Lesne et al study (2013), we found here that CaMKIIα activity was higher in older brains compared to young subjects' brains. Active CaMKII levels rose significantly in this cohort starting in the fifth decade of life and continued to rise with age in subjects in their 60s with intact cognition (**Fig. 26A**). In addition to the rise in parallel of Aβ*56 with pCaMKII, active CaMKII levels also positively correlated with Aβ*56 brain levels (Spearman Rho = 0.559, $P = 0.0001$, n = 46; **Fig. 8**) in unimpaired elderly subjects. These observations suggest that Aβ*56 is abnormally elevating the activity of CaMKII for up to 2-3 decades in humans, possibly creating a chronic sublethal stress level that might constitute one of the first initializing steps of the presymptomatic phase of AD.

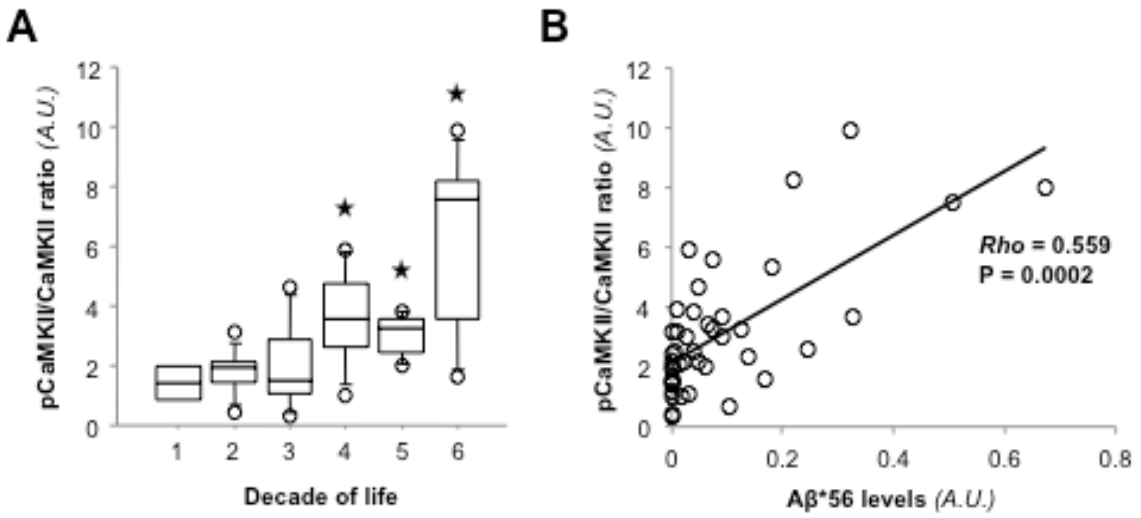

Figure 26. CaMKII activity increases with aging in the first six decades of life and is associated with Aβ*56 levels in human brain tissue. Total CaMKII, pT286-CaMKII and Aβ*56 protein levels were determined in the inferior temporal gyrus of cognitively intact subjects from the Brain and Tissue Bank for Developmental Disorders, University of Maryland Baltimore. (**A**) Box plot analyses revealed a rise of CaMKII phosphorylation at T286 with aging in postmortem brain tissue. (N = 46, ★P < 0.05 compared to second decade group, Kruskal-Wallis [$\chi^2_{(5,36)}$ = 15.1795, P = 0.0096] followed by Bonferroni-corrected Mann-Whitney U tests). (**B**) Regression analyses indicated that Aβ*56 levels positively correlated with active pCaMKII (N = 46; Spearman rank correlation, P = 0.0002).

III. Discussion

It is a widely accepted notion that Alzheimer's disease can be divided in three different clinical phases: a preclinical phase, an MCI and full-blown AD. Here we showed that Aβ*56 is elevated in human brains of cognitively intact individuals that could be in their asymptomatic (preclinical) phase starting in the 5th decade of life. Interesting previous a study has shown a decline of Aβ*56 levels in MCI and AD (Lesné et al., 2013), suggesting that Aβ*56 may be playing a more significant role in the preclinical phase of AD rather than in AD or MCI. Coincidently, levels of active CaMKII are elevated in that same group of subjects that could be in the preclinical phase of AD starting in their 40s.

Further we showed a strong correlation of pCaMKII with Aβ*56 in the same cohort, suggesting a relationship between the two proteins in this paradigm. Our findings support the idea that Aβ*56 effects in potential preclinical Alzheimer's disease could be mediated by CaMKII activity as found in mice and *in vivo*, providing insight on possible earlier molecular changes in AD.

Chapter 6
Discussion and future directions

In the previous studies we demonstrated that Aβ*56 coimmunoprecipitates with the NMDA receptor subunits GluN1, GluN2A and GluN2B in Tg2576 mice and brain of cognitively intact human subjects. Further, we showed that Aβ*56 binds to the GluN1 subunit and not the GluN2B subunit in HEK293T cells. This interaction of Aβ*56 with the NMDAR seemed to have functional implications as bath application of the oligomer to primary cortical neurons induced an enhanced Ca2+ influx through the NMDAR. Consequently, CaMKII activity is elevated in the presence of Aβ*56 both *in vivo* and *in vitro*. In both the young Tg2576 mice and in neurons treated with Aβ*56 purified from aged APP transgenic animals the elevation of CaMKII activity is paralleled with the translocation of the kinase to the PSD, in line with the described physiological behavior of CaMKII (Coultrap et al., 2011), that persist with the levels of Aβ*56. Interesting we also demonstrated a hyperphosphorylation of tau at two sites S202 and S416 in the presence of Aβ*56. This increase in tau phosphorylation by Aβ*56 is accompanied with a translocation of tau into the dendritic spines.

There are several important new concepts that can be derived from our findings. First of all, the increase in CaMKII in the membrane fraction followed the same profile as the detection of Aβ*56 in that same fraction. Aβ*56 is detected on the MB faction of Tg2576 mice starting at 6 month and slight increases with age (Lesné et al., 2006). Coincidently the interaction of Aβ*56 with the NMDAR subunit steadily increased with age in those same animals. This existing data supports the conclusion that CaMKII activity is modulated continuously by Aβ*56.

Second Aβ*56 seems to activate a pathway that is different from the signaling pathway that appear to be involved in mediating the toxicity of other Aβ species. For instance, even though Aβ*56 is capable of increasing activation of CaMKII by more than two fold, a thousand time higher concentrations of Aβ monomers, dimers, or timers could not induce modulation of the kinase activity. In addition to being specific, this activation of CaMKII by Aβ*56 is selective. Kinases previously described to be activated in the presence of other Aβ species (dimers and trimers) such as the member of the Sarc family kinase, Fyn do not appear to be modulated by the presence of Aβ*56 (Larson et al., 2012a).

Further, even though Aβ*56 has been shown to phosphorylate tau at two sites S202 and S416, that can be phosphorylated by multiple kinases, no other kinases beside CaMKII examined appeared to be modulated by the oligomer. Our results support the activation of Cdk5 and GSK3β in older Tg2576 mice at 12 and 16 months of age but not at 7m of age when Aβ*56 was already present (**Fig. 16**). These findings possibly reveal that other forms of Aβ accumulating with aging in Tg2576 animals might be responsible for activating these two kinases. Biochemical analysis using conformationally-distinct

classes of Aβ oligomers specific antibodies, non-fibrillar ($A11^+$) and prefibrillar (OC^+) oAβ revealed a strong correlation between OC^+ oligomers and Cdk5, but no correlations with the $A11^+$ (Aβ*56 belongs to this category, Larson et al., 2012). These findings seem to suggest that prefibrillar Aβ oligomers may be responsible for the increase in Cdk5 activation, while Aβ*56 would be responsible for the activation of CaMKII and subsequent hyperphosphorylation of tau noted, supporting the hypothesis that different Aβ species confer toxicity through distinct and selective pathways.

Third, Aβ*56 is present in potential preclinical AD and appears to be mediating its effects through the activation of CaMKII. It was demonstrated in the past that Aβ*56 is elevated in human brains starting in their 40s and accumulated with aging in non-demented subjects. However, the level of the soluble oligomers drops significantly in the brains of MCI and AD patients (Lesné et al., 2013). The greatest known risk factor for Alzheimer's disease is advancing age. Most individuals with the disease are age 65 or older. The likelihood of developing Alzheimer's disease doubles about every five years after age 65. After age 85, the risk reaches nearly 50 percent, putting the aging cohort in the category of potential preclinical AD. This combined with the fact that Aβ*56 brain levels are low in MCI and AD appear to suggest that Aβ*56 may be import in the asymptomatic phase of AD. Consistent with this argument, the temporal accumulation of pCaMKIIα matched well with the temporal profile of Aβ*56 levels. We showed that pCaMKII/CaMKII ratio rose sharply with aging in the temporal cortex of the studied cohort and was correlated with Aβ*56 levels in postmortem brain tissue of non-impaired human subjects across aging. Further, we showed that Aβ*56 levels correlated strongly with pS202-Tau levels in old non-demented subjects. Functionally, the consequence of

tau hyperphosphorylation at S202 by the Aβ*56/GluN/CaMKIIα axis could lead to a well-established disruption of microtubule dynamics (Trinczek et al., 1995). This fits with evidence of the already described medial temporal lobe hyperactivity in individuals at genetic risk for AD, in low-performing clinically normal and amyloid-positive MCI subjects (Miller et al., 2008; Putcha et al., 2011; Sperling et al., 2009). Interestingly, subtle cognitive impairment have been described in clinically intact subjects in which there is nonclinical memory deficits around the same age (Salthouse, 2009). All these findings together seem to suggest an intiator role of Aβ*56 in Alzheimer's disease.

Fourth, Aβ*56 appears to induce neuronal dysfunction via the Aβ*56/GluN/CaMKIIα axis without causing neuronal cell death. In the Tg2576 mice there is no known neurodegenration in the presence of Aβ*56. Similarly, even though the levels of Aβ*56 used *in vitro* is comparable to that present in 7 months old Tg2576 mice, as it caused changes in CaMKII activation and tau phosphorylation to the same extent then *in vivo*, we never observed any evidence that Aβ*56 was inducing cell death. Analysis of LDH release in neurons exposed to Aβ*56, modulations in intracellular messengers classically linked to neuronal cell death such as the activation of p38 or reductions in ERK/CREB activity (Hardingham & Bading, 2010), and evaluation of caspase-3 activation (**data not shown**) failed to show evidence of Aβ*56 causing cell death. These findings fit with the lack of frank neuronal loss in the Tg2576 and the fact that synaptic dysfunction is observed in preclinical AD but no neuronal cell death (Ashe & Zahs, 2010).

Finally, the data resonates with the emerging concept that CaMKII is altering neuronal physiology and cognition when aberrantly over-activated in the brain. Although CaMKII is typically involved in LTP giving it a crucial role in learning and memory, its abnormal

activation has been described in several other neuronal disorders (Picconi et al., 2004; Weeber et al., 2003; Yabuki et al., 2014). Increased phosphorylation of CaMKII accompanied by deficits in both context-dependent learning and hippocampal long-term potentiation (LTP) has been described in Angelman Syndrom (Weeber et al., 2003). Similarly, excessive CaMKII activation is observed in Attention Deficit Hyperactivity Disorder (ADHD) and in Parkingson's disease (Picconi et al., 2004; Yabuki et al., 2014). Now we describe an abnormal elevation of CaMKII phosphorylation in subjects that could be in preclinal AD leading to the hyperphosphorylation of tau that can be reversed both *in vivo* and *in vitro* by inhibiting the kinase directly or by uncoupling the NMDA receptor to the PSD.

Our findings appear to support the notion of Aβ*56 mediating its deleterious effects on cognition via the Aβ*56/GluN/Tau axis. However, we have yet to prove that the observed changes in CaMKII and tau are causing deficit in the synaptic function and that the cognitive deficit caused by Aβ*56 is dependent on the abnormal pCaMKII levels. In future directions it will be interesting to evaluate the effects Aβ*56, phosphorylation of tau at S202 and S416 has on dendritic spine morphology and proper functioning. Tau mutant with the pseudo phosphorylated and the non-phosphorylatable forms at S416 and S202 have already been generated. It will be important to determine the role of these phosphorylation sites on cellular distribution to infer impact on synaptic function. Additionally, the plane is to analyze spine morphology in the presence of Aβ*56 to determine if the oligomer has any effects on spine shape which are linked to their functions.

Furthermore, our data seems to suggest a binding of Aβ*56 to the NMDAR or more precisely to the GluN1 subunit. Since this binding to the receptor seems to modulate it, it will be interesting to determined where it is binding. To addressed this question multiple site on the GluN1 subunit will be altered to determine which region is important for binding of Aβ*56.

To conclude Aβ*56 appears to cause neuronal dysfunction by abnormally activating CaMKII in what could be the asymptomatic phase of AD that leads to the hyperphophorylation of tau possibly leading to the cognitive deficit in animals and potentially in human. However, further investigation is needed to definitively link these changes to synaptic dysfunction and cognitive deficit.

Chapter 7
Material and methods

Human brain tissue

De-identified *postmortem* brain tissue from the inferior temporal gyrus (Brodman Area 20) from subjects enrolled in the Religious Orders Study and in the Brain and Tissue Bank at the University of Maryland, Baltimore (National Institute of Child Health and Human Development Brain and Tissue Bank for developmental disorders brain specimens) underwent biochemical analyses. All brain tissue samples were selected to have a post-mortem interval <10 h. The characteristics of the clinical diagnostic groups used in this study are summarized elsewhere (Lesne et al., 2013).

The specimen used for the co-immunoprecipitation experiments in **Fig. 2** consisted in six randomly selected samples from individuals from 10-20 years of age of the Brain and

Tissue Bank at the University of Maryland, Baltimore and six randomly selected samples from subjects over 80 years of age from the Religious Orders Study, Rush University (**Table 1**). The cross-sectional analyses presented in **Fig. 26** were all from the Brain and Tissue Bank at the University of Maryland, Baltimore.

The University of Minnesota Institutional Review Board approved all human studies.

Transgenic animals

Mice from the APP line Tg2576, which express the human amyloid precursor protein with the Swedish mutation ($APP^{KM670/671NL}$), directed by the hamster prion promoter (Hsiao et al., 1996), were purchased from Taconic Farms, Inc. and bred to obtain wild-type and hemizygous animals. Mice from the J20, *MAPT*-null and Htau lines (Andorfer et al., 2003; Mucke et al., 2000) were purchased from The Jackson Laboratory. J20 animals bred following guidelines provided by the Mucke laboratory. Both male and female mice were used in all experiments. All mice were group housed by gender (aggressive animals were singly housed), given food and water *ad libitum* and maintained on a 12-hour light/dark cycle (7 a.m./7 p.m.). None of the animals analyzed were excluded.

All animal procedures and studies were reviewed and approved by the University of Minnesota Institutional Animal Care and Use Committee and Institutional Review Board.

Primary cell cultures

Mouse cortical cultures of neurons were prepared from 14- to 15-days-old embryos as described previously (Larson et al., 2012a) using $5x10^5$ cells/dish. After 3 days *in vitro* (DIV), neurons were treated with 10 μM AraC to inhibit proliferation of non-neuronal cells. All experiments were performed on near pure neuronal cultures (> 98% of

microtubule associated protein-2 immunoreactive cells) after 12-14 DIV. Three to nine 35mm dishes per culture per condition were used across three independent experiments.

The concentration and duration of the pretreatments with tatCN21 or with tatNR2B9c were determined by dose-response (1, 5 and 10 μM) and time-course (15, 30 and 60 minutes) experiments using CaMKII and neuronal cell death estimated by LDH assay. Accordingly, pretreatments were set to 15 minutes at 1 μM for both peptides as longer durations and higher concentrations prove toxic to cells (data not shown).

Following treatment(s), cells were harvested in an ice-cold lysis solution containing 50 mM Tris-HCl, pH 7.4, 150 mM NaCl, 0.1% Triton X-100 (Sigma) with 1 mM phenylmethylsulfonyl fluoride (PMSF), 2 mM 1,10-phenanthroline monohydrate (1,10-PTH), 1% (v/v) mammalian protease inhibitor cocktail (Sigma), 0.1% (v/v) phosphatase inhibitor cocktails A (Santa Cruz Biotechnology, Inc.) and 2 (Sigma-Aldrich). Cell lysates were centrifuged for 10 minutes at 13,000 x *g*, supernatants were isolated, and corresponding pellets were resuspended with the protease/phosphatase inhibitor-containing lysis buffer to extract membrane-bound proteins. Plasma membranes were solubilized in RIPA lysis buffer (50 mM Tris-HCl, pH 7.4, 150 mM NaCl, 0.5% Triton X-100, 1 mM EGTA, 3% SDS, 1% deoxycholate, 1 mM PMSF, 2 mM 1,10-PTH, 1% (v/v) mammalian protease inhibitor cocktail (Sigma), 0.1% (v/v) phosphatase inhibitor cocktails A (Santa Cruz Biotechnology, Inc.) and 2 (Sigma-Aldrich). Membrane lysates were then subjected to centrifugation for 10 minutes at 16,000 x *g*, and the soluble fraction was removed and stored for analysis.

Protein extractions

For analyzing Aβ species, we harvested one dissected hemi-forebrain per animal and used two extractions protocols described elsewhere (Lesne et al., 2006; Shankar et al., 2008). In particular, membrane-enriched protein extracts (or MB extracts) refer to protein lysates obtained following the third step of a serial extraction with a lysis RIPA buffer comprised of 50 mM Tris–HCl, pH 7.4, 150 mM NaCl, 0.5% Triton X-100, 1 mM EDTA, 3% SDS and 1% deoxycholate. Samples are then centrifuged at 16,100 x *g* for 90 minutes. Supernatants are collected and pellets further extracted with formic acid to analyze fibrillar/deposited proteins. It is possible that the use of the RIPA lysis buffer might strip loosely bound Aβ from plaques.

Protein amounts were determined by the Bradford protein assay (BCA Protein Assay, Pierce). All supernatants were ultra-centrifuged for 60 min at 100,000 x *g*. Finally, before analysis, fractions were endogenous immunoglobulins were depleted by sequentially incubating extracts for one hour at room temperature with 50 µL of Protein A-Sepharose, Fast Flow® followed by 50 µL of Protein G-Sepharose, Fast Flow® (GE Healthcare Life Sciences).

Tau dephosphorylation

Tau (50 µg IC lysate/reaction) was dephosphorylated by treatment with calf-intestinal alkaline phosphatase (CIP, New England BioLabs, Inc.) at 20 units/mL for 3 hours at 37°C. The reaction was stopped by adding SDS-PAGE loading buffer and heat denaturation at 95°C.

Affinity purification of human Aβ oligomers

One milligram of total brain proteins from Tg2576 or J20 APP transgenic mice were incubated for 3 hours at 4°C with Protein G-coupled magnetic beads (MagG beads, GE

Life Sciences) previously crosslinked with 200 µg of purified 6E10 antibody (Covance) or with 200 µg of Mab13.1.1 and Mab2.1.3 (100 µg of each). Immunocaptured proteins were eluted from the immune complexes using 1% *n*-octyl beta-D-thioglucopyranoside (OTG; Sigma Aldrich) in 100 mM Glycine, pH 2.8 for 1 minute (3 rounds).

Relative amounts of purified oligomeric Aβ were calculated based on synthetic A$\beta_{1\text{-}42}$ standards (0.001, 0.025, 0.05, 0.1, 0.25, 0.5, 1 and 2.5 ng) ran alongside the samples used for experiments. Since there are no reagents selective to each Aβ oligomer to date, we opted to determine the relative abundance of purified Aβ oligomers compared to eight Aβ standards. The mass of a given Aβ oligomer was estimated based on these standards and molar concentration was calculated based on the empirical molecular weight of each given Aβ oligomer (9, 14 and 56 kDa for putative Aβ dimers, trimers and Aβ*56 respectively).

Importantly, considering that the relative abundance of a given Aβ oligomer varies with aging, amyloid deposition and protein segregation (Fowler et al., 2014; Larson and Lesne, 2012; Lesne et al., 2006), protein lysates of 15-18-month-old APP Tg mice were screened by western blotting to measure the abundance of apparent Aβ dimers, trimers and Aβ*56 prior to be subjected to the purification steps consisting of sequential immune-affinity captures and size-exclusion chromatography (SEC). Similar segregations were obtained regardless of the line used although the relative yields for a given oAβ differed between lines.

Consistent with our previous findings (Fowler et al., 2014; Larson and Lesne, 2012; Lesne et al., 2006, Lesne et al., 2013), Aβ dimers are far more abundant in MB-enriched

protein lysates (MB) compared to extracellular-enriched lysates (EC), while this pattern is reversed for putative Aβ trimers. Similar biochemical segregation was also observed using postmortem human brain tissue (Lesne et al., 2013). The example provided in **Figure 3** using EC lysates reflects this segregation following our 4-step extraction protocol.

Size-exclusion chromatography (SEC)

Immunoaffinity purified protein extracts were loaded on Tricorn Superdex® 75 columns (Amersham Life Sciences, Piscataway, NJ, USA) and run at a flow rate of ~0.3 mL/min. Fractions of 250 µL of eluate in 50 mM Tris-HCl, 150 mM NaCl, 0.01% Triton X-100, pH 7.4, were collected using a BioLogic DuoFlow QuadTec 40 system (Bio-Rad) coupled to a microplate-format fraction collector. A280 was determined live during the experiments and confirmed following each run on a DTX800 Multimode microplate reader (Beckman Coulter).

Western blotting and quantification

SDS-PAGE. Electrophoreses were done on pre-cast 10-20% SDS-polyacrylamide Tris-Tricine gels, 10.5-14% and 4-10.5% Tris-HCl gels (Bio-Rad). Protein levels were normalized to 2-100 µg of protein per sample (depending on targeted protein) and resuspended with 4X loading buffer.

Transfer. Thereafter, proteins were transferred to 0.2 µm nitrocellulose membrane (Bio-Rad).

Blotting. To detect Aβ molecules, nitrocellulose membranes were boiled in 50 mL PBS by microwaving for 25 and 15 sec with 3 min intervals. Membranes were blocked in TTBS (Tris-Buffered Saline-0.1%Tween®20) containing 5% bovine serum albumin

(BSA) (Sigma) for 1-2 hours at room temperature, and probed with appropriate antisera/antibodies diluted in 5%BSA-TTBS. Primary antibodies were probed either with anti-IgG immunoglobulins conjugated with biotin or InfraRed dyes (Li-Cor Biosciences, USA). When biotin-conjugated secondary antibodies were used, IR-conjugated Neutravidin® (Thermo Scientific) was added to amplify the signal. Blots were revealed on an Odyssey platform (Li-Cor Biosciences). For the detection of A11-reactive A β species, all blotting steps were performed in total absence of detergent in the buffers used.

Stripping. When required, membranes were stripped using Restore™ Plus Stripping buffer (Pierce) for 30-180 min at room temperature depending on antibody affinity.

Quantification. Densitometry analyses were performed using OptiQuant software (Packard Bioscience, Meriden, CT) or using the Odyssey software (Li-Cor). Each protein of interest was probed in three individual experiments under the same conditions, and quantified by software analysis, following determination of experimental conditions ascertaining linearity in the detection of the signal. The method used allows for a dynamic range of ~100-fold above background. Respective averages were then determined across the triplicate western blots. Normalization was performed against the actin or the total form of the studied protein in the case of phosphorylated proteins. Importantly, due to the large number of samples analyzed, specimens were processed in two separate ways in order to compare possible effects induced by aging and by the transgene across groups.

Dot blotting

Two micrograms of MB protein extracts were mixed with sterile filtered deionized water in a total volume of 2.5 μ L. Each sample was adsorbed onto a nitrocellulose membrane

until dry for 30 minutes. Following a brief activation in 10% methanol-containing TBS, membranes were boiled in PBS to enhance antigen detection (Lesne et al., 2006). All steps were performed without detergent to enhance A11 and OC binding of oligomeric species (Lesne et al., 2006).

Immunoprecipitations

Aliquots (100-250 µg) of protein extracts were diluted to 1 mL with dilution buffer (50 mM Tris–HCl, pH 7.4, 150 mM NaCl) and incubated with appropriate antibodies (5 µg) overnight at 4°C, and added 50 µL of Protein G-Sepharose, Fast Flow® (GE Life Sciences) or Protein G-coupled magnetic beads (MagG beads, GE Life Sciences) 1:1 (v:v) slurry solution with dilution buffer (50 mM Tris-HCl, pH 7.4, 150 mM NaCl, pH 7.4) for two to 16 hours. The beads were washed twice in 1mL of dilution buffer and proteins were eluted in 25 μ L of loading SDS-PAGE buffer by boiling.

Antibodies

The following primary antibodies were used in this study: 6E10 [1:2,500], 4G8 [1:2500], biotinylated-6E10 [1:2,500] (Covance), 40/42-end specific Mab2.1.3 and Mab13.1.1 [1:1,000] (kind gift from Pritam Das, Mayo Clinic, Jacksonville, FL), A11 [1:1,000] (kind gift from Rakez Kayed University of Texas Medical Branch, Galveston, TX), Tau5 [1:2,000] (Covance), PS262-tau [1:2,000] (Cat.# AB9656, EMD Millipore), anti-pY18-tau [1:2,500] (kind gift from Gloria Lee, University of Iowa, Iowa City, IA), anti-pS416-tau [1:2,000] (Cat.# ab119391, Abcam), anti-pS409-tau [1:2,000] (Cat.# OPA1-03150, Thermo Scientific), pS202-tau(CP13) [1:500], PG5 [1:500], PHF1 [1:500], Alz50 [1:500] (kind gifts from Peter Davis, Albert Einstein College of Medicine, Yeshiva University, Manhasset, NY), 0N4R-tau [1:2,000] (Liu and Gotz, 2013), anti-GluN1 [1:1,000] (Cat.#

sc-1467 and sc-9058, Santa Cruz Biotechnology, Inc.), anti-GluN1-CT and anti-GluN2B [1:1,000] (Cat.# 05-432, #AB1557 and #06-600, EMD Millipore and Cat.# sc-1469 and sc-9057, Santa Cruz Biotechnology, Inc.), anti-GluN2A [1:1,000] (Cat.# sc-9056, Santa Cruz Biotechnology, Inc. and Cat.# 2720, Tocris bioscience), anti-mGluR5 [1:1,000] (Cat.# RA16100, Neuromics and Cat.# G9915, Sigma Aldrich), anti-AChR α 7 [1:1,000] (Cat.# sc-1447, Santa Cruz Biotechnology, Inc.), anti-GluA1 [1:1,000] (Cat.# sc-7609, Santa Cruz Biotechnology, Inc.), anti-GluA2 [1:1,000] (Cat.# sc-7610, Santa Cruz Biotechnology, Inc.), anti-EphB2 [1:2,000] (512012, R&D systems, Inc. and Cat.# sc-28980, Santa Cruz Biotechnology, Inc.), anti-Actin [1:10,000] (C4, EMD Millipore and Cat.# A2066, Sigma Aldrich), anti-CaMKII α [1:1,000] (Cat.# NBP1-20008, Novus Biological; Cat.# PA1-14077, Thermo Scientific and Cat.# sc-5306, Santa Cruz Biotechnology), pT286-CaMKII α [1:1,000] (Cat.# MA1-047, Thermo Scientific and Cat.# 3361, Cell Signaling), anti-MAP2 [1:500] (Cat.# NB300-213, Novus Biologicals), anti-PSD95 [1:200] (Cat.# sc-8575, Santa Cruz Biotechnology, Inc. and Cat.# ab18258, Abcam), anti-CREB [1:1,000] (Cat.# MAB5432, EMD Millipore), anti-pS133-CREB [1:1,000] (Cat.# 06-519, EMD Millipore), anti-p38 [1:1,000] (Cat.# 9212, Cell Signaling), pT180/Y182-P38 [1:2,000] (Cat.# 9216, Cell Signaling), anti-ERK [1:1,000] (Cat.# 06-182, EMD Millipore), anti-pERK [1:1,000] (12D4, EMD Millipore), anti-GSK3 α / β [1:1,000] (Cat.# sc-56913, Santa Cruz Biotechnology, Inc.), pS21/S9-GSK3 α / β [1:1,1000] (Cat.# 9327, Cell Signaling), pS9-GSK3 β [1:2,000] (Cat.# 9336, Cell Signaling), anti-p35 [1:1,000] (Cat.# sc-820, Santa Cruz Biotechnology, Inc.), anti-FOXO1 [1:1,000] (2H8.2, EMD Millipore), anti-Calcineurin A [1:1,000] (Cat.# 2614,

Cell Signaling), anti-PP1 α (Cat.# 2582, Cell Signaling), anti-$PP2A_C$ (1D6, EMD Millipore) and anti-cleaved Caspase-3 (Cat.# 9664, Cell Signaling).

Validation of the antibodies used was performed comparing the specificity and segregation pattern of the target protein using extracellular- (EC), intracellular- (IC) and membrane bound-enriched protein extracts as described in the section Protein Extractions.

Confocal imaging

Triple or Quadruple-label immunofluorescence was performed as previously described (Larson et al., 2012a; Larson et al., 2012b) using Alexa Fluor 488, 555, 635-conjugated secondary antibodies (Molecular Probes, Invitrogen). Mouse brain sections were treated for autofluorescence with 1% Sudan Black solution and coverslipped with ProLong mounting medium (Molecular Probes). Digital images were obtained using an Olympus IX81 FluoView1000 microscope with laser intensities ranging from 7-11%. Raw image z-stacks (0.1-0.5 μm intervals) were analyzed using Bitplane's Imaris7.x software suite. Frame size was maintained at 1024 × 800 and optical zoom of 1.00 was utilized to allow for maximum distribution of pixel size to tissue dimensions without over sampling. Six regions of interest (ROIs) per brain section (6 sections/brain) per animal (4-6 animals per group) were used. For *in vitro* analyses, eight ROIs/dish/group were used. *Z* stacks were reconstructed using the Surpass or Easy3D modules of the Imaris software package (version 7.x, Bitplane Inc., USA).

Statistical Analyses

When variables were non-normally distributed, nonparametric statistics were used (Spearman *rho* correlation coefficients, Kruskal-Wallis nonparametric analysis of variance followed by Bonferroni-corrected two-group *posthoc* Mann-Whitney U tests).

When variables were normally distributed, the following parametric statistics were used (one/two-way ANOVA followed by Bonferroni-corrected two-group *posthoc* Student t tests). Sample size was determined by power analysis to be able to detect statistically significant changes within a 20% variation of measured responses. Analyses were performed using JMP 11 (SAS Institute, USA).

References

Aarts, M., Liu, Y., Liu, L., Besshoh, S., Arundine, M., Gurd, J. W., … Tymianski, M. (2002). Treatment of ischemic brain damage by perturbing NMDA receptor- PSD-95 protein interactions. *Science (New York, N.Y.)*, *298*(5594), 846–50. http://doi.org/10.1126/science.1072873

Aizenstein, H. J., Nebes, R. D., Saxton, J. A., Price, J. C., Mathis, C. A., Tsopelas, N. D., … Klunk, W. E. (2008). Frequent amyloid deposition without significant cognitive impairment among the elderly. *Archives of Neurology*, *65*(11), 1509–17. http://doi.org/10.1001/archneur.65.11.1509

Altman, J., & Das, G. D. (1965). Autoradiographic and histological evidence of postnatal hippocampal neurogenesis in rats. *The Journal of Comparative Neurology*, *124*(3), 319–335. http://doi.org/10.1002/cne.901240303

Alvarez, A., Toro, R., Cáceres, A., & Maccioni, R. B. (1999). Inhibition of tau phosphorylating protein kinase cdk5 prevents β-amyloid-induced neuronal death. *FEBS Letters*, *459*(3), 421–426. http://doi.org/10.1016/S0014-5793(99)01279-X

Alzheimer, a, Förstl, H., & Levy, R. (1991). *On certain peculiar diseases of old age. History of psychiatry* (Vol. 2). http://doi.org/10.1177/0957154X9100200505

Amieva, H., Le Goff, M., Millet, X., Orgogozo, J. M., Pérès, K., Barberger-Gateau, P., … Dartigues, J. F. (2008). Prodromal Alzheimer's disease: successive emergence of the clinical symptoms. *Annals of Neurology*, *64*(5), 492–8. http://doi.org/10.1002/ana.21509

Andorfer, C., Kress, Y., Espinoza, M., De Silva, R., Tucker, K. L., Barde, Y. A., … Davies, P. (2003). Hyperphosphorylation and aggregation of tau in mice expressing normal human tau isoforms. *Journal of Neurochemistry*, *86*(3), 582–590. http://doi.org/10.1046/j.1471-4159.2003.01879.x

Arancio, O., Zhang, H. P., Chen, X., Lin, C., Trinchese, F., Puzzo, D., … Du Yan, S. S. (2004). RAGE potentiates Abeta-induced perturbation of neuronal function in transgenic mice. *The EMBO Journal*, *23*(20), 4096–105. http://doi.org/10.1038/sj.emboj.7600415

Arendt, T., Brückner, M. K., Mosch, B., & Lösche, A. (2010). Selective cell death of hyperploid neurons in Alzheimer's disease. *The American Journal of Pathology*, *177*(1), 15–20. http://doi.org/10.2353/ajpath.2010.090955

Arnold, C. S., Johnson, G. V, Cole, R. N., Dong, D. L., Lee, M., & Hart, G. W. (1996). The microtubule-associated protein tau is extensively modified with O-linked N-acetylglucosamine. *The Journal of Biological Chemistry*, *271*(46), 28741–4. Retrieved from http://www.ncbi.nlm.nih.gov/pubmed/8910513

Arriagada, P. V, Marzloff, K., & Hyman, B. T. (1992). Distribution of Alzheimer-type pathologic changes in nondemented elderly individuals matches the pattern in Alzheimer's disease. *Neurology*, *42*(9), 1681–1688. http://doi.org/10.1212/WNL.42.9.1681

Ashe, K. H., & Zahs, K. R. (2010). Probing the biology of Alzheimer's disease in mice. *Neuron*, *66*(5), 631–45. http://doi.org/10.1016/j.neuron.2010.04.031

Atwood, C. S., Obrenovich, M. E., Liu, T., Chan, H., Perry, G., Smith, M. a., & Martins, R. N. (2003). Amyloid-??: A chameleon walking in two worlds: A review of the trophic and toxic properties of amyloid-?? *Brain Research Reviews*, *43*(1), 1–16. http://doi.org/10.1016/S0165-0173(03)00174-7

Augustinack, J. C., Schneider, A., Mandelkow, E.-M., & Hyman, B. T. (2002). Specific tau phosphorylation sites correlate with severity of neuronal cytopathology in Alzheimer's disease. *Acta Neuropathologica*, *103*(1), 26–35. Retrieved from http://www.ncbi.nlm.nih.gov/pubmed/11837744

Avila, J., Lucas, J. J., Perez, M., & Hernandez, F. (2004). Role of tau protein in both physiological and pathological conditions. *Physiological Reviews*, *84*(2), 361–84. http://doi.org/10.1152/physrev.00024.2003

Baba, M., Nakajo, S., Tu, P. H., Tomita, T., Nakaya, K., Lee, V. M., … Iwatsubo, T. (1998). Aggregation of alpha-synuclein in Lewy bodies of sporadic Parkinson's disease and dementia with Lewy bodies. *The American Journal of Pathology*, *152*(4), 879–84. Retrieved from http://www.pubmedcentral.nih.gov/articlerender.fcgi?artid=1858234&tool=pmcentrez&rendertype=abstract

Balducci, C., Beeg, M., Stravalaci, M., Bastone, A., Sclip, A., Biasini, E., … Forloni, G. (2010). Synthetic amyloid-beta oligomers impair long-term memory independently of cellular prion protein. *Proceedings of the National Academy of Sciences of the United States of America*, *107*(5), 2295–300. http://doi.org/10.1073/pnas.0911829107

Barry, A. E., Klyubin, I., Mc Donald, J. M., Mably, A. J., Farrell, M. A., Scott, M., … Rowan, M. J. (2011). Alzheimer's disease brain-derived amyloid-β-mediated inhibition of LTP in vivo is prevented by immunotargeting cellular prion protein. *The Journal of Neuroscience : The Official Journal of the Society for Neuroscience*, *31*(20), 7259–63. http://doi.org/10.1523/JNEUROSCI.6500-10.2011

Bateman, R. J., Aisen, P. S., De Strooper, B., Fox, N. C., Lemere, C. A., Ringman, J. M., … Xiong, C. (2011). Autosomal-dominant Alzheimer's disease: a review and proposal for the prevention of Alzheimer's disease. *Alzheimer's Research & Therapy*, *3*(1), 1. http://doi.org/10.1186/alzrt59

Bateman, R. J., Xiong, C., Benzinger, T. L. S., Fagan, A. M., Goate, A., Fox, N. C., … Morris, J. C. (2012). Clinical and biomarker changes in dominantly inherited Alzheimer's disease. *The New England Journal of Medicine*, *367*(9), 795–804. http://doi.org/10.1056/NEJMoa1202753

Behl, C., Davis, J. B., Lesley, R., & Schubert, D. (1994). Hydrogen peroxide mediates amyloid ?? protein toxicity. *Cell*, *77*(6), 817–827. http://doi.org/10.1016/0092-8674(94)90131-7

Bennett, D. a, Schneider, J. a, Wilson, R. S., Bienias, J. L., & Arnold, S. E. (2004). Neurofibrillary tangles mediate the association of amyloid load with clinical Alzheimer disease and level of cognitive function. *Archives of Neurology*, *61*(3), 378–384. http://doi.org/10.1001/archneur.61.3.378

Benveniste, M., & Mayer, M. L. (1991). Kinetic analysis of antagonist action at N-methyl-D-aspartic acid receptors. Two binding sites each for glutamate and glycine. *Biophysical Journal*, *59*(3), 560–73. http://doi.org/10.1016/S0006-3495(91)82272-X

Bettens, K., Sleegers, K., & Broeckhoven, C. Van. (2013). Genetic insights in Alzheimer ' s disease. *The Lancet Neurology*, *12*(1), 92–104. http://doi.org/10.1016/S1474-4422(12)70259-4

Bhat, R. V, Shanley, J., Correll, M. P., Fieles, W. E., Keith, R. A., Scott, C. W., & Lee, C. M. (2000). Regulation and localization of tyrosine216 phosphorylation of glycogen synthase kinase-3beta in cellular and animal models of neuronal degeneration. *Proceedings of the National Academy of Sciences of the United States of America*, *97*(20), 11074–9. http://doi.org/10.1073/pnas.190297597

Binder, L. I., Guillozet-Bongaarts, A. L., Garcia-Sierra, F., & Berry, R. W. (2005). Tau, tangles, and Alzheimer's disease. *Biochimica et Biophysica Acta - Molecular Basis of Disease*, *1739*(2), 216–223. http://doi.org/10.1016/j.bbadis.2004.08.014

Bliss, T. V, & Collingridge, G. L. (1993). A synaptic model of memory: long-term potentiation in the hippocampus. *Nature*, *361*(6407), 31–9. http://doi.org/10.1038/361031a0

Borchelt, D. R., Thinakaran, G., Eckman, C. B., Lee, M. K., Davenport, F., Ratovitsky, T., … Sisodia, S. S. (1996). Familial Alzheimer's disease-linked presenilin 1 variants elevate Abeta1-42/1-40 ratio in vitro and in vivo. *Neuron*, *17*(5), 1005–1013. http://doi.org/10.1016/S0896-6273(00)80230-5

Braak, H., & Braak, E. (1991). Neuropathological stageing of Alzheimer-related changes. *Acta Neuropathologica*, *82*(4), 239–259. http://doi.org/10.1007/BF00308809

Braak, H., Thal, D. R., Ghebremedhin, E., & Del Tredici, K. (2011). Stages of the pathologic process in Alzheimer disease: age categories from 1 to 100 years. *Journal of Neuropathology and Experimental Neurology*, *70*(11), 960–9. http://doi.org/10.1097/NEN.0b013e318232a379

Braak, H., Zetterberg, H., Del Tredici, K., & Blennow, K. (2013). Intraneuronal tau aggregation precedes diffuse plaque deposition, but amyloid-?? changes occur before increases of tau in cerebrospinal fluid. *Acta Neuropathologica*, *126*(5), 631–641. http://doi.org/10.1007/s00401-013-1139-0

Burns, a, Tomlinson, B. E., & Mann, D. M. (1997). Observations on the brains of demented old people. B.E. Tomlinson, G. Blessed and M. Roth, Journal of the Neurological Sciences (1970) 11, 205-242 and Observations on the brains of non-demented old people. B.E. Tomlinson, G. Blessed and M. Roth, Journal o. *International Journal of Geriatric Psychiatry*, *12*(8), 785–790.

Cabrejo, L., Guyant-Maréchal, L., Laquerrière, A., Vercelletto, M., De La Fournière, F., Thomas-Antérion, C., … Hannequin, D. (2006). Phenotype associated with APP duplication in five families. *Brain*, *129*(11), 2966–2976. http://doi.org/10.1093/brain/awl237

Calella, A. M., Farinelli, M., Nuvolone, M., Mirante, O., Moos, R., Falsig, J., … Aguzzi, A. (2010). Prion protein and Abeta-related synaptic toxicity impairment. *EMBO Molecular Medicine*, *2*(8), 306–14. http://doi.org/10.1002/emmm.201000082

Camins, A., Verdaguer, E., Folch, J., Canudas, A. M., & Pallàs, M. (2006). The role of CDK5/P25 formation/inhibition in neurodegeneration. *Drug News & Perspectives*, *19*(8), 453–60. http://doi.org/10.1358/dnp.2006.19.8.1043961

Centelles, P. and. (1998). Departament de Bioquímica i Biologia Molecular, Facultat de Química, Universitat de Barcelona, Martí i Franquès, 1, 08028-Barcelona, Spain, 1–22.

Chang, K.-H., de Pablo, Y., Lee, H., Lee, H., Smith, M. A., & Shah, K. (2010). Cdk5 is a major regulator of p38 cascade: relevance to neurotoxicity in Alzheimer's disease.

Journal of Neurochemistry, *113*(5), 1221–9. http://doi.org/10.1111/j.1471-4159.2010.06687.x

Chapman, P. F., White, G. L., Jones, M. W., Cooper-Blacketer, D., Marshall, V. J., Irizarry, M., … Hsiao, K. K. (1999). Impaired synaptic plasticity and learning in aged amyloid precursor protein transgenic mice. *Nature Neuroscience*, *2*(3), 271–276. http://doi.org/10.1038/6374

Chen, J., Kanai, Y., Cowan, N. J., & Hirokawa, N. (1992). Projection domains of MAP2 and tau determine spacings between microtubules in dendrites and axons. *Nature*, *360*(6405), 674–7. http://doi.org/10.1038/360674a0

Chen, Q.-S., Wei, W.-Z., Shimahara, T., & Xie, C.-W. (2002). Alzheimer amyloid beta-peptide inhibits the late phase of long-term potentiation through calcineurin-dependent mechanisms in the hippocampal dentate gyrus. *Neurobiology of Learning and Memory*, *77*(3), 354–71. http://doi.org/10.1006/nlme.2001.4034

Chen, Y. R., & Glabe, C. G. (2006). Distinct early folding and aggregation properties of Alzheimer amyloid-?? peptides A??40 and A??42: Stable trimer or tetramer formation by A??42. *Journal of Biological Chemistry*, *281*(34), 24414–24422. http://doi.org/10.1074/jbc.M602363200

Cheng, I. H., Scearce-Levie, K., Legleiter, J., Palop, J. J., Gerstein, H., Bien-Ly, N., … Mucke, L. (2007). Accelerating amyloid-beta fibrillization reduces oligomer levels and functional deficits in Alzheimer disease mouse models. *The Journal of Biological Chemistry*, *282*(33), 23818–28. http://doi.org/10.1074/jbc.M701078200

Chetelat, G., Villemagne, V. L., Villain, N., Jones, G., Ellis, K. a, Ames, D., … Group, A. R. (2012). Accelerated cortical atrophy in cognitively normal elderly with high beta-amyloid deposition. *Neurology*, *78*(7), 477–484. http://doi.org/10.1212/WNL.0b013e318246d67a

Cissé, M., Halabisky, B., Harris, J., Devidze, N., Dubal, D. B., Sun, B., … Mucke, L. (2011). Reversing EphB2 depletion rescues cognitive functions in Alzheimer model. *Nature*, *469*(7328), 47–52. http://doi.org/10.1038/nature09635

Cissé, M., Sanchez, P. E., Kim, D. H., Ho, K., Yu, G.-Q., & Mucke, L. (2011). Ablation of cellular prion protein does not ameliorate abnormal neural network activity or cognitive dysfunction in the J20 line of human amyloid precursor protein transgenic mice. *The Journal of Neuroscience : The Official Journal of the Society for Neuroscience*, *31*(29), 10427–31. http://doi.org/10.1523/JNEUROSCI.1459-11.2011

Cleary, J. P., Walsh, D. M., Hofmeister, J. J., Shankar, G. M., Kuskowski, M. A., Selkoe, D. J., & Ashe, K. H. (2005). Natural oligomers of the amyloid-beta protein specifically disrupt cognitive function. *Nature Neuroscience*, *8*(1), 79–84. http://doi.org/10.1038/nn1372

Clements, J. D., & Westbrook, G. L. (1991). Activation kinetics reveal the number of glutamate and glycine binding sites on the N-methyl-d-aspartate receptor. *Neuron*, *7*(4), 605–613. http://doi.org/10.1016/0896-6273(91)90373-8

Cohen, T. J., Guo, J. L., Hurtado, D. E., Kwong, L. K., Mills, I. P., Trojanowski, J. Q., & Lee, V. M. Y. (2011). The acetylation of tau inhibits its function and promotes pathological tau aggregation. *Nature Communications*, *2*, 252. http://doi.org/10.1038/ncomms1255

Cole, A., Frame, S., & Cohen, P. (2004). Further evidence that the tyrosine phosphorylation of glycogen synthase kinase-3 (GSK3) in mammalian cells is an autophosphorylation event. *The Biochemical Journal*, *377*(Pt 1), 249–55. http://doi.org/10.1042/BJ20031259

Cook, C., Carlomagno, Y., Gendron, T. F., Dunmore, J., Scheffel, K., Stetler, C., … Petrucelli, L. (2013). Acetylation of the KXGS motifs in tau is a critical determinant in modulation of tau aggregation and clearance. *Human Molecular Genetics*, *23*(1), 104–116. http://doi.org/10.1093/hmg/ddt402

Cottrell, J. R., Dubé, G. R., Egles, C., & Liu, G. (2000). Distribution, density, and clustering of functional glutamate receptors before and after synaptogenesis in hippocampal neurons. *Journal of Neurophysiology*, *84*(3), 1573–87. Retrieved from http://www.ncbi.nlm.nih.gov/pubmed/10980028

Coultrap, S. J., & Bayer, K. U. (2012). CaMKII regulation in information processing and storage. *Trends in Neurosciences*, *35*(10), 607–618. http://doi.org/10.1016/j.tins.2012.05.003

Coultrap, S. J., Vest, R. S., Ashpole, N. M., Hudmon, A., & Bayer, K. U. (2011). CaMKII in cerebral ischemia. *Acta Pharmacologica Sinica*, *32*(7), 861–72. http://doi.org/10.1038/aps.2011.68

Cripps, D., Thomas, S. N., Jeng, Y., Yang, F., Davies, P., & Yang, A. J. (2006). Alzheimer Disease-specific Conformation of Hyperphosphorylated Paired Helical Filament-Tau Is Polyubiquitinated through Lys-48, Lys-11, and Lys-6 Ubiquitin Conjugation. *Journal of Biological Chemistry*, *281*(16), 10825–10838. http://doi.org/10.1074/jbc.M512786200

Cruts, M., Hendriks, L., & Van Broeckhoven, C. (1996). The presenilin genes: a new gene family involved in Alzheimer disease pathology. *Human Molecular Genetics*, *5 Spec No*, 1449–55. Retrieved from http://www.ncbi.nlm.nih.gov/pubmed/8875251

Cruz, J. C., Tseng, H.-C., Goldman, J. A., Shih, H., & Tsai, L.-H. (2003). Aberrant Cdk5 Activation by p25 Triggers Pathological Events Leading to Neurodegeneration and Neurofibrillary Tangles. *Neuron*, *40*(3), 471–483. http://doi.org/10.1016/S0896-6273(03)00627-5

Dajani, R., Fraser, E., Roe, S. M., Young, N., Good, V., Dale, T. C., & Pearl, L. H. (2001). Crystal Structure of Glycogen Synthase Kinase 3β. *Cell*, *105*(6), 721–732. http://doi.org/10.1016/S0092-8674(01)00374-9

Davies, S. N., Lester, R. A., Reymann, K. G., & Collingridge, G. L. (1989). Temporally distinct pre- and post-synaptic mechanisms maintain long-term potentiation. *Nature*, *338*(6215), 500–3. http://doi.org/10.1038/338500a0

Davies, S. P., Reddy, H., Caivano, M., & Cohen, P. (2000). Specificity and mechanism of action of some commonly used protein kinase inhibitors. *The Biochemical Journal*, *351*(Pt 1), 95–105. Retrieved from http://www.pubmedcentral.nih.gov/articlerender.fcgi?artid=1221339&tool=pmcentrez&rendertype=abstract

Deane, R., Du Yan, S., Submamaryan, R. K., LaRue, B., Jovanovic, S., Hogg, E., … Zlokovic, B. (2003). RAGE mediates amyloid-beta peptide transport across the blood-brain barrier and accumulation in brain. *Nature Medicine*, *9*(7), 907–13. http://doi.org/10.1038/nm890

DeKosky, S. T., & Scheff, S. W. (1990). Synapse loss in frontal cortex biopsies in Alzheimer's disease: correlation with cognitive severity. *Annals of Neurology*, *27*(5), 457–64. http://doi.org/10.1002/ana.410270502

Dewachter, I., Filipkowski, R. K., Priller, C., Ris, L., Neyton, J., Croes, S., … Van Leuven, F. (2009). Deregulation of NMDA-receptor function and down-stream signaling in APP[V717I] transgenic mice. *Neurobiology of Aging*, *30*(2), 241–56. http://doi.org/10.1016/j.neurobiolaging.2007.06.011

Dickerson, B. C., Bakkour, A., Salat, D. H., Feczko, E., Pacheco, J., Greve, D. N., … Buckner, R. L. (2009). The cortical signature of Alzheimer's disease: regionally specific cortical thinning relates to symptom severity in very mild to mild AD dementia and is detectable in asymptomatic amyloid-positive individuals. *Cerebral Cortex (New York, N.Y. : 1991)*, *19*(3), 497–510. http://doi.org/10.1093/cercor/bhn113

Donohue, M. C., Sperling, R. A., Salmon, D. P., Rentz, D. M., Raman, R., Thomas, R. G., … Aisen, P. S. (2015). HHS Public Access, *71*(8), 961–970. http://doi.org/10.1001/jamaneurol.2014.803.The
Eanes, I. E. S. (2015). thick.

Fagan, A. M., Head, D., Shah, A. R., Marcus, D., Mintun, M., Morris, J. C., & Holtzman, D. M. (2009). Decreased cerebrospinal fluid Abeta(42) correlates with brain atrophy in cognitively normal elderly. *Annals of Neurology*, *65*(2), 176–83. http://doi.org/10.1002/ana.21559

Fagan, A. M., Roe, C. M., Xiong, C., Mintun, M. A., Morris, J. C., & Holtzman, D. M. (2007). Cerebrospinal fluid tau/beta-amyloid(42) ratio as a prediction of cognitive decline in nondemented older adults. *Archives of Neurology*, *64*(3), 343–9. http://doi.org/10.1001/archneur.64.3.noc60123

Frandemiche, M. L., De Seranno, S., Rush, T., Borel, E., Elie, a, Arnal, I., … Buisson, a. (2014). Activity-dependent tau protein translocation to excitatory synapse is disrupted by exposure to amyloid-Beta oligomers. *J Neurosci*, *34*(17), 6084–6097. http://doi.org/10.1523/JNEUROSCI.4261-13.2014

Freir, D. B., Nicoll, A. J., Klyubin, I., Panico, S., Mc Donald, J. M., Risse, E., … Collinge, J. (2011). Interaction between prion protein and toxic amyloid β assemblies can be therapeutically targeted at multiple sites. *Nature Communications*, *2*, 336. http://doi.org/10.1038/ncomms1341

Funk, K. E., Thomas, S. N., Schafer, K. N., Cooper, G. L., Liao, Z., Clark, D. J., … Kuret, J. (2014). Lysine methylation is an endogenous post-translational modification of tau protein in human brain and a modulator of aggregation propensity. *The Biochemical Journal*, *462*(1), 77–88. http://doi.org/10.1042/BJ20140372

Gamblin, T. C., King, M. E., Dawson, H., Vitek, M. P., Kuret, J., Berry, R. W., & Binder, L. I. (2000). In vitro polymerization of tau protein monitored by laser light scattering: Method and application to the study of FTDP-17 mutants. *Biochemistry*, *39*(20), 6136–6144. http://doi.org/10.1021/bi000201f

Games et al 1995.pdf. (n.d.).

Gandy, S., Simon, A. J., Steele, J. W., Lublin, A. L., Lah, J. J., Walker, L. C., … Ehrlich, M. E. (2010). Days to criterion as an indicator of toxicity associated with human Alzheimer amyloid-beta oligomers. *Annals of Neurology*, *68*(2), 220–30. http://doi.org/10.1002/ana.22052

Gendron, T. F., & Petrucelli, L. (2009). The role of tau in neurodegeneration. *Molecular Neurodegeneration*, *4*, 13. http://doi.org/10.1186/1750-1326-4-13

Giannakopoulos, P., Herrmann, F. R., Bussière, T., Bouras, C., Kövari, E., Perl, D. P., … Hof, P. R. (2003). Tangle and neuron numbers, but not amyloid load, predict cognitive status in Alzheimer's disease. *Neurology*, *60*(9), 1495–1500. http://doi.org/10.1212/01.WNL.0000063311.58879.01

Giese, K. P. (1998). Autophosphorylation at Thr286 of the Calcium-Calmodulin Kinase II in LTP and Learning. *Science*, *279*(5352), 870–873. http://doi.org/10.1126/science.279.5352.870

Gimbel, D. A., Nygaard, H. B., Coffey, E. E., Gunther, E. C., Laurén, J., Gimbel, Z. A., & Strittmatter, S. M. (2010). Memory impairment in transgenic Alzheimer mice requires

cellular prion protein. *The Journal of Neuroscience : The Official Journal of the Society for Neuroscience*, *30*(18), 6367–74. http://doi.org/10.1523/JNEUROSCI.0395-10.2010

Glenner, G. G., & Wong, C. W. (1984). No Title, *120*(3), 885–890.

Goate, A., Chartier-Harlin, M. C., Mullan, M., Brown, J., Crawford, F., Fidani, L., … James, L. (1991). Segregation of a missense mutation in the amyloid precursor protein gene with familial Alzheimer's disease. *Nature*, *349*(6311), 704–6. http://doi.org/10.1038/349704a0

Gómez de Barreda, E., Pérez, M., Gómez Ramos, P., de Cristobal, J., Martín-Maestro, P., Morán, A., … Avila, J. (2010). Tau-knockout mice show reduced GSK3-induced hippocampal degeneration and learning deficits. *Neurobiology of Disease*, *37*(3), 622–9. http://doi.org/10.1016/j.nbd.2009.11.017

Gómez-Isla, T., Wasco, W., Pettingell, W. P., Gurubhagavatula, S., Schmidt, S. D., Jondro, P. D., … Tanzi, R. E. (1997). A novel presenilin-1 mutation: increased beta-amyloid and neurofibrillary changes. *Annals of Neurology*, *41*(6), 809–13. http://doi.org/10.1002/ana.410410618

Gong, Y., Chang, L., Viola, K. L., Lacor, P. N., Lambert, M. P., Finch, C. E., … Klein, W. L. (2003). Alzheimer's disease-affected brain: presence of oligomeric A beta ligands (ADDLs) suggests a molecular basis for reversible memory loss. *Proceedings of the National Academy of Sciences of the United States of America*, *100*(18), 10417–22. http://doi.org/10.1073/pnas.1834302100

Greenberg, S. G., Davies, P., Schein, J. D., & Binder, L. I. (1992). Hydrofluoric acid-treated tau PHF proteins display the same biochemical properties as normal tau. *The Journal of Biological Chemistry*, *267*(1), 564–9. Retrieved from http://www.ncbi.nlm.nih.gov/pubmed/1370450

Grundke-Iqbal, I., Iqbal, K., Tung, Y. C., Quinlan, M., Wisniewski, H. M., & Binder, L. I. (1986). Abnormal phosphorylation of the microtubule-associated protein tau (tau) in Alzheimer cytoskeletal pathology. *Proceedings of the National Academy of Sciences of the United States of America*, *83*(13), 4913–7. Retrieved from http://www.pubmedcentral.nih.gov/articlerender.fcgi?artid=323854&tool=pmcentrez&rendertype=abstract

Guidato, S., McLoughlin, D. M., Grierson, A. J., & Miller, C. C. J. (2002). Cyclin D2 Interacts with cdk-5 and Modulates Cellular cdk-5/p35 Activity. *Journal of Neurochemistry*, *70*(1), 335–340. http://doi.org/10.1046/j.1471-4159.1998.70010335.x
Guo, A., Gu, H., Zhou, J., Mulhern, D., Wang, Y., Lee, K. A., … Comb, M. J. (2014). Immunoaffinity enrichment and mass spectrometry analysis of protein methylation. *Molecular & Cellular Proteomics : MCP*, *13*(1), 372–87. http://doi.org/10.1074/mcp.O113.027870

Haass, C., & Selkoe, D. J. (2007). Soluble protein oligomers in neurodegeneration: lessons from the Alzheimer's amyloid beta-peptide. *Nature Reviews. Molecular Cell Biology*, *8*(2), 101–12. http://doi.org/10.1038/nrm2101

Hallows, J. L., Chen, K., DePinho, R. A., & Vincent, I. (2003). Decreased cyclin-dependent kinase 5 (cdk5) activity is accompanied by redistribution of cdk5 and cytoskeletal proteins and increased cytoskeletal protein phosphorylation in p35 null mice. *The Journal of Neuroscience : The Official Journal of the Society for Neuroscience*, *23*(33), 10633–44. Retrieved from http://www.ncbi.nlm.nih.gov/pubmed/14627648

Hamilton, R. L. (2000). Lewy bodies in Alzheimer's disease: a neuropathological review of 145 cases using alpha-synuclein immunohistochemistry. *Brain Pathology (Zurich, Switzerland)*, *10*(3), 378–84. Retrieved from http://www.ncbi.nlm.nih.gov/pubmed/10885656

Hanger, D. P., Seereeram, A., & Noble, W. (2009). Mediators of tau phosphorylation in the pathogenesis of Alzheimer's disease. *Expert Review of Neurotherapeutics*, *9*(11), 1647–66. http://doi.org/10.1586/ern.09.104

Harada, A., Oguchi, K., Okabe, S., Kuno, J., Terada, S., Ohshima, T., … Hirokawa, N. (1994). Altered microtubule organization in small-calibre axons of mice lacking tau protein. *Nature*, *369*(6480), 488–91. http://doi.org/10.1038/369488a0

Hardingham, G. E., & Bading, H. (2002). Coupling of extrasynaptic NMDA receptors to a CREB shut-off pathway is developmentally regulated. *Biochimica et Biophysica Acta (BBA) - Proteins and Proteomics*, *1600*(1-2), 148–153. http://doi.org/10.1016/S1570-9639(02)00455-7

Hardingham, G. E., & Bading, H. (2010). Synaptic versus extrasynaptic NMDA receptor signalling: implications for neurodegenerative disorders. *Nature Reviews. Neuroscience*, *11*(10), 682–696. http://doi.org/10.1038/nrn2911

Hardy, J. a, & Higgins, G. a. (1992). Disease : Alzheimer's Cascade Hypothesis Amyloid. *Science*, *256*(5054), 184–185.

Harper, J. D., Wong, S. S., Lieber, C. M., & Lansbury, P. T. (1997). Observation of metastable Aβ amyloid protofibrils by atomic force microscopy. *Chemistry & Biology*, *4*(2), 119–125. http://doi.org/10.1016/S1074-5521(97)90255-6

Hebert, L. E. (1995). Age-Specific Incidence of Alzheimer's Disease in a Community Population. *JAMA: The Journal of the American Medical Association*, *273*(17), 1354. http://doi.org/10.1001/jama.1995.03520410048025

Hellström-Lindahl, E., Viitanen, M., & Marutle, a. (2009). Comparison of Aβ levels in the brain of familial and sporadic Alzheimer's disease. *Neurochemistry International*, *55*(4), 243–252. http://doi.org/10.1016/j.neuint.2009.03.007

Hensley, K., Carney, J. M., Mattson, M. P., Aksenova, M., Harris, M., Wu, J. F., … Butterfield, D. a. (1994). A model for beta-amyloid aggregation and neurotoxicity based on free radical generation by the peptide: relevance to Alzheimer disease. *Proceedings of the National Academy of Sciences of the United States of America*, *91*(8), 3270–3274. http://doi.org/10.1073/pnas.91.8.3270

Hinds, H. L., Tonegawa, S., & Malinow, R. (1998). CA1 Long-Term Potentiation Is Diminished but Present in Hippocampal Slices from alpha -CaMKII Mutant Mice. *Learn. Mem.*, *5*(4), 344–354. http://doi.org/10.1101/lm.5.4.344

Hirokawa, N. (1988). Tau proteins: the molecular structure and mode of binding on microtubules. *The Journal of Cell Biology*, *107*(4), 1449–1459. http://doi.org/10.1083/jcb.107.4.1449

Hoover, B. R., Reed, M. N., Su, J., Penrod, R. D., Kotilinek, L. A., Grant, M. K., … Liao, D. (2010). Tau mislocalization to dendritic spines mediates synaptic dysfunction independently of neurodegeneration. *Neuron*, *68*(6), 1067–81. http://doi.org/10.1016/j.neuron.2010.11.030

Hsia, A. Y., Masliah, E., McConlogue, L., Yu, G. Q., Tatsuno, G., Hu, K., … Mucke, L. (1999). Plaque-independent disruption of neural circuits in Alzheimer's disease mouse models. *Proceedings of the National Academy of Sciences of the United States of America*, *96*(6), 3228–33. Retrieved from http://www.pubmedcentral.nih.gov/articlerender.fcgi?artid=15924&tool=pmcentrez&rendertype=abstract

Hsiao, K., Chapman, P., Nilsen, S., Eckman, C., Harigaya, Y., Younkin, S., … Cole, G. (1996). Correlative memory deficits, Abeta elevation, and amyloid plaques in transgenic mice. *Science (New York, N.Y.)*, *274*(5284), 99–102. http://doi.org/10.1126/science.274.5284.99

Hsieh, H., Boehm, J., Sato, C., Iwatsubo, T., Tomita, T., Sisodia, S., & Malinow, R. (2006). AMPAR removal underlies Abeta-induced synaptic depression and dendritic spine loss. *Neuron*, *52*(5), 831–43. http://doi.org/10.1016/j.neuron.2006.10.035

Huang, X., Atwood, C. S., Hartshorn, M. a., Multhaup, G., Goldstein, L. E., Scarpa, R. C., … Bush, A. I. (1999). The A?? peptide of Alzheimer's disease directly produces hydrogen peroxide through metal ion reduction. *Biochemistry*, *38*(24), 7609–7616. http://doi.org/10.1021/bi990438f

Ichinose, K., Juang, Y.-T., Crispín, J. C., Kis-Toth, K., & Tsokos, G. C. (2011). Suppression of autoimmunity and organ pathology in lupus-prone mice upon inhibition of calcium/calmodulin-dependent protein kinase type IV. *Arthritis and Rheumatism*, *63*(2), 523–9. http://doi.org/10.1002/art.30085

Iqbal, K., Alonso, A. C., Gong, C. X., Khatoon, S., Pei, J. J., Wang, J. Z., & Grundke-Iqbal, I. (1998). Mechanisms of neurofibrillary degeneration and the formation of neurofibrillary tangles. *Journal of Neural Transmission. Supplementum*, *53*, 169–80. Retrieved from http://www.ncbi.nlm.nih.gov/pubmed/9700655

Iqbal, K., Alonso, A. C., Gong, C. X., Khatoon, S., Singh, T. J., & Grundke-Iqbal, I. Mechanism of neurofibrillary degeneration in Alzheimer's disease. *Molecular Neurobiology*, *9*(1-3), 119–23. Retrieved from http://www.ncbi.nlm.nih.gov/pubmed/7888088

Irizarry, M. C., Soriano, F., McNamara, M., Page, K. J., Schenk, D., Games, D., & Hyman, B. T. (1997). Abeta deposition is associated with neuropil changes, but not with overt neuronal loss in the human amyloid precursor protein V717F (PDAPP) transgenic mouse. *The Journal of Neuroscience : The Official Journal of the Society for Neuroscience*, *17*(18), 7053–7059.

Ittner, L. M., & Götz, J. (2011). Amyloid-β and tau--a toxic pas de deux in Alzheimer's disease. *Nature Reviews. Neuroscience*, *12*(2), 65–72. http://doi.org/10.1038/nrn2967

Ittner, L. M., Ke, Y. D., Delerue, F., Bi, M., Gladbach, A., van Eersel, J., … Götz, J. (2010). Dendritic function of tau mediates amyloid-beta toxicity in Alzheimer's disease mouse models. *Cell*, *142*(3), 387–97. http://doi.org/10.1016/j.cell.2010.06.036

Jack, C. R., Knopman, D. S., Jagust, W. J., Shaw, L. M., Aisen, P. S., Weiner, M. W., … Trojanowski, J. Q. (2010). Hypothetical model of dynamic biomarkers of the Alzheimer's pathological cascade. *Lancet Neurology*, *9*(1), 119–28. http://doi.org/10.1016/S1474-4422(09)70299-6

Jin, M., Shepardson, N., Yang, T., Chen, G., Walsh, D., & Selkoe, D. J. (2011). Soluble amyloid beta-protein dimers isolated from Alzheimer cortex directly induce Tau hyperphosphorylation and neuritic degeneration. *Proceedings of the National Academy of Sciences of the United States of America*, *108*(14), 5819–24. http://doi.org/10.1073/pnas.1017033108

Johnson, J. W., & Ascher, P. (1987). Glycine potentiates the NMDA response in cultured mouse brain neurons. *Nature*, *325*(6104), 529–31. http://doi.org/10.1038/325529a0

Kang Et Al, 1987.Pdf. (n.d.).

Katzman, R. (2008). The Prevalence and Malignancy of Alzheimer Disease. A Major Killer. *Alzheimer's and Dementia*, *4*(6), 378–380. http://doi.org/10.1016/j.jalz.2008.10.003

Kawarabayashi, T., Shoji, M., Younkin, L. H., Wen-Lang, L., Dickson, D. W., Murakami, T., … Younkin, S. G. (2004). Dimeric amyloid beta protein rapidly accumulates in lipid rafts followed by apolipoprotein E and phosphorylated tau

accumulation in the Tg2576 mouse model of Alzheimer's disease. *The Journal of Neuroscience : The Official Journal of the Society for Neuroscience*, *24*(15), 3801–9. http://doi.org/10.1523/JNEUROSCI.5543-03.2004

Kessels, H. W., Nguyen, L. N., Nabavi, S., & Malinow, R. (2010). The prion protein as a receptor for amyloid-beta. *Nature*, *466*(7308), E3–4; discussion E4–5. http://doi.org/10.1038/nature09217

Kim, J.-H., Anwyl, R., Suh, Y.-H., Djamgoz, M. B. A., & Rowan, M. J. (2001). Use-Dependent Effects of Amyloidogenic Fragments of {beta}-Amyloid Precursor Protein on Synaptic Plasticity in Rat Hippocampus In Vivo. *J. Neurosci.*, *21*(4), 1327–1333. Retrieved from http://www.jneurosci.org/content/21/4/1327.long

King, M. E., Ahuja, V., Binder, L. I., & Kuret, J. (1999). Ligand-Dependent Tau Filament Formation : Implications for Alzheimer ' s Disease, *50*, 14851–14859.
Klunk, W. E., Price, J. C., Mathis, C. A., Tsopelas, N. D., Lopresti, B. J., Ziolko, S. K., … DeKosky, S. T. (2007). Amyloid deposition begins in the striatum of presenilin-1 mutation carriers from two unrelated pedigrees. *The Journal of Neuroscience : The Official Journal of the Society for Neuroscience*, *27*(23), 6174–84. http://doi.org/10.1523/JNEUROSCI.0730-07.2007

Klyubin, I., Betts, V., Welzel, A. T., Blennow, K., Zetterberg, H., Wallin, A., … Rowan, M. J. (2008). Amyloid beta protein dimer-containing human CSF disrupts synaptic plasticity: prevention by systemic passive immunization. *The Journal of Neuroscience : The Official Journal of the Society for Neuroscience*, *28*(16), 4231–7. http://doi.org/10.1523/JNEUROSCI.5161-07.2008

Knight, W. D., Okello, A. A., Ryan, N. S., Turkheimer, F. E., Rodríguez Martinez de Llano, S., Edison, P., … Rossor, M. N. (2011). Carbon-11-Pittsburgh compound B positron emission tomography imaging of amyloid deposition in presenilin 1 mutation carriers. *Brain : A Journal of Neurology*, *134*(Pt 1), 293–300. http://doi.org/10.1093/brain/awq310

Knopman, D. S., Parisi, J. E., Salviati, a, Floriach-Robert, M., Boeve, B. F., Ivnik, R. J., … Petersen, R. C. (2003). Neuropathology of cognitively normal elderly. *Journal of Neuropathology and Experimental Neurology*, *62*(11), 1087–1095. http://doi.org/10.1016/j.jalz.2008.05.2215

Koffie, R. M., Meyer-Luehmann, M., Hashimoto, T., Adams, K. W., Mielke, M. L., Garcia-Alloza, M., … Spires-Jones, T. L. (2009). Oligomeric amyloid beta associates with postsynaptic densities and correlates with excitatory synapse loss near senile plaques. *Proceedings of the National Academy of Sciences of the United States of America*, *106*(10), 4012–7. http://doi.org/10.1073/pnas.0811698106

Kostylev, M. A., Kaufman, A. C., Nygaard, H. B., Patel, P., Haas, L. T., Gunther, E. C., … Strittmatter, S. M. (2015). Prion-Protein-Interacting Amyloid-β Oligomers of High

Molecular Weight are Tightly Correlated with Memory Impairment in Multiple Alzheimer Mouse Models. *The Journal of Biological Chemistry*, *290*(28), 17415–38. http://doi.org/10.1074/jbc.M115.643577

Kuhn, H., Dickinson-Anson, H., & Gage, F. (1996). Neurogenesis in the dentate gyrus of the adult rat: age-related decrease of neuronal progenitor proliferation. *J. Neurosci.*, *16*(6), 2027–2033. Retrieved from http://www.jneurosci.org/content/16/6/2027.short

Kuperstein, I., Broersen, K., Benilova, I., Rozenski, J., Jonckheere, W., Debulpaep, M., … De Strooper, B. (2010). Neurotoxicity of Alzheimer's disease Aβ peptides is induced by small changes in the Aβ42 to Aβ40 ratio. *The EMBO Journal*, *29*(19), 3408–3420. http://doi.org/10.1038/emboj.2010.211

Lacor, P. N., Buniel, M. C., Chang, L., Fernandez, S. J., Gong, Y., Viola, K. L., … Klein, W. L. (2004). Synaptic targeting by Alzheimer's-related amyloid beta oligomers. *The Journal of Neuroscience : The Official Journal of the Society for Neuroscience*, *24*(45), 10191–200. http://doi.org/10.1523/JNEUROSCI.3432-04.2004

Lacor, P. N., Buniel, M. C., Furlow, P. W., Clemente, A. S., Velasco, P. T., Wood, M., … Klein, W. L. (2007). Abeta oligomer-induced aberrations in synapse composition, shape, and density provide a molecular basis for loss of connectivity in Alzheimer's disease. *The Journal of Neuroscience : The Official Journal of the Society for Neuroscience*, *27*(4), 796–807. http://doi.org/10.1523/JNEUROSCI.3501-06.2007

Larson, M. E., & Lesné, S. E. (2012). Soluble Aβ oligomer production and toxicity. *Journal of Neurochemistry*, *120*(SUPPL. 1), 125–139. http://doi.org/10.1111/j.1471-4159.2011.07478.x

Larson, M. E., Sherman, M. A., Greimel, S., Kuskowski, M., Schneider, J. A., Bennett, D. A., & Lesné, S. E. (2012). Soluble α-synuclein is a novel modulator of Alzheimer's disease pathophysiology. *The Journal of Neuroscience : The Official Journal of the Society for Neuroscience*, *32*(30), 10253–66. http://doi.org/10.1523/JNEUROSCI.0581-12.2012

Larson, M., Sherman, M. a, Amar, F., Nuvolone, M., Schneider, J. a, Bennett, D. a, … Lesné, S. E. (2012). The complex PrP(c)-Fyn couples human oligomeric Aβ with pathological tau changes in Alzheimer's disease. *The Journal of Neuroscience : The Official Journal of the Society for Neuroscience*, *32*(47), 16857–71a. Retrieved from http://www.pubmedcentral.nih.gov/articlerender.fcgi?artid=3568961&tool=pmcentrez&rendertype=abstract

Laurén, J., Gimbel, D. A., Nygaard, H. B., Gilbert, J. W., & Strittmatter, S. M. (2009). Cellular prion protein mediates impairment of synaptic plasticity by amyloid-β oligomers. *Nature*, *457*(7233), 1128–1132. http://doi.org/10.1038/nature07761

Lee, M. K., Stirling, W., Xu, Y., Xu, X., Qui, D., Mandir, A. S., … Price, D. L. (2002). Human -synuclein-harboring familial Parkinson's disease-linked Ala-53 -> Thr mutation causes neurodegenerative disease with -synuclein aggregation in transgenic mice. *Proceedings of the National Academy of Sciences*, *99*(13), 8968–8973. http://doi.org/10.1073/pnas.132197599

Lee, M. S., Kwon, Y. T., Li, M., Peng, J., Friedlander, R. M., & Tsai, L. H. (2000). Neurotoxicity induces cleavage of p35 to p25 by calpain. *Nature*, *405*(6784), 360–4. http://doi.org/10.1038/35012636

Leinenga, G., & Gotz, J. (2015). Scanning ultrasound removes amyloid- and restores memory in an Alzheimer's disease mouse model. *Science Translational Medicine*, *7*(278), 278ra33–278ra33. http://doi.org/10.1126/scitranslmed.aaa2512

Lemere, C. A., Lopera, F., Kosik, K. S., Lendon, C. L., Ossa, J., Saido, T. C., … Selkoe, D. J. (1996). The E280A presenilin 1 Alzheimer mutation produces increased A beta 42 deposition and severe cerebellar pathology. *Nature Medicine*, *2*(10), 1146–50. Retrieved from http://www.ncbi.nlm.nih.gov/pubmed/8837617

Leon, W. C., Canneva, F., Partridge, V., Allard, S., Ferretti, M. T., DeWilde, A., … Cuello, A. C. (2010). A novel transgenic rat model with a full Alzheimer's-like amyloid pathology displays pre-plaque intracellular amyloid-beta-associated cognitive impairment. *Journal of Alzheimer's Disease : JAD*, *20*(1), 113–26. http://doi.org/10.3233/JAD-2010-1349

Leroy, K., Yilmaz, Z., & Brion, J.-P. (2007). Increased level of active GSK-3beta in Alzheimer's disease and accumulation in argyrophilic grains and in neurones at different stages of neurofibrillary degeneration. *Neuropathology and Applied Neurobiology*, *33*(1), 43–55. http://doi.org/10.1111/j.1365-2990.2006.00795.x

Lesné, S. E., Sherman, M. A., Grant, M., Kuskowski, M., Schneider, J. A., Bennett, D. A., & Ashe, K. H. (2013). Brain amyloid-β oligomers in ageing and Alzheimer's disease. *Brain : A Journal of Neurology*, *136*(Pt 5), 1383–98. http://doi.org/10.1093/brain/awt062

Lesné, S., Koh, M. T., Kotilinek, L., Kayed, R., Glabe, C. G., Yang, A., … Ashe, K. H. (2006). A specific amyloid-beta protein assembly in the brain impairs memory. *Nature*, *440*(7082), 352–7. http://doi.org/10.1038/nature04533

Léveillé, F., El Gaamouch, F., Gouix, E., Lecocq, M., Lobner, D., Nicole, O., & Buisson, A. (2008). Neuronal viability is controlled by a functional relation between synaptic and extrasynaptic NMDA receptors. *FASEB Journal : Official Publication of the Federation of American Societies for Experimental Biology*, *22*(12), 4258–71. http://doi.org/10.1096/fj.08-107268

Levy, E., Carman, M. D., Fernandez-Madrid, I. J., Power, M. D., Lieberburg, I., van Duinen, S. G., … Frangione, B. (1990). Mutation of the Alzheimer's disease amyloid

gene in hereditary cerebral hemorrhage, Dutch type. *Science (New York, N.Y.)*, *248*(4959), 1124–1126. http://doi.org/10.1126/science.2111584

Lewis, J., Dickson, D. W., Lin, W. L., Chisholm, L., Corral, a, Jones, G., … McGowan, E. (2001). Enhanced neurofibrillary degeneration in transgenic mice expressing mutant tau and APP. *Science (New York, N.Y.)*, *293*(5534), 1487–1491. http://doi.org/10.1126/science.1058189

Li, L., Cheung, T., Chen, J., & Herrup, K. (2011). A comparative study of five mouse models of Alzheimer's disease: cell cycle events reveal new insights into neurons at risk for death. *International Journal of Alzheimer's Disease*, *2011*, 171464. http://doi.org/10.4061/2011/171464

Li, S., Hong, S., Shepardson, N. E., Walsh, D. M., Shankar, G. M., & Selkoe, D. (2009). Soluble oligomers of amyloid Beta protein facilitate hippocampal long-term depression by disrupting neuronal glutamate uptake. *Neuron*, *62*(6), 788–801. http://doi.org/10.1016/j.neuron.2009.05.012

Li, T., & Paudel, H. K. (2006). Glycogen synthase kinase 3beta phosphorylates Alzheimer's disease-specific Ser396 of microtubule-associated protein tau by a sequential mechanism. *Biochemistry*, *45*(10), 3125–33. http://doi.org/10.1021/bi051634r

Lippa, C. F., Fujiwara, H., Mann, D. M., Giasson, B., Baba, M., Schmidt, M. L., … Trojanowski, J. Q. (1998). Lewy bodies contain altered alpha-synuclein in brains of many familial Alzheimer's disease patients with mutations in presenilin and amyloid precursor protein genes. *The American Journal of Pathology*, *153*(5), 1365–70. Retrieved from http://www.pubmedcentral.nih.gov/articlerender.fcgi?artid=1853391&tool=pmcentrez&rendertype=abstract

Litersky, J. M., Johnson, G. V, Jakes, R., Goedert, M., Lee, M., & Seubert, P. (1996). Tau protein is phosphorylated by cyclic AMP-dependent protein kinase and calcium/calmodulin-dependent protein kinase II within its microtubule-binding domains at Ser-262 and Ser-356. *The Biochemical Journal*, *316 (Pt 2*, 655–60. Retrieved from http://www.pubmedcentral.nih.gov/articlerender.fcgi?artid=1217397&tool=pmcentrez&rendertype=abstract

Liu, C., & Götz, J. (2013). Profiling murine tau with 0N, 1N and 2N isoform-specific antibodies in brain and peripheral organs reveals distinct subcellular localization, with the 1N isoform being enriched in the nucleus. *PloS One*, *8*(12), e84849. http://doi.org/10.1371/journal.pone.0084849

Liu, L., Wong, T. P., Pozza, M. F., Lingenhoehl, K., Wang, Y., Sheng, M., … Wang, Y. T. (2004). Role of NMDA receptor subtypes in governing the direction of hippocampal synaptic plasticity. *Science (New York, N.Y.)*, *304*(5673), 1021–4. http://doi.org/10.1126/science.1096615

Liu, Y., Yoo, M.-J., Savonenko, A., Stirling, W., Price, D. L., Borchelt, D. R., … Lee, M. K. (2008). Amyloid pathology is associated with progressive monoaminergic neurodegeneration in a transgenic mouse model of Alzheimer's disease. *The Journal of Neuroscience : The Official Journal of the Society for Neuroscience*, *28*(51), 13805–14. http://doi.org/10.1523/JNEUROSCI.4218-08.2008

Lledo, P. M., Hjelmstad, G. O., Mukherji, S., Soderling, T. R., Malenka, R. C., & Nicoll, R. A. (1995). Calcium/calmodulin-dependent kinase II and long-term potentiation enhance synaptic transmission by the same mechanism. *Proceedings of the National Academy of Sciences of the United States of America*, *92*(24), 11175–9. Retrieved from http://www.pubmedcentral.nih.gov/articlerender.fcgi?artid=40594&tool=pmcentrez&rendertype=abstract

Loerch, P. M., Lu, T., Dakin, K. A., Vann, J. M., Isaacs, A., Geula, C., … Yankner, B. A. (2008). Evolution of the aging brain transcriptome and synaptic regulation. *PloS One*, *3*(10), e3329. http://doi.org/10.1371/journal.pone.0003329

Lopes, J. P., Oliveira, C. R., & Agostinho, P. (2010). Neurodegeneration in an Abeta-induced model of Alzheimer's disease: the role of Cdk5. *Aging Cell*, *9*(1), 64–77. http://doi.org/10.1111/j.1474-9726.2009.00536.x

Lou, L. L., Lloyd, S. J., & Schulman, H. (1986). Activation of the multifunctional Ca2+/calmodulin-dependent protein kinase by autophosphorylation: ATP modulates production of an autonomous enzyme. *Proceedings of the National Academy of Sciences of the United States of America*, *83*(24), 9497–501. Retrieved from http://www.pubmedcentral.nih.gov/articlerender.fcgi?artid=387167&tool=pmcentrez&rendertype=abstract

Lucas, J. J., Hernández, F., Gómez-Ramos, P., Morán, M. A., Hen, R., & Avila, J. (2001). Decreased nuclear beta-catenin, tau hyperphosphorylation and neurodegeneration in GSK-3beta conditional transgenic mice. *The EMBO Journal*, *20*(1-2), 27–39. http://doi.org/10.1093/emboj/20.1.27

Lue, L. F., Kuo, Y. M., Roher, a E., Brachova, L., Shen, Y., Sue, L., … Rogers, J. (1999). Soluble amyloid beta peptide concentration as a predictor of synaptic change in Alzheimer's disease. *The American Journal of Pathology*, *155*(3), 853–862. http://doi.org/10.1016/S0002-9440(10)65184-X

Luna-Muñoz, J., García-Sierra, F., Falcón, V., Menéndez, I., Chávez-Macías, L., & Mena, R. (2005). Regional conformational change involving phosphorylation of tau protein at the Thr231, precedes the structural change detected by Alz-50 antibody in Alzheimer's disease. *Journal of Alzheimer's Disease : JAD*, *8*(1), 29–41. Retrieved from http://www.ncbi.nlm.nih.gov/pubmed/16155347

Ma, Q.-L., Harris-White, M. E., Ubeda, O. J., Simmons, M., Beech, W., Lim, G. P., … Cole, G. M. (2007). Evidence of Abeta- and transgene-dependent defects in ERK-CREB

signaling in Alzheimer's models. *Journal of Neurochemistry*, *103*(4), 1594–607. http://doi.org/10.1111/j.1471-4159.2007.04869.x

Mairet-Coello, G., Courchet, J., Pieraut, S., Courchet, V., Maximov, A., & Polleux, F. (2013). The CAMKK2-AMPK Kinase Pathway Mediates the Synaptotoxic Effects of Aβ Oligomers through Tau Phosphorylation. *Neuron*, *78*(1), 94–108. http://doi.org/10.1016/j.neuron.2013.02.003

Mann, D. M. a, Iwatsubo, T., Cairns, T. N. J., Lantos, P. L., Nochlin, D., Prihar, G., … D, M. (1996). Amyloid p Protein (Ap) Deposition in Chromosome 14-linked Alzheimer ' s Disease : Predominance of ApB (G), 149–156.

Martin, L., Latypova, X., Wilson, C. M., Magnaudeix, A., Perrin, M., Yardin, C., & Terro, F. (2013). Tau protein kinases : Involvement in Alzheimer ' s disease. *Ageing Research Reviews*, *12*(1), 289–309. http://doi.org/10.1016/j.arr.2012.06.003

Masliah et al 1996. (n.d.).

Matsui, T., Sekiguchi, M., Hashimoto, A., Tomita, U., Nishikawa, T., & Wada, K. (1995). Functional comparison of D-serine and glycine in rodents: the effect on cloned NMDA receptors and the extracellular concentration. *Journal of Neurochemistry*, *65*(1), 454–8. Retrieved from http://www.ncbi.nlm.nih.gov/pubmed/7790891

Mayer, M. L., Westbrook, G. L., & Guthrie, P. B. (1984). Voltage-dependent block by Mg2+ of NMDA responses in spinal cord neurones. *Nature*, *309*(5965), 261–263. http://doi.org/10.1038/309261a0

McLaurin, J., Kierstead, M. E., Brown, M. E., Hawkes, C. A., Lambermon, M. H. L., Phinney, A. L., … St George-Hyslop, P. (2006). Cyclohexanehexol inhibitors of Abeta aggregation prevent and reverse Alzheimer phenotype in a mouse model. *Nature Medicine*, *12*(7), 801–8. http://doi.org/10.1038/nm1423

McLean, C. A., Cherny, R. A., Fraser, F. W., Fuller, S. J., Smith, M. J., Beyreuther, K., … Masters, C. L. (1999). Soluble pool of Abeta amyloid as a determinant of severity of neurodegeneration in Alzheimer's disease. *Annals of Neurology*, *46*(6), 860–6. Retrieved from http://www.ncbi.nlm.nih.gov/pubmed/10589538

Meilandt, W. J., Cisse, M., Ho, K., Wu, T., Esposito, L. A., Scearce-Levie, K., … Mucke, L. (2009). Neprilysin overexpression inhibits plaque formation but fails to reduce pathogenic Abeta oligomers and associated cognitive deficits in human amyloid precursor protein transgenic mice. *The Journal of Neuroscience : The Official Journal of the Society for Neuroscience*, *29*(7), 1977–86. http://doi.org/10.1523/JNEUROSCI.2984-08.2009

Meldrum, B. S. (2000). Glutamate as a neurotransmitter in the brain: review of physiology and pathology. *The Journal of Nutrition*, *130*(4S Suppl), 1007S–15S. Retrieved from http://www.ncbi.nlm.nih.gov/pubmed/10736372

Miller, S. (1986). Regulation of brain Type II Ca2+/calmodulin-dependent protein kinase by autophosphorylation: A Ca2+-triggered molecular switch. *Cell*, *44*(6), 861–870. http://doi.org/10.1016/0092-8674(86)90008-5
Miller, S. L., Fenstermacher, E., Bates, J., Blacker, D., Sperling, R. A., & Dickerson, B. C. (2008). Hippocampal activation in adults with mild cognitive impairment predicts subsequent cognitive decline. *Journal of Neurology, Neurosurgery, and Psychiatry*, *79*(6), 630–5. http://doi.org/10.1136/jnnp.2007.124149

Min, S.-W., Cho, S.-H., Zhou, Y., Schroeder, S., Haroutunian, V., Seeley, W. W., … Gan, L. (2010). Acetylation of tau inhibits its degradation and contributes to tauopathy. *Neuron*, *67*(6), 953–66. http://doi.org/10.1016/j.neuron.2010.08.044

Mintun, M. A., Larossa, G. N., Sheline, Y. I., Dence, C. S., Lee, S. Y., Mach, R. H., … Morris, J. C. (2006). [11C]PIB in a nondemented population: potential antecedent marker of Alzheimer disease. *Neurology*, *67*(3), 446–52. http://doi.org/10.1212/01.wnl.0000228230.26044.a4

Miyajima, M., Nornes, H. O., & Neuman, T. (1995). Cyclin E is expressed in neurons and forms complexes with cdk5. *Neuroreport*, *6*(8), 1130–2. Retrieved from http://www.ncbi.nlm.nih.gov/pubmed/7662893

Montgomery, J. M., Pavlidis, P., & Madison, D. V. (2001). Pair Recordings Reveal All-Silent Synaptic Connections and the Postsynaptic Expression of Long-Term Potentiation. *Neuron*, *29*(3), 691–701. http://doi.org/10.1016/S0896-6273(01)00244-6

Moonis, M., Swearer, J. M., Dayaw, M. P. E., St George-Hyslop, P., Rogaeva, E., Kawarai, T., & Pollen, D. A. (2005). Familial Alzheimer disease: decreases in CSF Abeta42 levels precede cognitive decline. *Neurology*, *65*(2), 323–5. http://doi.org/10.1212/01.wnl.0000171397.32851.bc

Morishima-Kawashima, M., Hasegawa, M., Takio, K., Suzuki, M., Titani, K., & Ihara, Y. (1993). Ubiquitin is conjugated with amino-terminally processed tau in paired helical filaments. *Neuron*, *10*(6), 1151–60. Retrieved from http://www.ncbi.nlm.nih.gov/pubmed/8391280

Mormino, E. C., Kluth, J. T., Madison, C. M., Rabinovici, G. D., Baker, S. L., Miller, B. L., … Jagust, W. J. (2009). Episodic memory loss is related to hippocampal-mediated beta-amyloid deposition in elderly subjects. *Brain : A Journal of Neurology*, *132*(Pt 5), 1310–23. http://doi.org/10.1093/brain/awn320

Morris, G. P., Clark, I. A., & Vissel, B. (2014). Inconsistencies and controversies surrounding the amyloid hypothesis of Alzheimer's disease. *Acta Neuropathologica Communications*, *2*, 135. http://doi.org/10.1186/s40478-014-0135-5

Morris, J. C., Roe, C. M., Grant, E. A., Head, D., Storandt, M., Goate, A. M., … Mintun, M. A. (2009). Pittsburgh compound B imaging and prediction of progression from cognitive normality to symptomatic Alzheimer disease. *Archives of Neurology*, *66*(12), 1469–75. http://doi.org/10.1001/archneurol.2009.269

Morris, M., Knudsen, G. M., Maeda, S., Trinidad, J. C., Ioanoviciu, A., Burlingame, A. L., & Mucke, L. (2015). Tau post-translational modifications in wild-type and human amyloid precursor protein transgenic mice. *Nature Neuroscience*, *18*(8), 1183–1189. http://doi.org/10.1038/nn.4067

Mucke, L., Masliah, E., Yu, G. Q., Mallory, M., Rockenstein, E. M., Tatsuno, G., … McConlogue, L. (2000). High-level neuronal expression of abeta 1-42 in wild-type human amyloid protein precursor transgenic mice: synaptotoxicity without plaque formation. *The Journal of Neuroscience : The Official Journal of the Society for Neuroscience*, *20*(11), 4050–4058. http://doi.org/20/11/4050 [pii]

Mucke, L., & Selkoe, D. J. (2012). Neurotoxicity of amyloid β-protein: Synaptic and network dysfunction. *Cold Spring Harbor Perspectives in Medicine*, *2*(7), 1–18. http://doi.org/10.1101/cshperspect.a006338

Noble, W., Olm, V., Takata, K., Casey, E., Mary, O., Meyerson, J., … Duff, K. (2003). Cdk5 Is a Key Factor in Tau Aggregation and Tangle Formation In Vivo. *Neuron*, *38*(4), 555–565. http://doi.org/10.1016/S0896-6273(03)00259-9

Oddo, S., Vasilevko, V., Caccamo, A., Kitazawa, M., Cribbs, D. H., & LaFerla, F. M. (2006). Reduction of soluble Abeta and tau, but not soluble Abeta alone, ameliorates cognitive decline in transgenic mice with plaques and tangles. *The Journal of Biological Chemistry*, *281*(51), 39413–23. http://doi.org/10.1074/jbc.M608485200

Olichney, J. M., Galasko, D., Salmon, D. P., Hofstetter, C. R., Hansen, L. A., Katzman, R., & Thal, L. J. (1998). Cognitive decline is faster in Lewy body variant than in Alzheimer's disease. *Neurology*, *51*(2), 351–7. Retrieved from http://www.ncbi.nlm.nih.gov/pubmed/9710002

Origlia, N., Righi, M., Capsoni, S., Cattaneo, A., Fang, F., Stern, D. M., … Domenici, L. (2008). Receptor for advanced glycation end product-dependent activation of p38 mitogen-activated protein kinase contributes to amyloid-beta-mediated cortical synaptic dysfunction. *The Journal of Neuroscience : The Official Journal of the Society for Neuroscience*, *28*(13), 3521–30. http://doi.org/10.1523/JNEUROSCI.0204-08.2008

Otmakhov, N., Griffith, L. C., & Lisman, J. E. (1997). Postsynaptic Inhibitors of Calcium/Calmodulin-Dependent Protein Kinase Type II Block Induction But Not

Maintenance of Pairing-Induced Long-Term Potentiation. *J. Neurosci.*, *17*(14), 5357–5365. Retrieved from http://www.jneurosci.org/content/17/14/5357.short

Palop, J. J., Chin, J., & Mucke, L. (2006). A network dysfunction perspective on neurodegenerative diseases. *Nature*, *443*(7113), 768–73. http://doi.org/10.1038/nature05289

Palop, J. J., Chin, J., Roberson, E. D., Wang, J., Thwin, M. T., Bien-Ly, N., … Mucke, L. (2007). Aberrant excitatory neuronal activity and compensatory remodeling of inhibitory hippocampal circuits in mouse models of Alzheimer's disease. *Neuron*, *55*(5), 697–711. http://doi.org/10.1016/j.neuron.2007.07.025

Patzke, H., & Tsai, L.-H. (2002). Calpain-mediated cleavage of the cyclin-dependent kinase-5 activator p39 to p29. *The Journal of Biological Chemistry*, *277*(10), 8054–60. http://doi.org/10.1074/jbc.M109645200

Pei, J. J., Tanaka, T., Tung, Y. C., Braak, E., Iqbal, K., & Grundke-Iqbal, I. (1997). Distribution, levels, and activity of glycogen synthase kinase-3 in the Alzheimer disease brain. *Journal of Neuropathology and Experimental Neurology*, *56*(1), 70–8. Retrieved from http://www.ncbi.nlm.nih.gov/pubmed/8990130

Petralia, R. S., Wang, Y. X., Hua, F., Yi, Z., Zhou, A., Ge, L., … Wenthold, R. J. (2010). Organization of NMDA receptors at extrasynaptic locations. *Neuroscience*, *167*(1), 68–87. http://doi.org/10.1016/j.neuroscience.2010.01.022

Pettit, D. L., Perlman, S., & Malinow, R. (1994). Potentiated transmission and prevention of further LTP by increased CaMKII activity in postsynaptic hippocampal slice neurons. *Science (New York, N.Y.)*, *266*(5192), 1881–5. Retrieved from http://www.ncbi.nlm.nih.gov/pubmed/7997883

Picconi, B., Gardoni, F., Centonze, D., Mauceri, D., Cenci, M. A., Bernardi, G., … Di Luca, M. (2004). Abnormal Ca2+-calmodulin-dependent protein kinase II function mediates synaptic and motor deficits in experimental parkinsonism. *The Journal of Neuroscience : The Official Journal of the Society for Neuroscience*, *24*(23), 5283–91. http://doi.org/10.1523/JNEUROSCI.1224-04.2004

Pike, K. E., Savage, G., Villemagne, V. L., Ng, S., Moss, S. a., Maruff, P., … Rowe, C. C. (2007). β-amyloid imaging and memory in non-demented individuals: Evidence for preclinical Alzheimer's disease. *Brain*, *130*(11), 2837–2844. http://doi.org/10.1093/brain/awm238

Price, J. L., & Morris, J. C. (1999). Tangles and plaques in nondemented aging and "preclinical" alzheimer's disease. *Annals of Neurology*, *45*(3), 358–368. http://doi.org/10.1002/1531-8249(199903)45:3<358::AID-ANA12>3.0.CO;2-X

Price, J. L., & Morris, J. C. (1999). Tangles and plaques in nondemented aging and "preclinical" Alzheimer's disease. *Annals of Neurology*, *45*(3), 358–68. Retrieved from http://www.ncbi.nlm.nih.gov/pubmed/10072051

Putcha, D., Brickhouse, M., O'Keefe, K., Sullivan, C., Rentz, D., Marshall, G., … Sperling, R. (2011). Hippocampal hyperactivation associated with cortical thinning in Alzheimer's disease signature regions in non-demented elderly adults. *The Journal of Neuroscience : The Official Journal of the Society for Neuroscience*, *31*(48), 17680–8. http://doi.org/10.1523/JNEUROSCI.4740-11.2011

Rapoport, M., Dawson, H. N., Binder, L. I., Vitek, M. P., & Ferreira, A. (2002). Tau is essential to beta -amyloid-induced neurotoxicity. *Proceedings of the National Academy of Sciences of the United States of America*, *99*(9), 6364–6369. http://doi.org/10.1073/pnas.092136199

Reed, M. N., Hofmeister, J. J., Jungbauer, L., Welzel, A. T., Yu, C., Sherman, M. A., … Cleary, J. P. (2011). Cognitive effects of cell-derived and synthetically derived Aβ oligomers. *Neurobiology of Aging*, *32*(10), 1784–94. http://doi.org/10.1016/j.neurobiolaging.2009.11.007

Rich, R. C., & Schulman, H. (1998). Substrate-directed function of calmodulin in autophosphorylation of Ca2+/calmodulin-dependent protein kinase II. *The Journal of Biological Chemistry*, *273*(43), 28424–9. Retrieved from http://www.ncbi.nlm.nih.gov/pubmed/9774470

Roberson, E. D., Scearce-Levie, K., Palop, J. J., Yan, F., Cheng, I. H., Wu, T., … Mucke, L. (2007). Reducing endogenous tau ameliorates amyloid beta-induced deficits in an Alzheimer's disease mouse model. *Science (New York, N.Y.)*, *316*(5825), 750–4. http://doi.org/10.1126/science.1141736

Rovelet-Lecrux, A., Hannequin, D., Raux, G., Le Meur, N., Laquerrière, A., Vital, A., … Campion, D. (2006). APP locus duplication causes autosomal dominant early-onset Alzheimer disease with cerebral amyloid angiopathy. *Nature Genetics*, *38*(1), 24–26. http://doi.org/10.1038/ng1718

Rowe, C. C., Ellis, K. A., Rimajova, M., Bourgeat, P., Pike, K. E., Jones, G., … Villemagne, V. L. (2010). Amyloid imaging results from the Australian Imaging, Biomarkers and Lifestyle (AIBL) study of aging. *Neurobiology of Aging*, *31*(8), 1275–83. http://doi.org/10.1016/j.neurobiolaging.2010.04.007

Saitoh, T., & Schwartz, J. H. (1985). Phosphorylation-dependent subcellular translocation of a Ca2+/calmodulin-dependent protein kinase produces an autonomous enzyme in Aplysia neurons. *The Journal of Cell Biology*, *100*(3), 835–42. Retrieved from http://www.pubmedcentral.nih.gov/articlerender.fcgi?artid=2113531&tool=pmcentrez&rendertype=abstract

Salthouse, T. A. (2009). When does age-related cognitive decline begin? *Neurobiology of Aging*, *30*(4), 507–14. http://doi.org/10.1016/j.neurobiolaging.2008.09.023

Samuels, B. A., Hsueh, Y.-P., Shu, T., Liang, H., Tseng, H.-C., Hong, C.-J., … Tsai, L.-H. (2007). Cdk5 promotes synaptogenesis by regulating the subcellular distribution of the MAGUK family member CASK. *Neuron*, *56*(5), 823–37. http://doi.org/10.1016/j.neuron.2007.09.035

Sato, K., Suematsu, A., Nakashima, T., Takemoto-Kimura, S., Aoki, K., Morishita, Y., … Takayanagi, H. (2006). Regulation of osteoclast differentiation and function by the CaMK-CREB pathway. *Nature Medicine*, *12*(12), 1410–6. http://doi.org/10.1038/nm1515

Scheuner, D., Eckman, C., Jensen, M., Song, X., Citron, M., Suzuki, N., … Younkin, S. (1996). Secreted amyloid beta-protein similar to that in the senile plaques of Alzheimer's disease is increased in vivo by the presenilin 1 and 2 and APP mutations linked to familial Alzheimer's disease. *Nature Medicine*, *2*(8), 864–70. Retrieved from http://www.ncbi.nlm.nih.gov/pubmed/8705854

Schwab, C., Hosokawa, M., & McGeer, P. L. (2004). Transgenic mice overexpressing amyloid beta protein are an incomplete model of Alzheimer disease. *Experimental Neurology*, *188*(1), 52–64. http://doi.org/10.1016/j.expneurol.2004.03.016

Scott, D. A., Tabarean, I., Tang, Y., Cartier, A., Masliah, E., & Roy, S. (2010). A pathologic cascade leading to synaptic dysfunction in alpha-synuclein-induced neurodegeneration. *The Journal of Neuroscience : The Official Journal of the Society for Neuroscience*, *30*(24), 8083–95. http://doi.org/10.1523/JNEUROSCI.1091-10.2010

Sengupta, A., Kabat, J., Novak, M., Wu, Q., Grundke-Iqbal, I., & Iqbal, K. (1998). Phosphorylation of tau at both Thr 231 and Ser 262 is required for maximal inhibition of its binding to microtubules. *Archives of Biochemistry and Biophysics*, *357*(2), 299–309. http://doi.org/10.1006/abbi.1998.0813

Sengupta, A., Wu, Q., Grundke-Iqbal, I., Iqbal, K., & Singh, T. J. (1997). Potentiation of GSK-3-catalyzed Alzheimer-like phosphorylation of human tau by cdk5. *Molecular and Cellular Biochemistry*, *167*(1-2), 99–105. Retrieved from http://www.ncbi.nlm.nih.gov/pubmed/9059986

Sergeant, N., Bretteville, A., Hamdane, M., Caillet-Boudin, M.-L., Grognet, P., Bombois, S., … Buée, L. (2008). Biochemistry of Tau in Alzheimer's disease and related neurological disorders. *Expert Review of Proteomics*, *5*(2), 207–24. http://doi.org/10.1586/14789450.5.2.207

Serrano-pozo, A., Frosch, M. P., Masliah, E., & Hyman, B. T. (2015). Neuropathological Alterations in Alzheimer Disease pic hallmarks, 1–24.

Seward, M. E., Swanson, E., Norambuena, A., Reimann, A., Cochran, J. N., Li, R., … Bloom, G. S. (2013). Amyloid-β signals through tau to drive ectopic neuronal cell cycle re-entry in Alzheimer's disease. *Journal of Cell Science*, *126*(Pt 5), 1278–86. http://doi.org/10.1242/jcs.1125880

Shankar, G. M., Bloodgood, B. L., Townsend, M., Walsh, D. M., Selkoe, D. J., & Sabatini, B. L. (2007). Natural oligomers of the Alzheimer amyloid-beta protein induce reversible synapse loss by modulating an NMDA-type glutamate receptor-dependent signaling pathway. *The Journal of Neuroscience : The Official Journal of the Society for Neuroscience*, *27*(11), 2866–75. http://doi.org/10.1523/JNEUROSCI.4970-06.2007

Shankar, G. M., Li, S., Mehta, T. H., Garcia-Munoz, A., Shepardson, N. E., Smith, I., … Selkoe, D. J. (2008). Amyloid-beta protein dimers isolated directly from Alzheimer's brains impair synaptic plasticity and memory. *Nature Medicine*, *14*(8), 837–42. http://doi.org/10.1038/nm1782

Silva, A. J., Stevens, C. F., Tonegawa, S., & Wang, Y. (1992). Deficient hippocampal long-term potentiation in alpha-calcium-calmodulin kinase II mutant mice. *Science (New York, N.Y.)*, *257*(5067), 201–6. Retrieved from http://www.ncbi.nlm.nih.gov/pubmed/1378648

Simakova, O., & Arispe, N. J. (2007). The cell-selective neurotoxicity of the Alzheimer's Abeta peptide is determined by surface phosphatidylserine and cytosolic ATP levels. Membrane binding is required for Abeta toxicity. *The Journal of Neuroscience : The Official Journal of the Society for Neuroscience*, *27*(50), 13719–29. http://doi.org/10.1523/JNEUROSCI.3006-07.2007

Simans, R., Mistretta, S., Durkin, T., Savage, M. J., Loh, T., Trusko, S., & Scott, R. W. (1993). Processing of the @ -Amyloid Precursor, *268*(22), 16602–16609.

Singh, T. J., Wang, J.-Z., Novak, M., Kontzekova, E., Grundke-Iqbal, I., & Iqbal, K. (1996). Calcium/calmodulin-dependent protein kinase II phosphorylates tau at Ser-262 but only partially inhibits its binding to microtubules. *FEBS Letters*, *387*(2-3), 145–148. http://doi.org/10.1016/0014-5793(96)00485-1

Skoog, I., Davidsson, P., Aevarsson, O., Vanderstichele, H., Vanmechelen, E., & Blennow, K. (2003). Cerebrospinal fluid beta-amyloid 42 is reduced before the onset of sporadic dementia: a population-based study in 85-year-olds. *Dementia and Geriatric Cognitive Disorders*, *15*(3), 169–76. http://doi.org/68478

Sleegers, K., Brouwers, N., Gijselinck, I., Theuns, J., Goossens, D., Wauters, J., … Van Broeckhoven, C. (2006). APP duplication is sufficient to cause early onset Alzheimer's dementia with cerebral amyloid angiopathy. *Brain*, *129*(11), 2977–2983. http://doi.org/10.1093/brain/awl203

Smith, D. (2003). Cdk5 in neuroskeletal dynamics. *Neuro-Signals*, *12*(4-5), 239–51. http://doi.org/74626

Snyder, E. M., Nong, Y., Almeida, C. G., Paul, S., Moran, T., Choi, E. Y., … Greengard, P. (2005). Regulation of NMDA receptor trafficking by amyloid-beta. *Nature Neuroscience*, *8*(8), 1051–8. http://doi.org/10.1038/nn1503

Sperling, R. A., Aisen, P. S., Beckett, L. A., Bennett, D. A., Craft, S., Fagan, A. M., … Phelps, C. H. (2011). Toward defining the preclinical stages of Alzheimer's disease: recommendations from the National Institute on Aging-Alzheimer's Association workgroups on diagnostic guidelines for Alzheimer's disease. *Alzheimer's & Dementia : The Journal of the Alzheimer's Association*, *7*(3), 280–92. http://doi.org/10.1016/j.jalz.2011.03.003

Sperling, R. A., Laviolette, P. S., O'Keefe, K., O'Brien, J., Rentz, D. M., Pihlajamaki, M., … Johnson, K. A. (2009). Amyloid deposition is associated with impaired default network function in older persons without dementia. *Neuron*, *63*(2), 178–88. http://doi.org/10.1016/j.neuron.2009.07.003

Spires, T. L., Meyer-Luehmann, M., Stern, E. a, McLean, P. J., Skoch, J., Nguyen, P. T., … Hyman, B. T. (2005). Dendritic spine abnormalities in amyloid precursor protein transgenic mice demonstrated by gene transfer and intravital multiphoton microscopy. *The Journal of Neuroscience : The Official Journal of the Society for Neuroscience*, *25*(31), 7278–7287. http://doi.org/10.1523/JNEUROSCI.1879-05.2005

Stambolic, V., & Woodgett, J. R. (1994). Mitogen inactivation of glycogen synthase kinase-3 beta in intact cells via serine 9 phosphorylation. *The Biochemical Journal*, *303 (Pt 3*, 701–4. Retrieved from http://www.pubmedcentral.nih.gov/articlerender.fcgi?artid=1137602&tool=pmcentrez&rendertype=abstract

Steiner, B., Mandelkow, E. M., Biernat, J., Gustke, N., Meyer, H. E., Schmidt, B., … Kirschner, M. W. (1990). Phosphorylation of microtubule-associated protein tau: identification of the site for Ca2(+)-calmodulin dependent kinase and relationship with tau phosphorylation in Alzheimer tangles. *The EMBO Journal*, *9*(11), 3539–44. Retrieved from /pmc/articles/PMC552103/?report=abstract

Stevens, C. F., Tonegawa, S., & Wang, Y. (1994). The role of calcium–calmodulin kinase II in three forms of synaptic plasticity. *Current Biology*, *4*(8), 687–693. http://doi.org/10.1016/S0960-9822(00)00153-6

Storandt, M., Mintun, M. A., Head, D., & Morris, J. C. (2009). Cognitive decline and brain volume loss as signatures of cerebral amyloid-beta peptide deposition identified with Pittsburgh compound B: cognitive decline associated with Abeta deposition. *Archives of Neurology*, *66*(12), 1476–81. http://doi.org/10.1001/archneurol.2009.272

Sturchler-Pierrat, C., Abramowski, D., Duke, M., Wiederhold, K. H., Mistl, C., Rothacher, S., … Sommer, B. (1997). Two amyloid precursor protein transgenic mouse models with Alzheimer disease-like pathology. *Proceedings of the National Academy of Sciences of the United States of America*, *94*(24), 13287–13292. http://doi.org/10.1073/pnas.94.24.13287

Sumi, M., Kiuchi, K., Ishikawa, T., Ishii, A., Hagiwara, M., Nagatsu, T., & Hidaka, H. (1991). The newly synthesized selective dependent protein kinase II inhibitor KN-93 reduces dopamine contents in PC12h cells. *Biochemical and Biophysical Research Communications*, *181*(3), 968–975. http://doi.org/10.1016/0006-291X(91)92031-E

Sunderland, T., Linker, G., Mirza, N., Putnam, K. T., Friedman, D. L., Kimmel, L. H., … Cohen, R. M. (2003). Decreased beta-amyloid1-42 and increased tau levels in cerebrospinal fluid of patients with Alzheimer disease. *JAMA*, *289*(16), 2094–103. http://doi.org/10.1001/jama.289.16.2094

Tariot, P. N., Farlow, M. R., Grossberg, G. T., Graham, S. M., McDonald, S., & Gergel, I. (2004). Memantine treatment in patients with moderate to severe Alzheimer disease already receiving donepezil: a randomized controlled trial. *JAMA*, *291*(3), 317–24. http://doi.org/10.1001/jama.291.3.317

Terasawa, M., Hidaka, H., & Chem, J. B. (1990). : H Tokumitsu , T Chijiwa , M Hagiwara , A KN-62 , a Specific Inhibitor of Ca2 ”/ Calmodulin-dependent Protein Kinase II *, *265*(8).

Terry, R. D., Masliah, E., Salmon, D. P., Butters, N., Deteresa, R., Hill, R., … Katzman, R. (1991). Physical Basis of Cognitive Alterations in Alzheimer ’ s Disease : Synapse h s s Is the Major Correlate of Cognitive Impairment, 572–580.

Thinakaran, G., & Parent, A. T. (2004). Identification of the role of presenilins beyond Alzheimer’s disease. *Pharmacological Research*, *50*(4), 411–8. http://doi.org/10.1016/j.phrs.2003.12.026

Thornton, T. M., Pedraza-Alva, G., Deng, B., Wood, C. D., Aronshtam, A., Clements, J. L., … Rincon, M. (2008). Phosphorylation by p38 MAPK as an alternative pathway for GSK3beta inactivation. *Science (New York, N.Y.)*, *320*(5876), 667–70. http://doi.org/10.1126/science.1156037

Tomiyama, T., Nagata, T., Shimada, H., Teraoka, R., Fukushima, A., Kanemitsu, H., … Mori, H. (2008). A new amyloid ?? variant favoring oligomerization in Alzheimer’s-type dementia. *Annals of Neurology*, *63*(3), 377–387. http://doi.org/10.1002/ana.21321

Townsend, M., Shankar, G. M., Mehta, T., Walsh, D. M., & Selkoe, D. J. (2006). Effects of secreted oligomers of amyloid beta-protein on hippocampal synaptic plasticity: a potent role for trimers. *The Journal of Physiology*, *572*(Pt 2), 477–92. http://doi.org/10.1113/jphysiol.2005.103754

Trinczek, B. (1995). Microtubule-associated Protein/Microtubule Affinity-regulating Kinase (p110[IMAGE]). *Journal of Biological Chemistry*, *270*(13), 7679–7688. http://doi.org/10.1074/jbc.270.13.7679

Trinczek, B., Biernat, J., Baumann, K., Mandelkow, E. M., & Mandelkow, E. (1995). Domains of tau protein, differential phosphorylation, and dynamic instability of microtubules. *Molecular Biology of the Cell*, *6*(12), 1887–902. Retrieved from /pmc/articles/PMC366657/?report=abstract

Tsubuki, S., Takaki, Y., & Saido, T. C. (2003). Dutch, Flemish, Italian, and Arctic mutations of APP and resistance of A?? to physiologically relevant proteolytic degradation. *Lancet*, *361*(9373), 1957–1958. http://doi.org/10.1016/S0140-6736(03)13555-6

Um, J. W., Kaufman, A. C., Kostylev, M., Heiss, J. K., Stagi, M., Takahashi, H., … Strittmatter, S. M. (2013). Metabotropic glutamate receptor 5 is a coreceptor for Alzheimer aβ oligomer bound to cellular prion protein. *Neuron*, *79*(5), 887–902. http://doi.org/10.1016/j.neuron.2013.06.036

Um, J. W., Nygaard, H. B., Heiss, J. K., Kostylev, M. a, Stagi, M., Vortmeyer, A., … Strittmatter, S. M. (2012). Alzheimer amyloid-β oligomer bound to postsynaptic prion protein activates Fyn to impair neurons. *Nature Neuroscience*, *15*(9), 1227–1235. http://doi.org/10.1038/nn.3178

Vest, R. S., Davies, K. D., O'Leary, H., Port, J. D., & Bayer, K. U. (2007). Dual mechanism of a natural CaMKII inhibitor. *Molecular Biology of the Cell*, *18*(12), 5024–33. http://doi.org/10.1091/mbc.E07-02-0185

Villemagne, V. L., Ataka, S., Mizuno, T., Brooks, W. S., Wada, Y., Kondo, M., … Rowe, C. C. (2009). High striatal amyloid beta-peptide deposition across different autosomal Alzheimer disease mutation types. *Archives of Neurology*, *66*(12), 1537–44. http://doi.org/10.1001/archneurol.2009.285

Vodopivec, I., Galichet, A., Knobloch, M., Bierhaus, A., Heizmann, C. W., & Nitsch, R. M. (2009). RAGE does not affect amyloid pathology in transgenic ArcAbeta mice. *Neuro-Degenerative Diseases*, *6*(5-6), 270–80. http://doi.org/10.1159/000261723
Walsh, D. M., Klyubin, I., Fadeeva, J. V, Cullen, W. K., Anwyl, R., Wolfe, M. S., … Selkoe, D. J. (2002). Naturally secreted oligomers of amyloid beta protein potently inhibit hippocampal long-term potentiation in vivo. *Nature*, *416*(6880), 535–9. http://doi.org/10.1038/416535a

Walsh, D. M., Lomakin, A., Benedek, G. B., Condron, M. M., & Teplow, D. B. (1997). Amyloid -Protein Fibrillogenesis: DETECTION OF A PROTOFIBRILLAR INTERMEDIATE. *Journal of Biological Chemistry*, *272*(35), 22364–22372. http://doi.org/10.1074/jbc.272.35.22364

Walsh, D. M., Townsend, M., Podlisny, M. B., Shankar, G. M., Fadeeva, J. V, El Agnaf, O., … Selkoe, D. J. (2005). Certain inhibitors of synthetic amyloid beta-peptide (Abeta) fibrillogenesis block oligomerization of natural Abeta and thereby rescue long-term potentiation. *The Journal of Neuroscience : The Official Journal of the Society for Neuroscience*, *25*(10), 2455–62. http://doi.org/10.1523/JNEUROSCI.4391-04.2005

Wang, Q. M., Fiol, C. J., DePaoli-Roach, A. A., & Roach, P. J. (1994). Glycogen synthase kinase-3 beta is a dual specificity kinase differentially regulated by tyrosine and serine/threonine phosphorylation. *The Journal of Biological Chemistry*, *269*(20), 14566–74. Retrieved from http://www.ncbi.nlm.nih.gov/pubmed/7514173

Weeber, E. J., Jiang, Y.-H., Elgersma, Y., Varga, A. W., Carrasquillo, Y., Brown, S. E., … Sweatt, J. D. (2003). Derangements of hippocampal calcium/calmodulin-dependent protein kinase II in a mouse model for Angelman mental retardation syndrome. *The Journal of Neuroscience : The Official Journal of the Society for Neuroscience*, *23*(7), 2634–44. Retrieved from http://www.ncbi.nlm.nih.gov/pubmed/12684449

Woods, Y. L., Cohen, P., Becker, W., Jakes, R., Goedert, M., Wang, X., & Proud, C. G. (2001). The kinase DYRK phosphorylates protein-synthesis initiation factor eIF2Bepsilon at Ser539 and the microtubule-associated protein tau at Thr212: potential role for DYRK as a glycogen synthase kinase 3-priming kinase. *The Biochemical Journal*, *355*(Pt 3), 609–15. Retrieved from /pmc/articles/PMC1221774/?report=abstract

Yabuki, Y., Shioda, N., Maeda, T., Hiraide, S., Togashi, H., & Fukunaga, K. (2014). Aberrant CaMKII activity in the medial prefrontal cortex is associated with cognitive dysfunction in ADHD model rats. *Brain Research*, *1557*, 90–100. http://doi.org/10.1016/j.brainres.2014.02.025

Yamaguchi, H., Ishiguro, K., Uchida, T., Takashima, A., Lemere, C. A., & Imahori, K. (1996). Preferential labeling of Alzheimer neurofibrillary tangles with antisera for tau protein kinase (TPK) I/glycogen synthase kinase-3 beta and cyclin-dependent kinase 5, a component of TPK II. *Acta Neuropathologica*, *92*(3), 232–41. Retrieved from http://www.ncbi.nlm.nih.gov/pubmed/8870824

Yamamoto, H., Hiragami, Y., Murayama, M., Ishizuka, K., Kawahara, M., & Takashima, A. (2005). Phosphorylation of tau at serine 416 by Ca2+/calmodulin-dependent protein kinase II in neuronal soma in brain. *Journal of Neurochemistry*, *94*(5), 1438–47. http://doi.org/10.1111/j.1471-4159.2005.03307.x

Yan, S. D., Chen, X., Fu, J., Chen, M., Zhu, H., Roher, A., … Schmidt, A. M. (1996). RAGE and amyloid-beta peptide neurotoxicity in Alzheimer's disease. *Nature*, *382*(6593), 685–91. http://doi.org/10.1038/382685a0

Yan, S. D., Roher, A., Schmidt, A. M., & Stern, D. M. (1999). Cellular cofactors for amyloid beta-peptide-induced cell stress. Moving from cell culture to in vivo. *The*

American Journal of Pathology, *155*(5), 1403–11. Retrieved from http://www.pubmedcentral.nih.gov/articlerender.fcgi?artid=1866992&tool=pmcentrez&rendertype=abstract

Yang, E., & Schulman, H. (1999). Structural examination of autoregulation of multifunctional calcium/calmodulin-dependent protein kinase II. *The Journal of Biological Chemistry*, *274*(37), 26199–208. Retrieved from http://www.ncbi.nlm.nih.gov/pubmed/10473573

Yoshimura, Y. (2003). Phosphorylation of tau protein to sites found in Alzheimer's disease brain is catalyzed by Ca2+/calmodulin-dependent protein kinase II as demonstrated tandem mass spectrometry. *Neuroscience Letters*, *353*(3), 185–188. http://doi.org/10.1016/j.neulet.2003.09.037

Youngjohn, J. R., & Crook, T. H. (1993). Learning, forgetting, and retrieval of everyday material across the adult life span. *Journal of Clinical and Experimental Neuropsychology*, *15*(4), 447–60. http://doi.org/10.1080/01688639308402570

Zhang, Y., Kurup, P., Xu, J., Carty, N., Fernandez, S. M., Nygaard, H. B., … Lombroso, P. J. (2010). Genetic reduction of striatal-enriched tyrosine phosphatase (STEP) reverses cognitive and cellular deficits in an Alzheimer's disease mouse model. *Proceedings of the National Academy of Sciences*, *107*(44), 19014–19019. http://doi.org/10.1073/pnas.1013543107

Zheng, W.-H., Bastianetto, S., Mennicken, F., Ma, W., & Kar, S. (2002). Amyloid β peptide induces tau phosphorylation and loss of cholinergic neurons in rat primary septal cultures. *Neuroscience*, *115*(1), 201–211. http://doi.org/10.1016/S0306-4522(02)00404-9